

SpatialBench

Is Your Spatial Foundation Model an All-Round Player?

Haosong Peng^{1,*} Hao Li^{2,3,*} Jiaqi Chen³ Yuhao Pan¹ Runmao Yao^{2,*} Yalun Dai²
 Fushuo Huo⁴ Fangzhou Hong^{2,*} Zhaoxi Chen^{2,*} Haozhao Wang⁵
 Dingwen Zhang³ Ziwei Liu^{2,*} Wenchao Xu^{1,†}

¹Hong Kong University of Science and Technology ²Nanyang Technological University *Ropedia

³Northwestern Polytechnical University ⁴Southeast University

⁵Huazhong University of Science and Technology

Project Page: ropedia.github.io/SpatialBench
 Code: github.com/Ropedia/SpatialBench

Dataset: ropedia-ai/DA-Next-5M
 Model: ropedia-ai/DA-Next

arXiv:2605.27367v1 [cs.CV] 26 May 2026

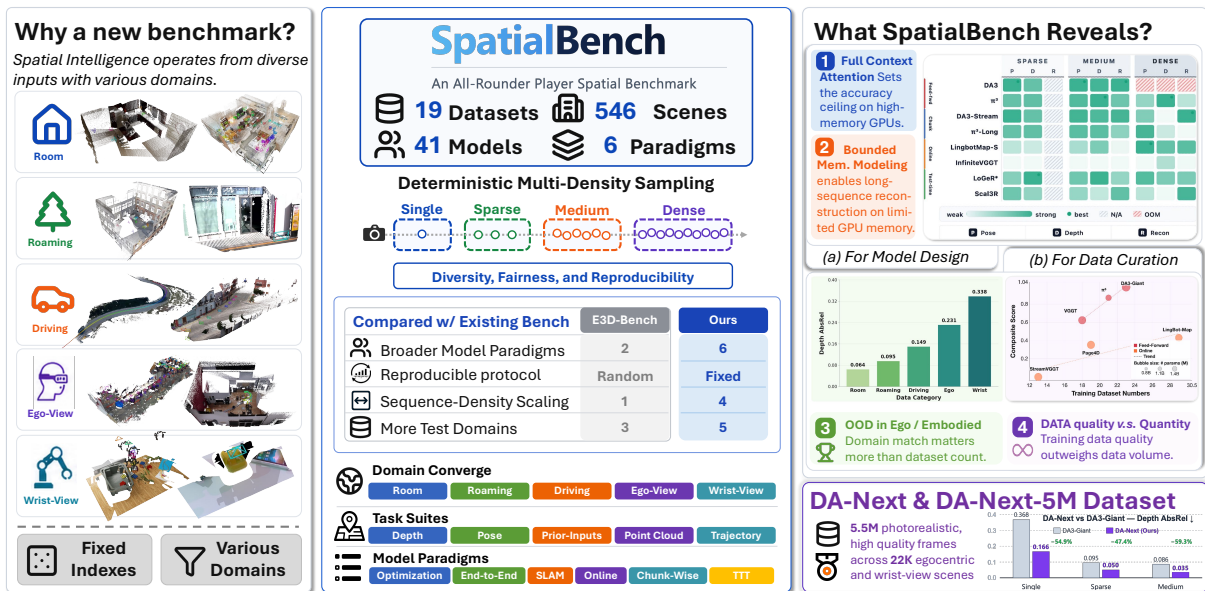


Figure 1 | **SpatialBench** provides a reproducible, cross-paradigm benchmark spanning 19 datasets, 546 scenes, 41 models, and 6 paradigms under deterministic multi-density sampling. Our analysis reveals insights on model design, domain generalization, data curation, and beyond, complemented by DA-Next and DA-Next-5M to address the embodied domain gap.

Abstract



While spatial foundation models have demonstrated impressive performance on standard datasets, a critical question remains: are they truly *all-round players* capable of generalizing robustly across diverse downstream tasks, arbitrary viewpoints, shifting scene domains, varying input densities, and specific hardware constraints? Answering this overarching question requires a holistic assessment, yet current models are

* Equal contribution. † Corresponding author.

mainly evaluated on specific domains for which they were specifically designed or trained. Such evaluations are intrinsically limited by narrow paradigm coverage, limited scene domains, and arbitrary frame sampling, making it fundamentally difficult to assess their true generalization capabilities. To address this gap, we present **SpatialBench**, a cross-paradigm, domain-diverse benchmark for spatial foundation models with deterministic sampling. SpatialBench features unprecedented scale and rigorous deterministic design, comprising **19** datasets and **546** scenes across **5** diverse spatial domains. It comprehensively evaluates **41** models across **6** paradigms on **5** task suites under **4** different input density settings. Our extensive evaluation reveals that current models are not yet all-round players, and uncovers crucial insights for future advancement. Specifically, we demonstrate that full-context attention maximizes accuracy while bounded-memory strategies unlock long-sequence scalability. Moreover, our empirical evaluations in challenging embodied and egocentric tasks demonstrate that strict domain alignment and high data quality are far more critical to performance than simple dataset scaling. Furthermore, to address the largest data gap identified in our analysis, we go beyond evaluation by introducing a large-scale dataset, **DA-Next-5M**, and a strong baseline model, **DA-Next**, pushing the boundaries of spatial representation learning.

1. Introduction

Spatial foundation models have already been widely deployed across robotics [117, 56, 128], AR/VR [119], autonomous driving [15], and embodied AI [41, 130]. This extensive adoption is driven by their remarkable ability to recover accurate 3D structures from mere images or videos, establishing them as general-purpose visual geometry backbones for spatial intelligence. However, operating in these real-world applications is inherently chaotic and far more demanding than standard reconstruction benchmarks. To truly support these downstream tasks, a robust model must maintain its reliability when confronting unpredictable scene domain shifts, highly variable sparse-to-dense input regimes, and strict hardware memory constraints. This raises the central question of this work: *if spatial foundation models are expected to support general-purpose spatial intelligence, can they truly serve as robust all-round players across the diverse conditions of the 3D world?*

However, existing evaluations fall short in several critical aspects. First, they cover only a narrow slice of today’s model paradigms. Spatial foundation models now span feed-forward [94, 42, 54], optimization-based [99, 48, 125], streaming [136, 46, 13], SLAM-based [62, 66], chunk-based [23], and test-time training (TTT) [16, 113, 126] approaches, yet most benchmarks evaluate only one or a few of them under separate protocols. Second, current comparisons are often not standardized. Even when papers report results on the same dataset, they may use different scene splits, private subsets, frame indices, temporal windows, or input densities, making direct comparison ambiguous. Third, existing protocols rarely expose how models scale with sequence density. For example, a model that works well on sparse image sets may fail on dense long videos because of memory growth, accumulated drift, or degraded global consistency; conversely, bounded-memory methods (e.g., online, chunk-wise, and TTT) may be undervalued when evaluation is restricted to short sequences. Finally, test domains remain too limited for assessing real-world spatial intelligence. Standard indoor or object-centric reconstruction datasets do not capture the diversity of robotics, autonomous driving, egocentric perception, and

wrist-mounted manipulation settings. These gaps motivate a benchmark that is cross-paradigm, deterministic, density-aware, and domain-diverse: one that can fairly compare models, reveal how performance changes from sparse views to dense streams, and diagnose where current spatial foundation models succeed or fail.

To address the aforementioned challenges, we introduce **SpatialBench**. By incorporating a deterministic density-aware protocol, broad domain diversity, and cross-paradigm comparisons, this comprehensive benchmark serves as a beacon to guide and verify spatial foundation models toward becoming true **all-round players**. SpatialBench is built around three core design principles: **(1) Deterministic Multi-Density Evaluation Protocol**. To systematically assess model robustness across varying input scales, SpatialBench adopts a deterministic sampling strategy to precompute frame indices across **4** distinct density regimes: *single-frame*, *sparse*, *medium*, and *dense*. By evaluating each scene under these standardized configurations across several key metrics, our protocol ensures both a comprehensive understanding of model performance and full reproducibility across different paradigms. **(2) Broad Domain Coverage Across 19 Datasets**. SpatialBench aggregates **19** datasets and **546** scenes in total, spanning a comprehensive range of conditions, including *indoor* and *outdoor* environments, *static* and *dynamic* scenes, *real-world* and *synthetic* data, and diverse viewpoint types. Each scene is annotated with orthogonal tags along these axes, enabling fine-grained cross-domain filtering and aggregation, supporting over 100 distinct evaluation configurations that far exceed any existing benchmark. **(3) Comprehensive and Cross-Paradigm Model Comparison**. SpatialBench provides unified adapters for **31** state-of-the-art models and **41** variants in total, spanning all six reconstruction paradigms: *optimization-based*, *end-to-end feed-forward*, *online streaming*, *chunk-wise*, *TTT-based*, and *SLAM-based* systems. All methods are evaluated under a unified protocol, enabling fair and direct comparison across several geometric tasks, including *depth* and *camera pose estimation*, *reconstruction*, *prior-enhanced geometry prediction*, and *trajectory estimation*.

We further conduct extensive analysis experiments on SpatialBench, revealing several key insights: **(1) Full-context attention defines the accuracy upper bound**, with globally coupled feed-forward models consistently outperforming bounded-memory approaches under the same input budget. **(2) Bounded-memory models unlock long-horizon scalability**, enabling continuous reconstruction beyond the memory limits of full-context models, at the cost of geometry estimation accuracy. **(3) Data quality outweighs data volume**, as carefully curated pseudo-GT supervision consistently outperforms larger but noisier training mixtures. **(4) Egocentric and wrist-view domains remain the dominant OOD failure modes**, exposing a field-level gap that cannot be addressed by scaling existing training mixtures alone.

To further address the gap in egocentric and wrist-view domains, we curate **DA-Next-5M**, a dataset comprising **22K** scenes with **5.5M** frames of 3D data in total from egocentric and robot wrist-view sources. We train our proposed **Depth-Anything-Next (DA-Next)** on DA-Next-5M, establishing a strong domain-specific baseline for these underexplored viewpoints. The key contributions of our work are summarized as follows.

- SpatialBench is the first standardized benchmark for comprehensive evaluation of 3D spatial foundation models on several geometry tasks, aggregating 19 diverse datasets and 546 scenes, and providing unified adapters for 32 methods and 41 variants across all six paradigms.
- Through extensive experiments on SpatialBench, we conduct a comprehensive cross-paradigm analysis and derive key insights into model robustness, domain generalization, and input-density scaling behavior, highlighting promising directions for future research.

- Experiments show that DA-Next achieves substantial gains over DA3-Giant: +47%/+59% in depth estimation and +3.1%/+5.5% in pose estimation on sparse/medium inputs, demonstrating that targeted in-domain data curation effectively closes the embodied domain gap.

2. Related Work

Spatial foundation models for visual geometry. Recent advances in visual geometry have shifted 3D reconstruction from optimization-heavy pipelines toward spatial foundation models that directly infer scene geometry, camera parameters, and point cloud from images. Early influential systems such as DUS_t3R [99] and MAS_t3R [48] reformulate geometric reconstruction as dense pointmap prediction, substantially simplifying pose-free 3D reconstruction and 3D-grounded image matching. Although these methods still rely on global alignment or optimization-based post-processing, they establish a strong foundation for subsequent feed-forward reconstruction models. Building on this direction, end-to-end feed-forward methods aim to recover visual geometry in a single network pass. VGGT [94] predicts camera parameters, depth maps, pointmaps, and point tracks in a unified transformer framework, while Fast3R [116] scales feed-forward reconstruction to large unordered image collections and FastVGGT [82] accelerates VGGT-style inference without retraining. MUS_t3R [9] extends stereo-style reconstruction to multi-view settings, and MapAnything [42] supports flexible geometric inputs such as poses, depths, intrinsics, and partial reconstructions for universal metric 3D reconstruction. More model families further expand this paradigm: OmniVGGT [71] incorporates omni-modality prior for reconstruction; π^3 removes the dependence on reference frames through a fully permutation-equivariant architecture, predicting affine-invariant camera poses, and scale-invariant local pointmaps; AMB3R [93] introduces a backend module for more accurate metric-scale reconstruction; DA3 and its variants [54] recover consistent 3D geometry from arbitrary visual inputs across multiple model scales; and WorldMirror [59] explores any-prior prompting to unify diverse 3D representations. Together, these feed-forward spatial foundation models demonstrate strong reconstruction capability on bounded image sets, but their performance can degrade when applied to long videos, streaming inputs, or large-scale scenes where memory, consistency, and drift become critical. Moreover, processing long sequences with these models incurs prohibitive GPU memory consumption and increased inference latency.

Long-sequence, online, and test-time training models. To handle realistic video streams, recent work has extended spatial foundation models from bounded image sets to online, chunk-wise, SLAM-based, and test-time adaptive settings. Online and streaming methods maintain temporal or spatial memory, recurrent states, or compact historical context as new frames arrive. Spann3R [92] introduces spatial memory for incremental 3D reconstruction, CUT3R [98] uses a persistent recurrent state for continuous 3D perception, and MonST3R [125] extends DUS_t3R-style reconstruction to dynamic scenes with motion. Point3R [107] employs explicit spatial pointer memory for streaming reconstruction, while Stream3R [46], StreamVGGT [136], Page4D [133], InfiniteVGGT [123], WinT3R [52], LongStream [17], and LingBot-Map [13] investigate different memory mechanisms, window designs, causal attention strategies, and long-horizon update rules for scalable online geometry estimation. Another line processes long videos in chunks and then aligns local reconstructions into a global scene. VGGT-Long [23], π^3 -Long [23], and DA3-Streaming [23] follow this chunk-wise strategy to extend powerful feed-forward backbones or model variants to kilometer-scale or long-sequence reconstruction. In parallel, SLAM-based systems such as MAS_t3R-SLAM [66] and VGGT-SLAM [62] combine learned 3D priors with classical mapping and tracking components to improve real-time dense reconstruction. Finally, test-time training methods, including TTT3R [16], Scal3R [113],

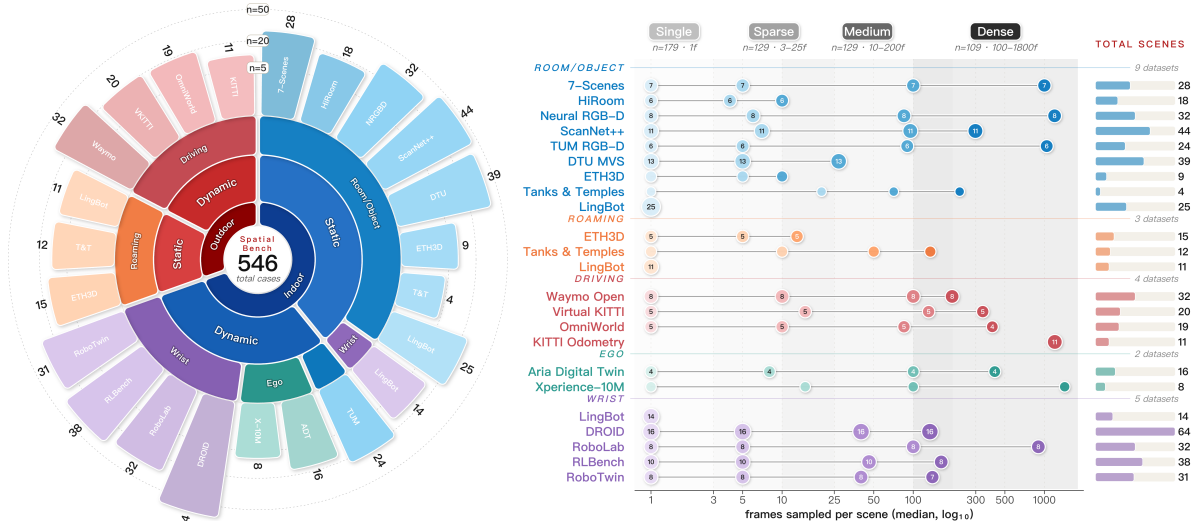


Figure 2 | **Overview of SpatialBench.** (Left) Distribution of all scene categories and their corresponding counts. (Right) Data sources and the median number of frames per scene under sparse, medium, and dense input settings. The number on each circle indicates the number of scenes.

ZipMap [39] and LoGeR [126], adapt the model or scene representation during inference to improve large-scale consistency and reduce drift. These methods reveal an emerging trend: the central challenge of spatial foundation models is no longer only accurate single-shot reconstruction, but also scalable memory management, temporal consistency, dynamic-scene robustness, and long-range geometric alignment under realistic visual streams.

Related benchmarks for visual geometry. Several recent efforts have introduced systematic benchmarks for 3D reconstruction and visual geometry. Robust MVD [81] focuses on cross-dataset generalization for multi-view depth estimation, while E3D-Bench [19] provides a broader evaluation covering depth, reconstruction, pose estimation, and novel-view synthesis. In addition, several model works construct their own evaluation protocols, including DA3 [54], π^3 [101], and MapAnything [42]. Among these, E3D-Bench is the most comprehensive standalone effort, supporting cross-method comparison across multiple tasks. However, it does not provide comparisons across various domains and paradigms. The remaining model-specific suites are largely tied to individual model studies and lack a unified protocol for controlled cross-paradigm comparison. In contrast, SpatialBench provides a standalone, deterministic, and tag-aware benchmark that enables systematic analysis across diverse input densities, viewpoint types, scene dynamics, and foundation model paradigms.

3. SpatialBench Design

SpatialBench is built upon a large-scale collection of heterogeneous 3D vision datasets, covering a diverse spectrum of scene categories, capture conditions, and viewpoint configurations. Fig. 2 provides an overview of SpatialBench: the left panel shows the breakdown of scene categories and their corresponding counts, and the right panel reports the data sources alongside the median number of frames per scene across different settings. This multi-dimensional design allows SpatialBench to evaluate model capabilities across a wide range of conditions in a principled and systematic way.

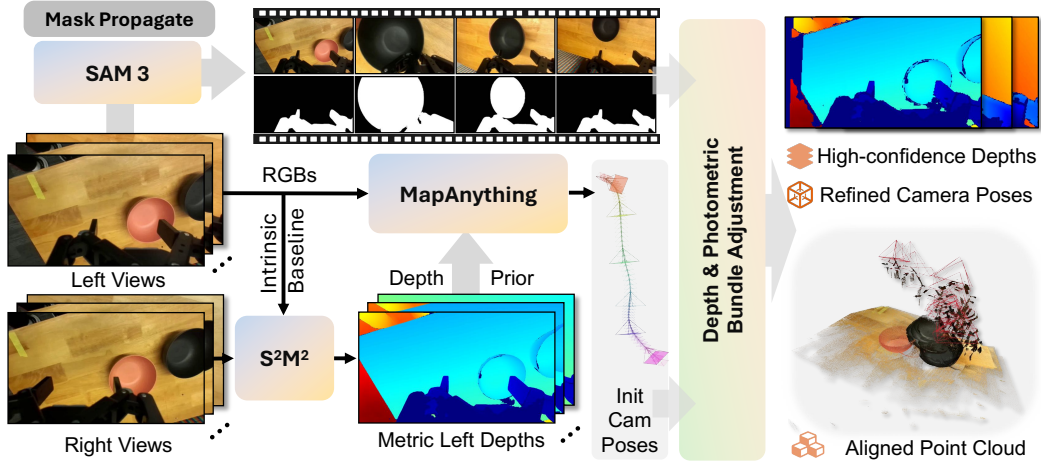


Figure 3 | **DROID data curation pipeline.** We obtain metric depth from stereo sequences via S^2M^2 [65], with initial camera poses estimated by MapAnything [42]. Gripper and contact affordance masks are segmented using SAM3. Then the camera poses are refined via bundle adjustment using the RGBs, initial camera poses, and masks.

3.1. Data Collection and Curation

SpatialBench unifies heterogeneous 3D vision datasets under a common, deterministic evaluation protocol. Raw datasets are first normalized into a shared per-scene representation comprising *RGB frames*, *metric depth maps*, *camera-to-world poses*, and *camera intrinsics*, and are subsequently curated into a fixed set of evaluation scene indices. Each scene index is stored as a JSON record that specifies, for every (scene, view-density) pair, the exact frame indices to be consumed by a method. By decoupling data ingestion from evaluation, this design ensures that all methods are assessed on identical inputs and that results remain fully reproducible across repeated runs.

We aggregate 19 publicly available real-world and synthetic datasets, spanning the principal axes relevant to modern 3D perception: *environment* (indoor/outdoor), *dynamics* (static/dynamic), *viewpoint* (normal/egocentric/wrist), and *data type* (real/synthetic). For example, the whole dataset can be classified into four distinct subsets according to the *dynamics* and *data type* axes: static-real, static-synthetic, dynamic-real, and dynamic-synthetic: (1) **Static-real**. 7-Scenes [83], DTU [37], NRGBD [4], Scannet++ [121], Tanks & Temples [44], and ETH3D [80] provide high-quality ground-truth geometry under static conditions, covering settings from close-range tabletop scans to large-scale outdoor architecture. (2) **Static-synthetic**. Hiroom [54]. (3) **Dynamic-real**. TUM-Dynamic [86], DROID [43], Xperience [78], Waymo [87], and KITTI-Odometry [26] capture dynamic indoor activities as well as street-scale driving scenarios. (4) **Dynamic-synthetic**. ADT [69], RLBench [36] with Colosseum [72], RoboTwin [14], Robolab [118], Virtual KITTI 2 [8], and OmniWorld-Game [135] provide dense photorealistic sequences for dynamic and robotic settings that are otherwise costly to acquire in the real world. We also collect a **Single-frame Mixture** including Lingbot-Depth [88] and all the above datasets, which contributes one-shot rgb/depth/intrinsic triplets, used exclusively in the monocular depth evaluation. We refer the reader to Tab. 4 in Appendix B.1 for a complete overview of all datasets included in SpatialBench.

To obtain high-quality, depth-consistent real-world wrist-view sequences, we design a dedicated data curation pipeline for the DROID [43] dataset, as illustrated in Fig. 3. We feed stereo video sequences into the S^2M^2 [65] stereo depth estimation model to obtain per-frame metric depth for the left image, with unreliable points filtered out via confidence thresholding. The

resulting image sequence and metric depth maps are then passed to MapAnything [42] to obtain initial camera poses. In parallel, we apply SAM3 [10] to segment dynamic regions, including the gripper and objects it interacts with, on a set of keyframes, and propagate the masks to the full sequence. These masks exclude dynamic foreground regions from the Bundle Adjustment optimization, which assumes a static scene background. Finally, leveraging the initial camera poses along with RGB images and the obtained masks, we perform depth & photometric bundle adjustment to refine the camera poses, yielding globally aligned point clouds. Other data pipeline and implementation details are provided in Appendix A.

3.2. Multi-density Evaluation Regimes

A central principle of our benchmark is that each method is evaluated across multiple temporal resolutions on the same scene, rather than on arbitrarily truncated clips. From each curated scene, we generate four parallel entries corresponding to distinct view-density regimes: **SINGLE**, **SPARSE**, **MEDIUM**, and **DENSE**. These regimes are designed to probe complementary failure modes: **SINGLE** isolates monocular depth priors; **SPARSE** stresses wide-baseline reconstruction from unordered views; **MEDIUM** reflects the moderate-overlap inputs typical of SfM and SLAM; and **DENSE** evaluates long-horizon online estimation. Because all four regimes are derived from the same underlying scene, scene difficulty and density-related difficulty can be disentangled.

SINGLE. For each scene, we fix a single deterministic frame index that is consistent across all evaluations. This ensures that frame selection is reproducible across machines and independent of wall-clock time.

SPARSE. Sparse-view selection is formulated as a *weighted set-cover problem* over the scene’s 3D voxel support. Let \mathcal{V} denote the set of all voxels in the scene, and let \mathcal{F} denote the candidate frames. Each frame $f \in \mathcal{F}$ covers a subset of voxels $V_f \subseteq \mathcal{V}$. We greedily select frames to maximize cumulative voxel coverage until a small frame budget K is reached. This deterministic procedure promotes viewpoint diversity and is robust to variations in trajectory speed, producing a compact set of views that jointly covers the scene rather than merely temporally distant frames. The full selection objective is given in Appendix B.2.

MEDIUM. The medium regime retains the set-cover formulation of the sparse regime but favors view overlap over diversity. Let \mathcal{V} be the coarsened voxel set and \mathcal{F} the candidate frames. The selected frame set \mathcal{S} is obtained by greedily maximizing voxel coverage, subject to a length-adaptive frame budget. This procedure encourages mid-range overlap among views rather than extreme viewpoint diversity. The corresponding budgeted objective is detailed in Appendix B.2.

DENSE. The dense regime targets the opposite end of the spectrum: an online, long-horizon setting in which a method must ingest essentially every frame of a trajectory and reconstruct temporally coherent geometry. Accordingly, the goal is not to *select* views in the set-cover sense, but to preserve temporal continuity while avoiding the trivial inflation of evaluation cost caused by near-duplicate consecutive frames. In practice, however, processing arbitrarily long trajectories can exceed the memory limits of some methods; therefore, we impose a maximum frame budget to ensure that the dense evaluation remains feasible across all methods.

3.3. Evaluated Models

In this work, we evaluate 31 methods with 41 model variants in total. We categorize the evaluated methods into six paradigms: 1) *Optimization-based* methods, including DUS3R [99] and MAST3R [48]; 2) *End-to-End Feed-Forward* methods, including VGGT [94], Fast3R [116],

FastVGGT [82], MUST3R [9], MapAnything [42], OmniVGGT [71], π^3 [101], AMB3R [93], DepthAnything3 [54], WorldMirror [59], and VGGT-Omega [95]; 3) *Online/Streaming* methods, including Spann3r [92], CUT3R [98], MonST3R [125], Point3R [107], Stream3R [46], StreamVGGT [136], PAGE4D [133], InfiniteVGGT [123], WinT3R [52], LongStream [17] and LingBot-Map [13]; 4) *Chunk-based* methods, including VGGT-Long [23], Pi-Long [23] and DA3-Streaming [23]; 5) *SLAM-based* methods, including MAST3R-SLAM [66] and VGGT-SLAM [61]; and 6) *Test-Time Training* methods, including TTT3R [16], Scal3R [113] and LoGeR [126]. All evaluated models are listed in Table 1.

3.4. Task Description and Metrics

To comprehensively assess the capabilities of each model, we design five general evaluation tasks across different settings as follows. Appendix B.4 reports complete metric definitions.

Camera Pose Estimation. Given an input image sequence, we evaluate pairwise camera geometry using Relative Rotation Accuracy (RRA) and Relative Translation Accuracy (RTA), following Wang et al. [94]. We use R_{Acc_x} and T_{Acc_x} to denote the fraction of pairs with angular errors below threshold x , and AUC_x as the area under the joint accuracy curve of RRA and RTA up to threshold x .

Camera Trajectory Estimation. For continuous image sequences, *i.e.*, our medium and dense input settings, we additionally compute Absolute Trajectory Error (ATE), Relative Translation Error (RPE_t), and Relative Rotation Error (RPE_r), all evaluated after global Sim(3) alignment with the ground-truth trajectory, following Teed and Deng [89].

Depth Estimation. For single/multi-view depth estimation, we compute $AbsRel$, $SqRel$, $RMSE$, $LogRMSE$, and threshold (inlier, δ_r) metrics over all valid pixels with respect to the ground-truth depth, where the inlier ratio indicates the percentage of pixels with correct predictions. Predicted depths are aligned to the ground truth via median alignment by default. For models with metric-scale prediction capability, we additionally report $AbsRel$ both before and after alignment.

Dense-View Reconstruction. We evaluate scene-level 3D reconstruction on a subset of scenes. Given the ground-truth and reconstructed point sets, we compute *Accuracy* and *Completeness*, and report the *F-score* (harmonic mean of Precision and Recall) and the *Overall* score, defined as $(Accuracy + Completeness) / 2$, following Lin et al. [54].

Prior-Enhanced Prediction. This task targets methods that accept auxiliary prior inputs (e.g., MapAnything, OmniVGGT [42, 71]). We evaluate their performance under two settings: with all ground-truth depth priors provided, and with all ground-truth camera pose priors provided.

4. Depth-Anything-Next

To fill the gap of 3D foundation models in the egocentric and wrist-view domains, we introduce Depth-Anything-Next and our DA-Next-5M dataset in this section.

4.1. DA-Next-5M Dataset

We curate **DA-Next-5M**, a large-scale 3D dataset comprising 5.5M high-quality frames across 22K scenes, primarily collected from egocentric and wrist-view perspectives. This category of views presents unique challenges, including high motion dynamics, frequent occlusions, and ultra-close-range capture, making it a critical data paradigm for embodied intelligence

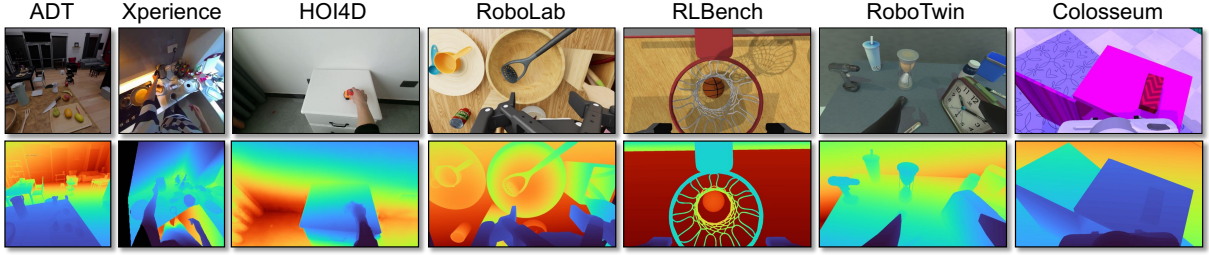


Figure 4 | **DA-Next-5M Data Samples.** The dataset showcases a diverse array of assets and episodes.

applications. Tab. 7 presents the statistics of DA-Next-5M, where all datasets provide image sequences, metric depths, camera intrinsics, and extrinsics. For simulation-based datasets, extensive domain randomization is applied to various factors, including background appearance, object size, color, and wrist camera placement. Please refer to Appendix C for the data collection pipeline.

4.2. Model Architecture

Depth-Anything-Next builds upon the architecture of DA3 [54], while extending it with the capability to predict absolute scale in an end-to-end manner. Fig. 5 illustrates the overall architecture of DA-Next. Specifically, DA-Next takes a sequence of frames $\mathbf{I} = \{I_i\}_{i=1}^N$ and auxiliary camera information $\mathbf{C} = \{C_i\}_{i=1}^N$ as input, where each $C_i = \{K_i, G_i\}$ comprises the intrinsics $K_i \in \mathbb{R}^{3 \times 3}$ and the pose $G_i \in \text{SE}(3)$. All the frames are first patchified into patch tokens \mathbf{e}_f . The patch tokens from all frames are then concatenated with camera tokens \mathbf{e}_c and scale tokens \mathbf{e}_s , and jointly processed by the transformer encoder \mathcal{E} : $(\hat{\mathbf{e}}_c, \hat{\mathbf{e}}_s, \hat{\mathbf{e}}_f) = \mathcal{E}(\mathbf{e}_c, \mathbf{e}_s, \mathbf{e}_f)$. Here, \mathbf{e}_c represents GT camera tokens when auxiliary camera information is available, and defaults to learnable camera tokens otherwise. DA-Next adopts pure transformer blocks as its encoder, where frame-wise self-attention and global self-attention alternate throughout the layers. After being processed by the encoder (L layers), the patch tokens $\hat{\mathbf{e}}_f$ and camera tokens $\hat{\mathbf{e}}_c$ are fed into the Dual-DPT heads to produce the final depth map $\hat{\mathbf{D}}$ and ray map $\hat{\mathbf{R}}$ predictions, while the scale tokens $\hat{\mathbf{e}}_s$ are passed through a lightweight MLP to regress a scalar scale factor \hat{S} . Finally, the scene point cloud is reconstructed from the predicted depth map $\hat{\mathbf{D}}$, ray map $\hat{\mathbf{R}}$, and scale factor \hat{S} .

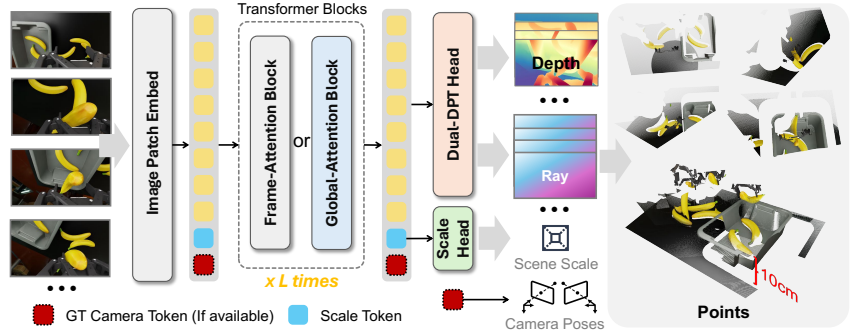


Figure 5 | **Overview of Depth-Anything-Next.** The model incorporates additional scale tokens to learn the scene-level metric scale. Optionally, camera pose information can be embedded as GT camera tokens to serve as auxiliary input to provide geometric guidance.

4.3. Implementation Details

Training Objectives. Following DA3 [54], our training objective is a multi-task loss comprising five components: depths $\{\hat{\mathbf{D}}, \mathbf{D}\}$, depth gradients $\{\nabla \hat{\mathbf{D}}, \nabla \mathbf{D}\}$, ray maps $\{\hat{\mathbf{R}}, \mathbf{R}\}$, points $\{\hat{\mathbf{P}}, \mathbf{P}\}$, and scale $\{\hat{S}, S\}$ supervision. The total loss is defined as $\mathcal{L} = \mathcal{L}_{\text{depth}} + \alpha \mathcal{L}_{\text{grad}} + \mathcal{L}_{\text{ray}} + \mathcal{L}_{\text{pmap}} + \mathcal{L}_{\text{scale}}$. Prior to loss computation, all ground-truth signals are canonicalized into the first-camera

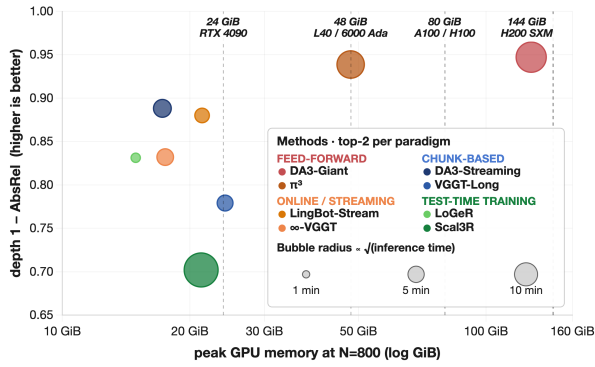


Figure 6 | **Operating snapshot.** Memory, depth error, and inference time at $N = 800$.

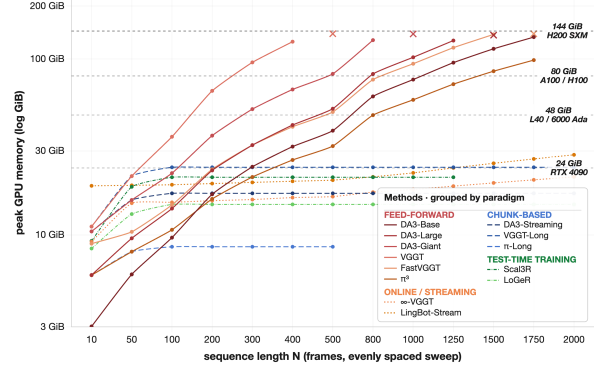


Figure 7 | **Memory scaling.** Peak GPU memory versus input sequence length.

coordinate frame and then normalized by a per-scene scale factor S , defined as the mean ℓ_2 norm of the valid ground-truth world points \mathbf{P} . We divide \mathbf{P} , \mathbf{D} , and the camera translations by S , and use S itself as the regression target of the scale head, so that \hat{S} recovers the absolute metric scale to which the other predictions are invariant. All loss terms are based on the ℓ_1 norm with $\alpha = 1$, where the scale loss is defined as: $\mathcal{L}_{\text{scale}} = \|f_{\log}(\hat{S}) - f_{\log}(S)\|_1$ and $f_{\log} : \mathbf{x} \rightarrow (\mathbf{x}/\|\mathbf{x}\|) \cdot \log(1 + \|\mathbf{x}\|)$.

Datasets. We train our model mainly on DA-Next-5M. To mitigate potential generalization degradation, we retain data from 11 general 3D datasets for joint training, including Mapfree [2], Hypersim [76], Infinigen [73], etc. The full datasheet and dataset mixture can be found in the Appendix D.

Training Details. Our DA-Next architecture follows DA3-Giant [54] with $L = 41$ Transformer blocks and is initialized by pre-trained weights. During training, each batch incorporates ground-truth camera information as auxiliary input with probability $p = 20\%$. The training runs end-to-end on 4 NVIDIA H200 GPUs over seven days. We provide complete implementation details in Appendix D.

5. Findings: How to Train Your Best Spatial Foundation Models?

Tab. 1 presents the main results on SpatialBench, reporting depth, camera pose, trajectory, and point cloud metrics across single-frame, sparse, medium, dense, and average settings for 41 models spanning six reconstruction paradigms. We refer the reader to Appendix F for per-regime sub-tables and per-dataset metric breakdowns.

Full-Context Attention Sets the Accuracy Upper Bound on High-Memory GPUs. Fig. 6 compares representative models at a fixed sequence length of $N = 800$, where all compared methods successfully complete the input. Under this shared input budget, full-context feed-forward models occupy the strongest accuracy region of the memory–accuracy Pareto plot. In particular, DA3-Giant and π^3 achieve the lowest depth errors among the compared paradigms, outperforming streaming and online-map variants in reconstruction accuracy. This indicates that globally coupled attention over the input sequence remains a highly effective representation mechanism for geometric reasoning. By jointly resolving cross-view correspondences and enforcing scene-level consistency, full-context models provide stronger reconstruction accuracy and generalization under the same budget.

Table 1 | **Main Results on SpatialBench.** We report performance across four input settings: *Single Frame*, *Sparse*, *Medium*, *Dense*, and their *Average* across all settings. *Time* is the per-sequence inference time in seconds reported in the sparse regime, averaged over all scenes. The best, second-best, and third-best results in each column are highlighted in **deep blue**, **medium blue**, and **light blue**, respectively. Out-of-memory (OOM, > 140G) and Timeout (T.O., > 4h per scene) cells are shaded **light red**. Within each sub-category, the **bold** value marks the in-group best.

Method	#Params (M)	Time (s)	Single Frame		Sparse		Medium				Dense				Average			
			AbsRel↓	AUC@30↑	AbsRel↓	AUC@30↑	AbsRel↓	AUC@30↑	ATE↓	F-Score↑	AbsRel↓	AUC@30↑	ATE↓	F-Score↑	AbsRel↓	AUC@30↑	ATE↓	F-Score↑
Optimization-based																		
DUST3R	571.17	7.59	0.385	0.257	0.498	0.276	0.448	1.691	0.340	OOM	OOM	OOM	OOM	(0.306)	(0.473)	(1.691)	(0.343)	
MAS3R	688.64	8.17	0.456	0.209	0.568	0.259	0.522	1.911	0.373	OOM	OOM	OOM	OOM	(0.308)	(0.545)	(1.911)	(0.370)	
End-to-End Feed-Forward																		
VGGT	1256.54	0.40	0.184	0.105	0.700	0.125	0.687	0.727	0.661	OOM	OOM	OOM	OOM	(0.138)	(0.694)	(0.727)	(0.661)	
Fast3R	647.55	0.90	0.350	0.260	0.392	0.255	0.386	6.582	0.300	0.331	0.232	13.68	0.224	0.299	0.337	10.13	0.262	
FastVGGT	1157.94	0.24	0.183	0.113	0.631	0.105	0.662	0.738	0.576	0.120	0.588	19.23	0.479	0.130	0.627	9.984	0.527	
MUS3R	423.43	0.96	0.429	0.165	0.614	0.162	0.643	3.097	0.507	T.O.	T.O.	T.O.	T.O.	(0.252)	(0.629)	(3.097)	(0.507)	
MapAnything	1228.49	0.22	0.451	0.153	0.579	0.146	0.579	1.737	0.420	OOM	OOM	OOM	OOM	(0.250)	(0.579)	(1.737)	(0.420)	
OmniVGGT	1217.49	0.22	0.188	0.117	0.665	0.111	0.665	1.491	0.595	OOM	OOM	OOM	OOM	(0.139)	(0.665)	(1.491)	(0.595)	
π^3	958.70	0.20	0.478	0.092	0.742	0.082	0.749	0.565	0.649	0.109	0.524	16.39	0.332	0.190	0.672	8.478	0.491	
π^3 -X	1360.03	0.24	0.371	0.084	0.741	0.078	0.744	0.369	0.658	OOM	OOM	OOM	OOM	(0.178)	(0.742)	(0.369)	(0.658)	
AMB3R	1563.12	0.53	0.466	0.088	0.739	0.085	0.727	0.645	0.554	OOM	OOM	OOM	OOM	(0.213)	(0.733)	(0.645)	(0.554)	
DA3-Small	34.30	0.39	0.385	0.191	0.476	0.176	0.479	4.850	0.432	0.208	0.368	28.12	0.325	0.240	0.441	16.48	0.379	
DA3-Base	135.37	0.40	0.349	0.159	0.566	0.142	0.562	3.865	0.515	0.166	0.436	26.35	0.399	0.204	0.521	15.11	0.457	
DA3-Large	410.94	0.41	0.333	0.128	0.688	0.105	0.701	2.722	0.626	OOM	OOM	OOM	OOM	(0.189)	(0.694)	(2.722)	(0.626)	
DA3-Giant	1355.67	0.47	0.368	0.095	0.785	0.086	0.776	1.161	0.742	OOM	OOM	OOM	OOM	(0.183)	(0.780)	(1.161)	(0.742)	
DA3-Nested	1689.85	0.52	0.364	0.106	0.779	0.086	0.770	1.980	0.737	OOM	OOM	OOM	OOM	(0.185)	(0.774)	(1.980)	(0.737)	
WorldMirror	1263.34	0.22	0.349	0.139	0.660	0.118	0.674	1.357	0.575	OOM	OOM	OOM	OOM	(0.202)	(0.667)	(1.357)	(0.575)	
VGGT-Omega	1143.81	0.48	0.516	0.077	0.803	0.067	0.795	0.659	0.706	-	-	-	-	(0.220)	(0.799)	(0.659)	(0.706)	
DA-Next [†] (Ours)	1303.76	0.50	0.166	0.050	0.809	0.035	0.819	1.442	0.727	OOM	OOM	OOM	OOM	(0.084)	(0.814)	(1.442)	(0.727)	
Online																		
Spann3r ²²⁴	658.69	0.55	0.370	0.274	0.329	0.252	0.361	4.312	0.254	0.315	0.246	26.48	0.159	0.303	0.312	15.4	0.207	
CUT3R	793.31	0.41	0.247	0.196	0.519	0.189	0.469	2.676	0.286	0.260	0.165	25.54	0.109	0.223	0.384	14.11	0.197	
MonST3R	571.17	20.81	0.309	0.227	0.269	0.241	0.195	2.234	0.081	OOM	OOM	OOM	OOM	(0.259)	(0.232)	(2.234)	(0.081)	
Point3R	828.01	1.05	0.379	0.221	0.339	0.228	0.303	6.512	0.211	0.285	0.212	28.09	0.139	0.278	0.285	17.3	0.175	
Stream3R-S	1190.60	0.62	0.409	0.114	0.603	0.204	0.427	5.717	0.348	OOM	OOM	OOM	OOM	(0.242)	(0.515)	(5.717)	(0.348)	
Stream3R-W	1190.60	0.62	0.409	0.117	0.597	0.240	0.364	6.756	0.323	OOM	OOM	OOM	OOM	(0.255)	(0.480)	(6.756)	(0.323)	
StreamVGGT	1256.54	0.85	0.219	0.154	0.598	0.171	0.562	4.940	0.397	0.198	0.413	26.9	0.251	0.185	0.524	15.92	0.324	
Page4D	1256.81	0.56	0.228	0.112	0.608	0.107	0.618	0.855	0.423	OOM	OOM	OOM	OOM	(0.149)	(0.613)	(0.855)	(0.423)	
InfiniteVGGT	1256.54	0.46	0.217	0.154	0.596	0.170	0.563	4.964	0.402	0.197	0.416	27.01	0.254	0.184	0.525	15.99	0.328	
Wint3R	749.46	0.41	0.619	0.157	0.499	0.144	0.444	3.944	0.401	0.234	0.202	27.8	0.114	0.288	0.382	15.87	0.258	
LongStream-B	1190.60	0.59	0.523	0.153	0.549	0.224	0.455	0.925	0.135	0.269	0.294	5.766	0.083	0.292	0.433	3.345	0.109	
LongStream-S	1190.60	0.83	0.523	0.151	0.543	0.166	0.385	1.188	0.126	0.279	0.218	10.08	0.083	0.280	0.382	5.634	0.105	
LingbotMap [†] -W	1157.94	0.30	0.333	0.138	0.650	0.114	0.641	0.509	0.362	0.167	0.553	4.694	0.352	0.188	0.615	2.602	0.357	
LingbotMap [†] -S	1157.94	0.33	0.333	0.138	0.650	0.114	0.647	0.508	0.411	0.139	0.627	3.470	0.472	0.181	0.641	1.989	0.442	
Chunk-wise																		
VGGT-Long	1256.54	0.20	0.184	0.105	0.700	0.131	0.679	0.512	0.633	0.222	0.507	8.467	0.467	0.161	0.629	4.490	0.550	
π^3 -Long	958.70	0.23	0.478	0.092	0.742	0.097	0.740	0.465	0.590	0.216	0.614	4.021	0.251	0.221	0.699	2.243	0.420	
DA3-Streaming	1355.67	0.51	0.368	0.095	0.785	0.091	0.767	0.563	0.725	0.245	0.546	8.575	0.516	0.200	0.699	4.569	0.621	
SLAM-based																		
MAS3R-SLAM	688.64	3.04	0.348	0.336	0.190	0.348	0.262	6.075	0.130	0.404	0.311	25.7	0.121	0.359	0.254	15.89	0.126	
VGGT-SLAM	1256.54	0.57	0.184	0.105	0.700	0.129	0.645	0.686	0.610	0.211	0.441	9.069	0.384	0.157	0.595	4.878	0.497	
Test-Time Training																		
TTT3R	793.31	0.61	0.247	0.202	0.469	0.179	0.493	2.343	0.294	0.222	0.321	21.07	0.173	0.212	0.428	11.71	0.233	
Scal3R	1266.14	2.32	0.227	0.114	0.732	0.147	0.670	0.400	0.671	0.244	0.480	2.396	0.498	0.183	0.627	1.398	0.585	
LoGeR	1254.62	0.26	0.251	0.095	0.687	0.113	0.693	0.591	0.504	0.197	0.552	5.217	0.335	0.164	0.644	2.904	0.419	
LoGeR*	1254.60	0.30	0.200	0.077	0.708	0.083	0.714	0.566	0.574	0.156	0.598	4.598	0.421	0.129	0.673	2.582	0.497	

“S” denotes **stream**, “B” denotes **batch**, and “W” denotes **window**. LingbotMap* indicates the best checkpoint is selected in each regime. DA-Next[†]: Numbers in (parentheses) below each DA-Next entry give the relative gap to DA3-Giant. Values in parentheses in the *Average* column indicate that the method runs OOM on the dense regime, and the average is therefore computed over fewer settings. Such methods are excluded from per-column rankings in the *Average* column. Note that DA-Next is excluded from the per-column rankings.

Takeaway: *Under the same input budget, the full-context attention models still define the accuracy upper bound, suggesting that globally coupled representations remain crucial for high-fidelity 3D geometry estimation and reconstruction.*

Bounded-Memory Modeling Enables Long-Sequence Reconstruction on Limited GPUs. The accuracy advantage of full-context models comes with a clear physical constraint. As shown in Fig. 7, their GPU memory consumption grows rapidly with sequence length and eventually reaches the out-of-memory boundary on dense long-horizon inputs. Streaming, online, chunk-

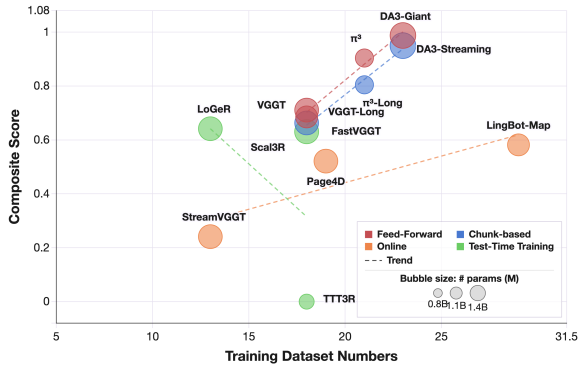


Figure 8 | **Training coverage.** Dataset count, parameter scale, and SpatialBench accuracy.

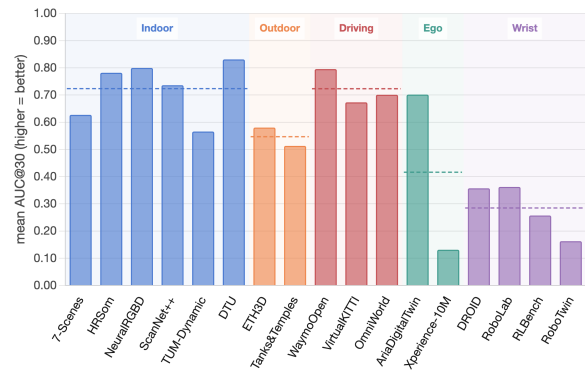


Figure 9 | **Domain-level OOD severity.** Mean AUC@30 grouped by evaluation domain.

wise, and TTT variants exhibit a different scaling behavior: by restricting the active context through causal updates, sliding windows, or chunked inference, they maintain substantially flatter memory curves and can continue processing sequences that full-context models cannot complete under the same hardware budget. As sequence length grows, these methods show stronger trajectory-level consistency (lower ATE), reflecting their ability to maintain long-range geometric alignment. However, their depth estimation accuracy remains below that of full-context models across all input regimes, indicating that bounded-memory inference trades pairwise geometric precision for scalability. Thus, these two model families occupy complementary operating regimes: full-context models are preferable when accuracy on bounded inputs is the priority, while bounded-memory methods are better suited for long-horizon or resource-constrained deployment.

Takeaway: *Streaming, chunk-wise, and TTT models trade part of the full-context accuracy advantage for bounded-memory inference, enabling continuous long-horizon reconstruction under realistic hardware constraints.*

Training Data Volume Correlates with Performance, but Data Quality is the a Critical Factor.

Tab. 5 summarizes the training datasets used across all evaluated methods, showing considerable variation in both dataset count and domain coverage. As shown in Fig. 8, there is a clear positive correlation between the number of training datasets and composite benchmark score within the end-to-end and online paradigms: methods trained on more diverse data sources consistently achieve higher performance. However, data volume alone does not tell the full story. Within comparable dataset counts, data quality plays a more decisive role than sheer dataset quantity. A representative example is DA3, which leverages synthetic datasets to train a teacher model and subsequently refines noisy depth estimates to generate high-quality pseudo-GT supervision. This careful curation strategy enables DA3 to achieve the highest composite scores among feed-forward models, despite not relying on the largest training corpus.

Takeaway: *Training data volume and performance are positively correlated, but data quality is the more decisive factor: carefully curated, high-quality pseudo-GT supervision consistently outperforms larger but noisier training mixtures under comparable dataset scales.*

Egocentric-View and Wrist-View Remain the Dominant OOD Failure Modes. The most severe generalization gap exposed by SpatialBench is not on standard indoor reconstruction datasets, but on embodied-view domains. As shown in Fig. 9, the cross-method average remains relatively strong on indoor datasets, while performance drops sharply on ego-view and especially wrist-

view sequences. This failure is not caused by a single weak model: the OOD curve averages over the full evaluated method pool, indicating a field-level limitation. The training-data analysis explains this behavior. Current pre-training mixtures heavily cover standard indoor and outdoor reconstruction data, but real robot wrist-view data is systematically absent, and real egocentric coverage is sparse.

To address this gap, DA-Next is trained on DA-Next-5M, which explicitly incorporates egocentric and wrist-view data into the training mixture. As shown in Tab. 1, DA-Next achieves consistent and substantial improvements over DA3-Giant across depth and camera pose metrics: depth AbsRel improves by 47% from 0.095 to 0.050 on sparse inputs and 59% from 0.086 to 0.035 on medium inputs, while AUC@30 improves by +3.1% and +5.5% respectively. These gains confirm that targeted in-domain data curation is an effective and practical strategy for closing the OOD gap.

Takeaway: *The largest remaining data gap is domain diversity, not only data volume: ego-view and wrist-view data are underrepresented in current training mixtures and produce the strongest OOD failures on SpatialBench. DA-Next, trained on DA-Next-5M, directly addresses this gap.*

Is Test-Time Training a Free Lunch?

Tab. 2 contrasts three pairs of feed-forward 3D foundation models with their test-time training (TTT) descendants: CUT3R [98] / TTT3R [16], VGGT [94] / Scal3R [113], and Pi3 [101] / LoGeR [126] across *Sparse*, *Medium*, and *Dense*, summarized by aggregate camera-pose AUC@30 (\uparrow) and global trajectory ATE (\downarrow). Specifically, the TTT methods are designed to digest sequences longer than the context their base models were trained on. For example, Scal3R inserts chunk-wise Global Context Memory into VGGT, and LoGeR aug-

ments Pi3 with a parametric TTT memory plus sliding-window attention. Therefore, the natural prior is that TTT should pay off most when sequences are long, and least when they are short and discontinuous. The *Dense* block confirms this expectation. TTT3R nearly doubles AUC@30 (0.165 \rightarrow 0.321, +95%) and cuts ATE by 17.5%; LoGeR lifts AUC@30 by 14.1% and reduces ATE by 72% over Pi3; Scal3R is the *only* VGGT-family model that runs at all, since vanilla VGGT OOMs under thousand-frame inputs. In the *Medium* setting, inputs contain a mix of short and moderately long segments, which limits the benefit of TTT. Gains become inconsistent across metrics: AUC@30 improves only for TTT3R (+5.1%) while regressing for Scal3R (-2.5%) and LoGeR (-4.7%); ATE narrows for TTT3R (-12.7%) and Scal3R (-45.2%) but stays flat for LoGeR (0.57 \rightarrow 0.57). In the *Sparse* setting, inputs consist of only 4–15 frames with large baselines and limited temporal continuity, making it difficult for TTT methods to perform effective test-time updates. As a result, the end-to-end base models outperform their TTT counterparts on AUC@30 in two of the three pairs, with only Scal3R holding even (+4.7%).

Takeaway: *TTT’s gains are concentrated on dense long sequences, where it consistently improves both pairwise camera pose accuracy and global trajectory consistency over the base models, which confirms*

Table 2 | **TTT vs. Base model across input length regimes.** For each (Base model, TTT) pair, we report aggregate camera-pose AUC@30 (\uparrow) and global trajectory ATE (\downarrow), formatted as *base* \rightarrow *TTT*. **Green** marks improvement, **red** marks regression. \dagger Vanilla VGGT OOMs under *Dense*.

Regime	Pair	AUC@30 \uparrow	ATE \downarrow
Sparse	CUT3R / TTT3R	0.519 \rightarrow 0.470	—
	VGGT / Scal3R	0.700 \rightarrow 0.732	—
	Pi3 / LoGeR	0.742 \rightarrow 0.708	—
Medium	CUT3R / TTT3R	0.469 \rightarrow 0.493	2.68 \rightarrow 2.34
	VGGT / Scal3R	0.687 \rightarrow 0.670	0.73 \rightarrow 0.40
	Pi3 / LoGeR	0.749 \rightarrow 0.714	0.57 \rightarrow 0.57
Dense	CUT3R / TTT3R	0.165 \rightarrow 0.321	25.5 \rightarrow 21.1
	VGGT † / Scal3R	N/A \rightarrow 0.480	N/A \rightarrow 2.40
	Pi3 / LoGeR	0.524 \rightarrow 0.598	16.4 \rightarrow 4.60

Table 3 | **Effect of GT Priors across Sparse / Medium.** We inject ground-truth depth and/or camera (pose + intrinsic) priors for each prior-aware model. Trajectory and point-cloud metrics are not reported for the sparse regime.

Method	Aux. Prior		Depth						Camera						Trajectory		PointCloud			
	Depth	Camera	AbsRel \downarrow	SqRel \downarrow	RMSE \downarrow	$\delta_{1.05}\uparrow$	$\delta_{1.10}\uparrow$	$\delta_{1.10}\uparrow$	RAcc \uparrow	RAcc \uparrow	TAcc \uparrow	TAcc \uparrow	AUC@5 \uparrow	AUC@15 \uparrow	AUC@30 \uparrow	ATE \downarrow	RPE \downarrow	RPE \downarrow	F-Score \uparrow	Overall \downarrow
Sparse																				
DA3-Giant	\times	\times	0.095	0.107	0.608	0.563	0.689	0.821	0.791	0.870	0.587	0.682	0.525	0.699	0.785	-	-	-	-	-
	\times	\checkmark	0.078	0.100	0.586	0.635	0.749	0.859	0.968	0.981	0.965	0.989	0.918	0.969	0.984	-	-	-	-	-
MapAnything	\times	\times	0.153	1.079	1.337	0.361	0.512	0.701	0.608	0.762	0.300	0.423	0.244	0.446	0.579	-	-	-	-	-
	\checkmark	\times	0.029	0.048	0.415	0.726	0.845	0.940	0.651	0.783	0.404	0.507	0.317	0.547	0.674	-	-	-	-	-
	\times	\checkmark	0.143	1.172	1.192	0.427	0.580	0.755	1.000	1.000	0.779	0.894	0.741	0.883	0.934	-	-	-	-	-
	\checkmark	\checkmark	0.020	0.040	0.368	0.861	0.906	0.949	1.000	1.000	0.956	0.981	0.913	0.966	0.982	-	-	-	-	-
OmniVGGT	\times	\times	0.117	0.119	0.669	0.534	0.671	0.810	0.620	0.746	0.416	0.507	0.332	0.537	0.665	-	-	-	-	-
	\checkmark	\times	0.023	0.061	0.479	0.840	0.913	0.963	0.613	0.723	0.385	0.479	0.313	0.505	0.631	-	-	-	-	-
	\times	\checkmark	0.115	0.117	0.665	0.545	0.680	0.814	0.896	0.953	0.819	0.896	0.697	0.858	0.921	-	-	-	-	-
	\checkmark	\checkmark	0.021	0.044	0.427	0.850	0.919	0.969	0.907	0.959	0.833	0.917	0.715	0.876	0.934	-	-	-	-	-
π^3 -X	\times	\times	0.084	0.084	0.599	0.576	0.710	0.833	0.756	0.837	0.491	0.595	0.427	0.627	0.741	-	-	-	-	-
	\checkmark	\times	0.009	0.017	0.255	0.959	0.979	0.992	0.787	0.860	0.540	0.645	0.476	0.667	0.769	-	-	-	-	-
	\times	\checkmark	0.080	0.082	0.589	0.640	0.757	0.858	0.936	0.979	0.715	0.834	0.636	0.827	0.901	-	-	-	-	-
	\checkmark	\checkmark	0.009	0.017	0.255	0.960	0.980	0.992	0.940	0.981	0.758	0.848	0.679	0.843	0.908	-	-	-	-	-
WorldMirror	\times	\times	0.139	0.165	0.803	0.443	0.585	0.747	0.701	0.796	0.400	0.507	0.328	0.537	0.666	-	-	-	-	-
	\checkmark	\times	0.081	0.243	0.933	0.510	0.643	0.789	0.695	0.808	0.377	0.507	0.329	0.544	0.672	-	-	-	-	-
	\times	\checkmark	0.127	0.158	0.759	0.559	0.688	0.811	0.812	0.899	0.629	0.762	0.534	0.762	0.863	-	-	-	-	-
	\checkmark	\checkmark	0.058	0.282	0.945	0.674	0.772	0.868	0.826	0.911	0.620	0.753	0.533	0.764	0.864	-	-	-	-	-
Medium																				
DA3-Giant	\times	\times	0.086	0.088	0.578	0.572	0.686	0.812	0.750	0.834	0.587	0.663	0.532	0.684	0.776	1.161	0.284	2.275	0.742	0.073
	\times	\checkmark	0.078	0.111	0.579	0.644	0.756	0.862	0.984	0.992	0.970	0.987	0.951	0.978	0.987	0.000	0.000	0.002	0.772	0.062
MapAnything	\times	\times	0.146	0.490	1.052	0.347	0.491	0.681	0.563	0.702	0.312	0.419	0.254	0.451	0.579	1.737	0.533	2.852	0.420	0.114
	\checkmark	\times	0.032	0.037	0.380	0.683	0.811	0.933	0.597	0.733	0.393	0.499	0.316	0.529	0.664	2.053	0.512	2.521	0.539	0.086
	\times	\checkmark	0.126	0.225	0.893	0.429	0.567	0.737	0.998	1.000	0.786	0.881	0.740	0.879	0.930	0.051	0.029	0.270	0.521	0.108
	\checkmark	\checkmark	0.019	0.034	0.356	0.857	0.910	0.955	1.000	1.000	0.940	0.969	0.896	0.953	0.972	0.042	0.023	0.216	0.773	0.056
OmniVGGT	\times	\times	0.111	0.096	0.649	0.518	0.645	0.780	0.609	0.726	0.426	0.527	0.340	0.542	0.665	1.491	0.355	2.768	0.595	0.104
	\checkmark	\times	0.023	0.056	0.454	0.838	0.914	0.966	0.602	0.727	0.418	0.520	0.325	0.531	0.663	1.904	0.404	2.949	0.582	0.094
	\times	\checkmark	0.108	0.106	0.668	0.521	0.650	0.786	0.870	0.936	0.792	0.878	0.664	0.834	0.905	0.513	0.111	0.589	0.673	0.073
	\checkmark	\checkmark	0.023	0.064	0.479	0.839	0.910	0.961	0.870	0.930	0.804	0.895	0.671	0.843	0.910	0.639	0.133	0.576	0.693	0.068
π^3 -X	\times	\times	0.078	0.061	0.538	0.582	0.712	0.831	0.741	0.827	0.536	0.628	0.463	0.644	0.744	0.369	0.108	1.459	0.658	0.074
	\checkmark	\times	0.008	0.013	0.239	0.969	0.984	0.993	0.761	0.844	0.547	0.638	0.478	0.659	0.763	0.478	0.129	1.277	0.667	0.074
	\times	\checkmark	0.070	0.060	0.536	0.652	0.759	0.856	0.912	0.960	0.721	0.827	0.641	0.818	0.889	0.373	0.075	0.453	0.703	0.067
	\checkmark	\checkmark	0.008	0.013	0.238	0.969	0.984	0.993	0.914	0.958	0.747	0.840	0.677	0.829	0.890	0.112	0.040	0.461	0.748	0.057
WorldMirror	\times	\times	0.118	0.129	0.745	0.446	0.574	0.721	0.676	0.777	0.419	0.535	0.354	0.557	0.674	1.356	0.342	2.046	0.576	0.090
	\checkmark	\times	0.082	0.132	0.726	0.512	0.638	0.782	0.694	0.797	0.420	0.540	0.354	0.564	0.685	1.797	0.479	1.974	0.643	0.073
	\times	\checkmark	0.101	0.117	0.700	0.572	0.682	0.790	0.766	0.863	0.621	0.744	0.528	0.740	0.838	0.276	0.093	0.937	0.664	0.077
	\checkmark	\checkmark	0.057	0.126	0.688	0.668	0.755	0.851	0.793	0.872	0.633	0.754	0.542	0.752	0.845	0.313	0.107	0.894	0.755	0.058

that TTT is engineered as a length-generalization mechanism rather than as a universal free lunch.

Can Injecting GT Priors Drive Performance to a Perfect Level?

Tab. 3 presents an ablation study on the effect of injecting ground-truth depth and camera pose priors for five prior-aware models (DA3-Giant, MapAnything, OmniVGGT, π^3 -X, and WorldMirror) across sparse and medium input settings, evaluated on depth, camera, trajectory, and point cloud metrics. All prior-aware models benefit from depth prior injection to varying degrees, with depth metrics approaching near-GT-level accuracy across the board. However, the effect of camera pose priors is more nuanced. DA3-Giant and MapAnything exhibit strong prior adherence: injecting GT camera poses leads to highly consistent pose predictions, with AUC@15 maintained above 90% under all settings. In contrast, OmniVGGT, π^3 -X, and WorldMirror show moderate improvements but fail to fully conform to the injected camera poses under challenging conditions (see Fig. 19 in Appendix. B.6), partially overriding them with their own predictions.

Takeaway: *Injecting GT depth priors consistently drives depth estimation to near-perfect accuracy, yet camera pose priors yield inconsistent gains. Some models partially override the injected poses with their own predictions and fail under challenging conditions.*

Fig. 10 presents a qualitative comparison against representative baselines, where DA-Next

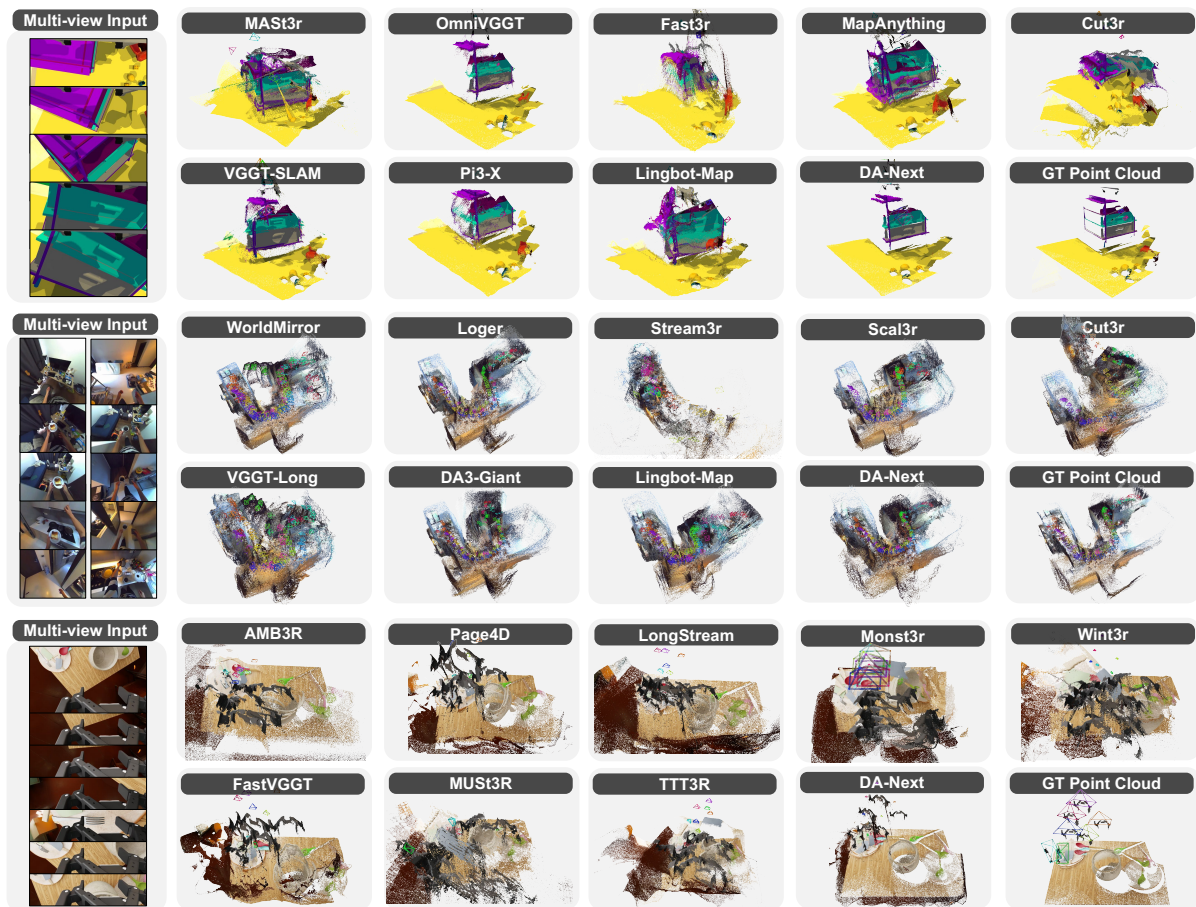


Figure 10 | Qualitative comparison of multi-view 3D reconstruction on SpatialBench.

yields a more accurate camera trajectory and sharper geometry under challenging viewpoints. Due to space limitations, we provide additional visualizations in Appendix B.6 and findings in Appendix E.

6. Conclusion

We presented SpatialBench, a comprehensive, reproducible, and cross-paradigm benchmark for evaluating spatial foundation models across diverse domains, input densities, and reconstruction task suites. Through extensive experiments on 41 models across 6 paradigms, SpatialBench reveals that current spatial foundation models are not yet all-round players, exposing critical gaps in domain generalization, input-density robustness. To address the most significant data gap identified, we introduced DA-Next-5M, a large-scale egocentric and wrist-view dataset, and trained DA-Next as a strong baseline. We hope SpatialBench serves as a rigorous foundation for future research toward more generalizable and robust 3D foundation models.

References

- [1] Manuel López Antequera, Pau Gargallo, Markus Hofinger, Samuel Rota Bulo, Yubin Kuang, and Peter Kotschieder. 2020. Mapillary planet-scale depth dataset. In *European Conference on Computer Vision*, pages 589–604. Springer.
- [2] Eduardo Arnold, Jamie Wynn, Sara Vicente, Guillermo Garcia-Hernando, Áron Monzpart, Victor Prisacariu, Daniyar Turmukhambetov, and Eric Brachmann. 2022. [Map-free visual relocalization: Metric pose relative to a single image](#). In *Computer Vision - ECCV 2022 - 17th European Conference, Tel Aviv, Israel, October 23-27, 2022, Proceedings, Part I*, volume 13661 of *Lecture Notes in Computer Science*, pages 690–708. Springer.
- [3] Armen Avetisyan, Christopher Xie, Henry Howard-Jenkins, Tsun-Yi Yang, Samir Aroudj, Suvam Patra, Fuyang Zhang, Duncan Frost, Luke Holland, Campbell Orme, and 1 others. 2024. Scenescript: Reconstructing scenes with an autoregressive structured language model. In *European Conference on Computer Vision*, pages 247–263. Springer.
- [4] Dejan Azinović, Ricardo Martin-Brualla, Dan B Goldman, Matthias Nießner, and Justus Thies. 2022. Neural rgb-d surface reconstruction. In *Proceedings of the IEEE/CVF conference on computer vision and pattern recognition*, pages 6290–6301.
- [5] Gilad Baruch, Zhuoyuan Chen, Afshin Dehghan, Tal Dimry, Yuri Feigin, Peter Fu, Thomas Gebauer, Brandon Joffe, Daniel Kurz, Arik Schwartz, and 1 others. 2021. Arkitscenes: A diverse real-world dataset for 3d indoor scene understanding using mobile rgb-d data. *arXiv preprint arXiv:2111.08897*.
- [6] Zuria Bauer, Francisco Gomez-Donoso, Edmanuel Cruz, Sergio Orts-Escolano, and Miguel Cazorla. 2019. Uasol, a large-scale high-resolution outdoor stereo dataset. *Scientific data*, 6(1):162.
- [7] Michael J Black, Priyanka Patel, Joachim Tesch, and Jinlong Yang. 2023. Bedlam: A synthetic dataset of bodies exhibiting detailed lifelike animated motion. In *Proceedings of the IEEE/CVF Conference on Computer Vision and Pattern Recognition*, pages 8726–8737.
- [8] Yohann Cabon, Naila Murray, and Martin Humenberger. 2020. [Virtual KITTI 2](#). *CoRR*, abs/2001.10773.
- [9] Yohann Cabon, Lucas Stoffl, Leonid Antsfeld, Gabriela Csurka, Boris Chidlovskii, Jerome Revaud, and Vincent Leroy. 2025. Must3r: Multi-view network for stereo 3d reconstruction. In *Proceedings of the IEEE/CVF Conference on Computer Vision and Pattern Recognition*, pages 1050–1060.
- [10] Nicolas Carion, Laura Gustafson, Yuan-Ting Hu, Shoubhik Debnath, Ronghang Hu, Didac Suris, Chaitanya Ryali, Kalyan Vasudev Alwala, Haitham Khedr, Andrew Huang, Jie Lei, Tengyu Ma, Baishan Guo, Arpit Kalla, Markus Marks, Joseph Greer, Meng Wang, Peize Sun, Roman Rädle, and 19 others. 2025. [Sam 3: Segment anything with concepts](#). *Preprint*, arXiv:2511.16719.
- [11] Angel Chang, Angela Dai, Thomas Funkhouser, Maciej Halber, Matthias Niessner, Manolis Savva, Shuran Song, Andy Zeng, and Yinda Zhang. 2017. Matterport3d: Learning from rgb-d data in indoor environments. *arXiv preprint arXiv:1709.06158*.
- [12] Ming-Fang Chang, John Lambert, Patsorn Sangkloy, Jagjeet Singh, Slawomir Bak, Andrew Hartnett, De Wang, Peter Carr, Simon Lucey, Deva Ramanan, and 1 others. 2019. Argoverse: 3d tracking and forecasting with rich maps. In *Proceedings of the IEEE/CVF conference on computer vision and pattern recognition*, pages 8748–8757.
- [13] Lin-Zhuo Chen, Jian Gao, Yihang Chen, Ka Leong Cheng, Yipengjing Sun, Liangxiao Hu, Nan Xue, Xing Zhu, Yujun Shen, Yao Yao, and Yinghao Xu. 2026. Geometric context transformer for streaming 3d reconstruction. *arXiv preprint arXiv:2604.14141*.
- [14] Tianxing Chen, Zanzin Chen, Baijun Chen, Zijian Cai, Yibin Liu, Zixuan Li, Qiwei Liang, Xianliang Lin, Yiheng Ge, Zhenyu Gu, and 1 others. 2025. Robotwin 2.0: A scalable data generator and benchmark with strong domain randomization for robust bimanual robotic manipulation. *arXiv preprint arXiv:2506.18088*.
- [15] Xiaoxue Chen, Ziyi Xiong, Yuantao Chen, Gen Li, Nan Wang, Hongcheng Luo, Long Chen, Haiyang Sun, Bing Wang, Guang Chen, and 1 others. 2025. Dggt: Feedforward 4d reconstruction of dynamic driving scenes using unposed images. *arXiv preprint arXiv:2512.03004*.
- [16] Xingyu Chen, Yue Chen, Yuliang Xiu, Andreas Geiger, and Anpei Chen. 2025. Ttt3r: 3d reconstruction as test-time training. *arXiv preprint arXiv:2509.26645*.
- [17] Chong Cheng, Xianda Chen, Tao Xie, Wei Yin, Weiqiang Ren, Qian Zhang, Xiaoyang Guo, and Hao Wang. 2026. [Longstream: Long-sequence streaming autoregressive visual geometry](#). *Preprint*, arXiv:2602.13172.
- [18] Jaehoon Cho, Dongbo Min, Youngjung Kim, and Kwanghoon Sohn. 2021. Diml/cvl rgb-d dataset: 2m rgb-d images of natural indoor and outdoor scenes. *arXiv preprint arXiv:2110.11590*.

- [19] Wenyan Cong, Yiqing Liang, Yancheng Zhang, Ziyi Yang, Yan Wang, Boris Ivanovic, Marco Pavone, Chen Chen, Zhangyang Wang, and Zhiwen Fan. 2025. E3d-bench: A benchmark for end-to-end 3d geometric foundation models. *arXiv preprint arXiv:2506.01933*.
- [20] Marius Cordts, Mohamed Omran, Sebastian Ramos, Timo Rehfeld, Markus Enzweiler, Rodrigo Benenson, Uwe Franke, Stefan Roth, and Bernt Schiele. 2016. The cityscapes dataset for semantic urban scene understanding. In *Proceedings of the IEEE conference on computer vision and pattern recognition*, pages 3213–3223.
- [21] Angela Dai, Angel X. Chang, Manolis Savva, Maciej Halber, Thomas A. Funkhouser, and Matthias Nießner. 2017. *Scannet: Richly-annotated 3d reconstructions of indoor scenes*. In *2017 IEEE Conference on Computer Vision and Pattern Recognition, CVPR 2017, Honolulu, HI, USA, July 21-26, 2017*, pages 2432–2443. IEEE Computer Society.
- [22] Matt Deitke, Dustin Schwenk, Jordi Salvador, Luca Weihs, Oscar Michel, Eli VanderBilt, Ludwig Schmidt, Kiana Ehsani, Aniruddha Kembhavi, and Ali Farhadi. 2023. Objaverse: A universe of annotated 3d objects. In *Proceedings of the IEEE/CVF conference on computer vision and pattern recognition*, pages 13142–13153.
- [23] Kai Deng, Zexin Ti, Jiawei Xu, Jian Yang, and Jin Xie. 2025. *Vggt-long: Chunk it, loop it, align it – pushing vggt’s limits on kilometer-scale long rgb sequences*. *Preprint*, arXiv:2507.16443.
- [24] Michael Fonder and Marc Van Droogenbroeck. 2019. Mid-air: A multi-modal dataset for extremely low altitude drone flights. In *Proceedings of the IEEE/CVF conference on computer vision and pattern recognition workshops*, pages 0–0.
- [25] Mathias Gehrig, Willem Aarents, Daniel Gehrig, and Davide Scaramuzza. 2021. Dsec: A stereo event camera dataset for driving scenarios. *IEEE Robotics and Automation Letters*, 6(3):4947–4954.
- [26] Andreas Geiger, Philip Lenz, and Raquel Urtasun. 2012. Are we ready for autonomous driving? the kitti vision benchmark suite. In *2012 IEEE conference on computer vision and pattern recognition*, pages 3354–3361. IEEE.
- [27] Yotam Gil, Shay Elmaleh, Harel Haim, Emanuel Marom, and Raja Giryes. 2021. Online training of stereo self-calibration using monocular depth estimation. *IEEE Transactions on Computational Imaging*, 7:812–823.
- [28] Jose L Gómez, Manuel Silva, Antonio Seoane, Agnès Borrás, Mario Noriega, Germán Ros, Jose A Iglesias-Guitian, and Antonio M López. 2025. All for one, and one for all: Urbansyn dataset, the third musketeer of synthetic driving scenes. *Neurocomputing*, 637:130038.
- [29] Klaus Greff, Francois Belletti, Lucas Beyer, Carl Doersch, Yilun Du, Daniel Duckworth, David J Fleet, Dan Gnanapragasam, Florian Golemo, Charles Herrmann, and 1 others. 2022. Kubric: A scalable dataset generator. In *Proceedings of the IEEE/CVF conference on computer vision and pattern recognition*, pages 3749–3761.
- [30] Vitor Guizilini, Rares Ambrus, Sudeep Pillai, Allan Raventos, and Adrien Gaidon. 2020. 3d packing for self-supervised monocular depth estimation. In *Proceedings of the IEEE/CVF conference on computer vision and pattern recognition*, pages 2485–2494.
- [31] John Houston, Guido Zuidhof, Luca Bergamini, Yawei Ye, Long Chen, Ashesh Jain, Sammy Omari, Vladimir Igloukov, and Peter Ondruska. 2021. One thousand and one hours: Self-driving motion prediction dataset. In *Conference on Robot Learning*, pages 409–418. PMLR.
- [32] Yuan-Ting Hu, Jiahong Wang, Raymond A Yeh, and Alexander G Schwing. 2021. Sail-vos 3d: A synthetic dataset and baselines for object detection and 3d mesh reconstruction from video data. In *Proceedings of the IEEE/CVF Conference on Computer Vision and Pattern Recognition*, pages 1418–1428.
- [33] Jiahui Huang, Qunjie Zhou, Hesam Rabeti, Aleksandr Korovko, Huan Ling, Xuanchi Ren, Tianchang Shen, Jun Gao, Dmitry Slepichev, Chen-Hsuan Lin, Jiawei Ren, Kevin Xie, Joydeep Biswas, Laura Leal-Taixe, and Sanja Fidler. 2025. Vipe: Video pose engine for 3d geometric perception. In *NVIDIA Research Whitepapers arXiv:2508.10934*.
- [34] Po-Han Huang, Kevin Matzen, Johannes Kopf, Narendra Ahuja, and Jia-Bin Huang. 2018. *Deepmvs: Learning multi-view stereopsis*. In *2018 IEEE Conference on Computer Vision and Pattern Recognition, CVPR 2018, Salt Lake City, UT, USA, June 18-22, 2018*, pages 2821–2830. Computer Vision Foundation / IEEE Computer Society.
- [35] Physical Intelligence, Kevin Black, Noah Brown, James Darpinian, Karan Dhabalia, Danny Driess, Adnan Esmail, Michael Equi, Chelsea Finn, Niccolo Fusai, and 1 others. 2025. $\pi_{0.5}$: A vision-language-action model with open-world generalization. *arXiv preprint arXiv:2504.16054*.
- [36] Stephen James, Zicong Ma, David Rovick Arrojo, and Andrew J Davison. 2020. Rlbench: The robot learning benchmark & learning environment. *IEEE Robotics and Automation Letters*, 5(2):3019–3026.
- [37] Rasmus Jensen, Anders Dahl, George Vogiatzis, Engin Tola, and Henrik Aanæs. 2014. Large scale multi-view stereopsis evaluation. In *Proceedings of the IEEE conference on computer vision and pattern recognition*, pages 406–413.

- [38] Hanwen Jiang, Zexiang Xu, Desai Xie, Ziwen Chen, Haian Jin, Fujun Luan, Zhixin Shu, Kai Zhang, Sai Bi, Xin Sun, and 1 others. 2025. Megasynt: Scaling up 3d scene reconstruction with synthesized data. In *Proceedings of the Computer Vision and Pattern Recognition Conference*, pages 16441–16452.
- [39] Haian Jin, Rundi Wu, Tianyuan Zhang, Ruiqi Gao, Jonathan T. Barron, Noah Snavely, and Aleksander Holynski. 2026. ZipMap: Linear-time stateful 3d reconstruction via test-time training. In *Proceedings of the IEEE/CVF Conference on Computer Vision and Pattern Recognition*.
- [40] Nikita Karaev, Ignacio Rocco, Benjamin Graham, Natalia Neverova, Andrea Vedaldi, and Christian Rupprecht. 2023. Dynamicstereo: Consistent dynamic depth from stereo videos. In *Proceedings of the IEEE/CVF Conference on Computer Vision and Pattern Recognition (CVPR)*, pages 13229–13239.
- [41] Simar Kareer, Dhruv Patel, Ryan Punamiya, Pranay Mathur, Shuo Cheng, Chen Wang, Judy Hoffman, and Danfei Xu. 2025. Egomimic: Scaling imitation learning via egocentric video. In *2025 IEEE International Conference on Robotics and Automation (ICRA)*, pages 13226–13233. IEEE.
- [42] Nikhil Keetha, Norman Müller, Johannes Schönberger, Lorenzo Porzi, Yuchen Zhang, Tobias Fischer, Arno Knapitsch, Duncan Zauss, Ethan Weber, Nelson Antunes, Jonathon Luiten, Manuel Lopez-Antequera, Samuel Rota Bulò, Christian Richardt, Deva Ramanan, Sebastian Scherer, and Peter Kotschieder. 2026. MapAnything: Universal feed-forward metric 3D reconstruction. In *International Conference on 3D Vision (3DV)*. IEEE.
- [43] Alexander Khazatsky, Karl Pertsch, Suraj Nair, Ashwin Balakrishna, Sudeep Dasari, Siddharth Karamcheti, Soroush Nasiriany, Mohan Kumar Srirama, Lawrence Yunliang Chen, Kirsty Ellis, and 1 others. 2024. Droid: A large-scale in-the-wild robot manipulation dataset. *arXiv preprint arXiv:2403.12945*.
- [44] Arno Knapitsch, Jaesik Park, Qian-Yi Zhou, and Vladlen Koltun. 2017. Tanks and temples: Benchmarking large-scale scene reconstruction. *ACM Transactions on Graphics*, 36(4).
- [45] Anastasiia Kornilova, Marsel Faizullin, Konstantin Pakulev, Andrey Sadkov, Denis Kukushkin, Azat Akhmetyanov, Timur Akhtyamov, Hekmat Taherinejad, and Gonzalo Ferrer. 2022. Smartportraits: Depth powered handheld smartphone dataset of human portraits for state estimation, reconstruction and synthesis. In *Proceedings of the IEEE/CVF Conference on Computer Vision and Pattern Recognition*, pages 21318–21329.
- [46] Yushi Lan, Yihang Luo, Fangzhou Hong, Shangchen Zhou, Honghua Chen, Zhaoyang Lyu, Shuai Yang, Bo Dai, Chen Change Loy, and Xingang Pan. 2026. SStream3R: Scalable sequential 3D reconstruction with causal transformer. In *ICLR*.
- [47] Hoang-An Le, Thomas Mensink, Partha Das, Sezer Karaoglu, and Theo Gevers. 2021. Eden: Multimodal synthetic dataset of enclosed garden scenes. In *Proceedings of the IEEE/CVF Winter Conference on Applications of Computer Vision*, pages 1579–1589.
- [48] Vincent Leroy, Yohann Cabon, and Jérôme Revaud. 2024. [Grounding image matching in 3d with mast3r](#). In *Computer Vision - ECCV 2024 - 18th European Conference, Milan, Italy, September 29–October 4, 2024, Proceedings, Part LXXII*, volume 15130 of *Lecture Notes in Computer Science*, pages 71–91. Springer.
- [49] Yixuan Li, Lihan Jiang, Linning Xu, Yuanbo Xiangli, Zhenzhi Wang, Dahua Lin, and Bo Dai. 2023. Matrixcity: A large-scale city dataset for city-scale neural rendering and beyond. In *Proceedings of the IEEE/CVF International Conference on Computer Vision*, pages 3205–3215.
- [50] Zhengqi Li and Noah Snavely. 2018. Megadepth: Learning single-view depth prediction from internet photos. In *Proceedings of the IEEE conference on computer vision and pattern recognition*, pages 2041–2050.
- [51] Zhengqi Li, Richard Tucker, Forrester Cole, Qianqian Wang, Linyi Jin, Vickie Ye, Angjoo Kanazawa, Aleksander Holynski, and Noah Snavely. 2025. MegaSaM: Accurate, Fast and Robust Structure and Motion from Casual Dynamic Videos. In *Proceedings of the IEEE/CVF Conference on Computer Vision and Pattern Recognition*.
- [52] Zizun Li, Jianjun Zhou, Yifan Wang, Haoyu Guo, Wenzheng Chang, Yang Zhou, Haoyi Zhu, Junyi Chen, Chunhua Shen, and Tong He. 2025. [Wint3r: Window-based streaming reconstruction with camera token pool](#). *Preprint*, arXiv:2509.05296.
- [53] Yiyi Liao, Jun Xie, and Andreas Geiger. 2022. Kitti-360: A novel dataset and benchmarks for urban scene understanding in 2d and 3d. *IEEE Transactions on Pattern Analysis and Machine Intelligence*, 45(3):3292–3310.
- [54] Haotong Lin, Sili Chen, Junhao Liew, Donny Y Chen, Zhenyu Li, Guang Shi, Jiashi Feng, and Bingyi Kang. 2025. Depth anything 3: Recovering the visual space from any views. *arXiv preprint arXiv:2511.10647*.
- [55] Haotong Lin, Sida Peng, Jingxiao Chen, Songyou Peng, Jiaming Sun, Minghuan Liu, Hujun Bao, Jiashi Feng, Xiaowei Zhou, and Bingyi Kang. 2025. Prompting depth anything for 4k resolution accurate metric depth estimation. In *Proceedings of the Computer Vision and Pattern Recognition Conference*, pages 17070–17080.

- [56] Tao Lin, Gen Li, Yilei Zhong, Yanwen Zou, Yuxin Du, Jiting Liu, Encheng Gu, and Bo Zhao. 2025. Evo-0: Vision-language-action model with implicit spatial understanding. *arXiv preprint arXiv:2507.00416*.
- [57] Lu Ling, Yichen Sheng, Zhi Tu, Wentian Zhao, Cheng Xin, Kun Wan, Lantao Yu, Qianyu Guo, Zixun Yu, Yawen Lu, and 1 others. 2024. D13dv-10k: A large-scale scene dataset for deep learning-based 3d vision. In *Proceedings of the IEEE/CVF Conference on Computer Vision and Pattern Recognition*, pages 22160–22169.
- [58] Minghuan Liu, Zhengbang Zhu, Xiaoshen Han, Peng Hu, Haotong Lin, Xinyao Li, Jingxiao Chen, Jiafeng Xu, Yichu Yang, Yunfeng Lin, Xinghang Li, Yong Yu, Weinan Zhang, Tao Kong, and Bingyi Kang. 2025. Manipulation as in simulation: Enabling accurate geometry perception in robots. *arXiv preprint*.
- [59] Yifan Liu, Zhiyuan Min, Zhenwei Wang, Junta Wu, Tengfei Wang, Yixuan Yuan, Yawei Luo, and Chunchao Guo. 2025. Worldmirror: Universal 3d world reconstruction with any-prior prompting. *arXiv preprint arXiv:2510.10726*.
- [60] Yunze Liu, Yun Liu, Che Jiang, Kangbo Lyu, Weikang Wan, Hao Shen, Boqiang Liang, Zhoujie Fu, He Wang, and Li Yi. 2022. Hoi4d: A 4d egocentric dataset for category-level human-object interaction. In *Proceedings of the IEEE/CVF Conference on Computer Vision and Pattern Recognition*, pages 21013–21022.
- [61] Dominic Maggio and Luca Carlone. 2026. Vggt-slam 2.0: Real-time dense feed-forward scene reconstruction. *arXiv preprint arXiv:2601.19887*.
- [62] Dominic Maggio, Hyungtae Lim, and Luca Carlone. 2025. Vggt-slam: Dense rgb slam optimized on the sl (4) manifold. *Advances in Neural Information Processing Systems*, 39.
- [63] John McCormac, Ankur Handa, Stefan Leutenegger, and Andrew J Davison. 2016. Scenenet rgb-d: 5m photorealistic images of synthetic indoor trajectories with ground truth. *arXiv preprint arXiv:1612.05079*.
- [64] Lukas Mehl, Jenny Schmalfluss, Azin Jahedi, Yaroslava Nalivayko, and Andrés Bruhn. 2023. Spring: A high-resolution high-detail dataset and benchmark for scene flow, optical flow and stereo. In *Proceedings of the IEEE/CVF Conference on Computer Vision and Pattern Recognition*, pages 4981–4991.
- [65] Junhong Min, Youngpil Jeon, Jimin Kim, and Minyong Choi. 2025. S²M²: Scalable stereo matching model for reliable depth estimation. In *Proceedings of the IEEE/CVF International Conference on Computer Vision (ICCV)*.
- [66] Riku Murai, Eric Dexheimer, and Andrew J. Davison. 2025. MAST3R-SLAM: Real-time dense SLAM with 3D reconstruction priors. In *Proceedings of the IEEE/CVF Conference on Computer Vision and Pattern Recognition*.
- [67] Simon Niklaus, Long Mai, Jimei Yang, and Feng Liu. 2019. 3d ken burns effect from a single image. *ACM Transactions on Graphics (ToG)*, 38(6):1–15.
- [68] Maxime Oquab, Timothée Darcet, Théo Moutakanni, Huy V. Vo, Marc Szafraniec, Vasil Khalidov, Pierre Fernandez, Daniel Haziza, Francisco Massa, Alaaeldin El-Nouby, Mido Assran, Nicolas Ballas, Wojciech Galuba, Russell Howes, Po-Yao Huang, Shang-Wen Li, Ishan Misra, Michael Rabbat, Vasu Sharma, and 7 others. 2024. **Dinov2: Learning robust visual features without supervision**. *Trans. Mach. Learn. Res.*, 2024.
- [69] Xiaqing Pan, Nicholas Charron, Yongqian Yang, Scott Peters, Thomas Whelan, Chen Kong, Omkar Parkhi, Richard Newcombe, and Yuheng Carl Ren. 2023. Aria digital twin: A new benchmark dataset for egocentric 3d machine perception. In *Proceedings of the IEEE/CVF International Conference on Computer Vision*, pages 20133–20143.
- [70] Manthan Patel, Fan Yang, Yuheng Qiu, Cesar Cadena, Sebastian Scherer, Marco Hutter, and Wenshan Wang. 2025. Tartanground: A large-scale dataset for ground robot perception and navigation. In *2025 IEEE/RSJ International Conference on Intelligent Robots and Systems (IROS)*, pages 20524–20531. IEEE.
- [71] Haosong Peng, Hao Li, Yalun Dai, Yushi Lan, Yihang Luo, Tianyu Qi, Zhengshen Zhang, Yufeng Zhan, Junfei Zhang, Wenchao Xu, and 1 others. 2025. Omnivggt: Omni-modality driven visual geometry grounded transformer. *arXiv preprint arXiv:2511.10560*.
- [72] Wilbert Pumacay, Ishika Singh, Jiafei Duan, Ranjay Krishna, Jesse Thomason, and Dieter Fox. 2024. The colosseum: A benchmark for evaluating generalization for robotic manipulation. *arXiv preprint arXiv:2402.08191*.
- [73] Alexander Raistrick, Lingjie Mei, Karhan Kayan, David Yan, Yiming Zuo, Beining Han, Hongyu Wen, Meenal Parakh, Stamatis Alexandropoulos, Lahav Lipson, and 1 others. 2024. Infinigen indoors: Photorealistic indoor scenes using procedural generation. In *Proceedings of the IEEE/CVF Conference on Computer Vision and Pattern Recognition*, pages 21783–21794.
- [74] Santhosh K. Ramakrishnan, Aaron Gokaslan, Erik Wijmans, Oleksandr Maksymets, Alexander Clegg, John M. Turner, Eric Undersander, Wojciech Galuba, Andrew Westbury, Angel X. Chang, Manolis Savva, Yili Zhao, and Dhruv Batra. 2021. **Habitat-matterport 3d dataset (HM3D): 1000 large-scale 3d environments for embodied AI**. *CoRR*, abs/2109.08238.

- [75] Jeremy Reizenstein, Roman Shapovalov, Philipp Henzler, Luca Sbordone, Patrick Labatut, and David Novotny. 2021. Common objects in 3d: Large-scale learning and evaluation of real-life 3d category reconstruction. In *Proceedings of the IEEE/CVF international conference on computer vision*, pages 10901–10911.
- [76] Mike Roberts, Jason Ramapuram, Anurag Ranjan, Atulit Kumar, Miguel Ángel Bautista, Nathan Paczan, Russ Webb, and Joshua M. Susskind. 2021. *Hypersim: A photorealistic synthetic dataset for holistic indoor scene understanding*. In *2021 IEEE/CVF International Conference on Computer Vision, ICCV 2021, Montreal, QC, Canada, October 10-17, 2021*, pages 10892–10902. IEEE.
- [77] Eric Rohmer, Surya PN Singh, and Marc Freese. 2013. V-rep: A versatile and scalable robot simulation framework. In *2013 IEEE/RSJ international conference on intelligent robots and systems*, pages 1321–1326. IEEE.
- [78] Ropedia. 2026. Xperience-10m: A large-scale egocentric multimodal dataset with structured 3d/4d annotations. Dataset.
- [79] Manolis Savva, Abhishek Kadian, Aleksandr Maksymets, Yili Zhao, Erik Wijmans, Bhavana Jain, Julian Straub, Jia Liu, Vladlen Koltun, Jitendra Malik, and 1 others. 2019. Habitat: A platform for embodied ai research. In *Proceedings of the IEEE/CVF international conference on computer vision*, pages 9339–9347.
- [80] Thomas Schops, Johannes L Schonberger, Silvano Galliani, Torsten Sattler, Konrad Schindler, Marc Pollefeys, and Andreas Geiger. 2017. A multi-view stereo benchmark with high-resolution images and multi-camera videos. In *Proceedings of the IEEE conference on computer vision and pattern recognition*, pages 3260–3269.
- [81] Philipp Schröppel, Jan Bechtold, Artemij Amiranashvili, and Thomas Brox. 2022. A benchmark and a baseline for robust multi-view depth estimation. In *2022 International Conference on 3D Vision (3DV)*, pages 637–645. IEEE.
- [82] You Shen, Zhipeng Zhang, Yansong Qu, and Liujuan Cao. 2025. Fastvggt: Training-free acceleration of visual geometry transformer. *arXiv preprint arXiv:2509.02560*.
- [83] Jamie Shotton, Ben Glocker, Christopher Zach, Shahram Izadi, Antonio Criminisi, and Andrew Fitzgibbon. 2013. Scene coordinate regression forests for camera relocalization in rgb-d images. In *Proceedings of the IEEE conference on computer vision and pattern recognition*, pages 2930–2937.
- [84] Samarth Sinha, Roman Shapovalov, Jeremy Reizenstein, Ignacio Rocco, Natalia Neverova, Andrea Vedaldi, and David Novotny. 2023. Common pets in 3d: Dynamic new-view synthesis of real-life deformable categories. In *Proceedings of the IEEE/CVF Conference on Computer Vision and Pattern Recognition*, pages 4881–4891.
- [85] Julian Straub, Thomas Whelan, Lingni Ma, Yufan Chen, Erik Wijmans, Simon Green, Jakob J Engel, Raul Mur-Artal, Carl Ren, Shobhit Verma, and 1 others. 2019. The replica dataset: A digital replica of indoor spaces. *arXiv preprint arXiv:1906.05797*.
- [86] J. Sturm, N. Engelhard, F. Endres, W. Burgard, and D. Cremers. 2012. A benchmark for the evaluation of rgb-d slam systems. In *Proc. of the International Conference on Intelligent Robot Systems (IROS)*.
- [87] Pei Sun, Henrik Kretschmar, Xerxes Dotiwalla, Aurelien Chouard, Vijaysai Patnaik, Paul Tsui, James Guo, Yin Zhou, Yuning Chai, Benjamin Caine, Vijay Vasudevan, Wei Han, Jiquan Ngiam, Hang Zhao, Aleksei Timofeev, Scott Ettinger, Maxim Krivokon, Amy Gao, Aditya Joshi, and 4 others. 2020. *Scalability in perception for autonomous driving: Waymo open dataset*. In *2020 IEEE/CVF Conference on Computer Vision and Pattern Recognition, CVPR 2020, Seattle, WA, USA, June 13-19, 2020*, pages 2443–2451. Computer Vision Foundation / IEEE.
- [88] Bin Tan, Changjiang Sun, Xiage Qin, Hanat Adai, Zelin Fu, Tianxiang Zhou, Han Zhang, Yinghao Xu, Xing Zhu, Yujun Shen, and Nan Xue. 2026. Masked depth modeling for spatial perception. *arXiv preprint arXiv:2601.17895*.
- [89] Zachary Teed and Jia Deng. 2021. Droid-slam: Deep visual slam for monocular, stereo, and rgb-d cameras. *Advances in neural information processing systems*, 34:16558–16569.
- [90] Fabio Tosi, Yiyi Liao, Carolin Schmitt, and Andreas Geiger. 2021. *Smd-nets: Stereo mixture density networks*. In *IEEE Conference on Computer Vision and Pattern Recognition, CVPR 2021, virtual, June 19-25, 2021*, pages 8942–8952. Computer Vision Foundation / IEEE.
- [91] Basile Van Hoorick, Rundi Wu, Ege Ozguroglu, Kyle Sargent, Ruoshi Liu, Pavel Tokmakov, Achal Dave, Changxi Zheng, and Carl Vondrick. 2024. Generative camera dolly: Extreme monocular dynamic novel view synthesis. In *European Conference on Computer Vision*, pages 313–331. Springer.
- [92] Hengyi Wang and Lourdes Agapito. 2024. 3d reconstruction with spatial memory. *arXiv preprint arXiv:2408.16061*.
- [93] Hengyi Wang and Lourdes Agapito. 2025. Amb3r: Accurate feed-forward metric-scale 3d reconstruction with backend. *arXiv preprint arXiv:2511.20343*.

- [94] Jianyuan Wang, Minghao Chen, Nikita Karaev, Andrea Vedaldi, Christian Rupprecht, and David Novotný. 2025. **VGGT: visual geometry grounded transformer**. In *IEEE/CVF Conference on Computer Vision and Pattern Recognition, CVPR 2025, Nashville, TN, USA, June 11-15, 2025*, pages 5294–5306. Computer Vision Foundation / IEEE.
- [95] Jianyuan Wang, Minghao Chen, Shangzhan Zhang, Nikita Karaev, Johannes Schönberger, Patrick Labatut, Piotr Bojanowski, David Novotny, Andrea Vedaldi, and Christian Rupprecht. 2026. **Vggt- ω** . *Preprint*, arXiv:2605.15195.
- [96] Kaixuan Wang and Shaojie Shen. 2020. Flow-motion and depth network for monocular stereo and beyond. *IEEE Robotics and Automation Letters*, 5(2):3307–3314.
- [97] Qiang Wang, Shizhen Zheng, Qingsong Yan, Fei Deng, Kaiyong Zhao, and Xiaowen Chu. 2021. Irs: A large naturalistic indoor robotics stereo dataset to train deep models for disparity and surface normal estimation. In *2021 IEEE International Conference on Multimedia and Expo (ICME)*, pages 1–6. IEEE.
- [98] Qianqian Wang, Yifei Zhang, Aleksander Holynski, Alexei A Efros, and Angjoo Kanazawa. 2025. Continuous 3d perception model with persistent state. In *Proceedings of the Computer Vision and Pattern Recognition Conference*, pages 10510–10522.
- [99] Shuzhe Wang, Vincent Leroy, Yohann Cabon, Boris Chidlovskii, and Jérôme Revaud. 2024. **Dust3r: Geometric 3d vision made easy**. In *IEEE/CVF Conference on Computer Vision and Pattern Recognition, CVPR 2024, Seattle, WA, USA, June 16-22, 2024*, pages 20697–20709. IEEE.
- [100] Wenshan Wang, DeLong Zhu, Xiangwei Wang, Yaoyu Hu, Yuheng Qiu, Chen Wang, Yafei Hu, Ashish Kapoor, and Sebastian A. Scherer. 2020. **Tartanair: A dataset to push the limits of visual SLAM**. In *IEEE/RSJ International Conference on Intelligent Robots and Systems, IROS 2020, Las Vegas, NV, USA, October 24, 2020 - January 24, 2021*, pages 4909–4916. IEEE.
- [101] Yifan Wang, Jianjun Zhou, Haoyi Zhu, Wenzheng Chang, Yang Zhou, Zizun Li, Junyi Chen, Jiangmiao Pang, Chunhua Shen, and Tong He. 2025. π^3 : Permutation-equivariant visual geometry learning. *arXiv preprint arXiv:2507.13347*.
- [102] Yihan Wang and Jia Deng. 2026. Waft-stereo: Warping-alone field transforms for stereo matching. *arXiv preprint arXiv:2603.24836*.
- [103] Zehan Wang, Siyu Chen, Lihe Yang, Jialei Wang, Ziang Zhang, Hengshuang Zhao, and Zhou Zhao. 2025. **Depth anything with any prior**. *Preprint*, arXiv:2505.10565.
- [104] Bowen Wen, Matthew Trepte, Joseph Aribido, Jan Kautz, Orazio Gallo, and Stan Birchfield. 2025. Foundationstereo: Zero-shot stereo matching. In *Proceedings of the IEEE/CVF conference on computer vision and pattern recognition*, pages 5249–5260.
- [105] Magnus Wrenninge and Jonas Unger. 2018. Synscapes: A photorealistic synthetic dataset for street scene parsing. *arXiv preprint arXiv:1810.08705*.
- [106] Tong Wu, Jiarui Zhang, Xiao Fu, Yuxin Wang, Jiawei Ren, Liang Pan, Wayne Wu, Lei Yang, Jiaqi Wang, Chen Qian, and 1 others. 2023. Omniobject3d: Large-vocabulary 3d object dataset for realistic perception, reconstruction and generation. In *Proceedings of the IEEE/CVF conference on computer vision and pattern recognition*, pages 803–814.
- [107] Yuqi Wu, Wenzhao Zheng, Jie Zhou, and Jiwen Lu. 2025. Point3r: Streaming 3d reconstruction with explicit spatial pointer memory. *arXiv preprint arXiv:2507.02863*.
- [108] Fei Xia, Amir R Zamir, Zhiyang He, Alexander Sax, Jitendra Malik, and Silvio Savarese. 2018. Gibson env: Real-world perception for embodied agents. In *Proceedings of the IEEE conference on computer vision and pattern recognition*, pages 9068–9079.
- [109] Hongchi Xia, Yang Fu, Sifei Liu, and Xiaolong Wang. 2024. Rgb-d objects in the wild: Scaling real-world 3d object learning from rgb-d videos. In *Proceedings of the IEEE/CVF Conference on Computer Vision and Pattern Recognition*, pages 22378–22389.
- [110] Jianfeng Xiang, Zelong Lv, Sicheng Xu, Yu Deng, Ruicheng Wang, Bowen Zhang, Dong Chen, Xin Tong, and Jiaolong Yang. 2025. Structured 3d latents for scalable and versatile 3d generation. In *Proceedings of the IEEE/CVF conference on computer vision and pattern recognition*, pages 21469–21480.
- [111] Pengchuan Xiao, Zhenlei Shao, Steven Hao, Zishuo Zhang, Xiaolin Chai, Judy Jiao, Zesong Li, Jian Wu, Kai Sun, Kun Jiang, and 1 others. 2021. Pandaset: Advanced sensor suite dataset for autonomous driving. In *2021 IEEE international intelligent transportation systems conference (ITSC)*, pages 3095–3101. IEEE.
- [112] Enze Xie, Wenhai Wang, Zhiding Yu, Anima Anandkumar, Jose M Alvarez, and Ping Luo. 2021. Segformer: Simple and efficient design for semantic segmentation with transformers. In *Neural Information Processing Systems (NeurIPS)*.

- [113] Tao Xie, Peishan Yang, Yudong Jin, Yingfeng Cai, Wei Yin, Weiqiang Ren, Qian Zhang, Wei Hua, Sida Peng, Xiaoyang Guo, and 1 others. 2026. Scal3r: Scalable test-time training for large-scale 3d reconstruction. *arXiv preprint arXiv:2604.08542*.
- [114] Gangwei Xu, Xianqi Wang, Zhaoxing Zhang, Junda Cheng, Chunyuan Liao, and Xin Yang. 2025. Igev++: Iterative multi-range geometry encoding volumes for stereo matching. *IEEE Transactions on Pattern Analysis and Machine Intelligence*.
- [115] Guorun Yang, Xiao Song, Chaoqin Huang, Zhidong Deng, Jianping Shi, and Bolei Zhou. 2019. Drivingstereo: A large-scale dataset for stereo matching in autonomous driving scenarios. In *Proceedings of the IEEE/CVF conference on computer vision and pattern recognition*, pages 899–908.
- [116] Jianing Yang, Alexander Sax, Kevin J. Liang, Mikael Henaff, Hao Tang, Ang Cao, Joyce Chai, Franziska Meier, and Matt Feiszli. 2025. **Fast3r: Towards 3d reconstruction of 1000+ images in one forward pass**. In *IEEE/CVF Conference on Computer Vision and Pattern Recognition, CVPR 2025, Nashville, TN, USA, June 11-15, 2025*, pages 21924–21935. Computer Vision Foundation / IEEE.
- [117] Sizhe Yang, Linning Xu, Hao Li, Juncheng Mu, Jia Zeng, Dahua Lin, and Jiangmiao Pang. 2026. Robo3r: Enhancing robotic manipulation with accurate feed-forward 3d reconstruction. *arXiv preprint arXiv:2602.10101*.
- [118] Xuning Yang, Rishit Dagli, Alex Zook, Hugo Hadfield, Ankit Goyal, Stan Birchfield, Fabio Ramos, and Jonathan Tremblay. 2026. Robolab: A high-fidelity simulation benchmark for analysis of task generalist policies. *arXiv preprint arXiv:2604.09860*.
- [119] Yuxue Yang, Lue Fan, Ziqi Shi, Junran Peng, Feng Wang, and Zhaoxiang Zhang. 2026. Neoverse: Enhancing 4d world model with in-the-wild monocular videos. *arXiv preprint arXiv:2601.00393*.
- [120] Yao Yao, Zixin Luo, Shiwei Li, Jingyang Zhang, Yufan Ren, Lei Zhou, Tian Fang, and Long Quan. 2020. **Blendedmvs: A large-scale dataset for generalized multi-view stereo networks**. In *2020 IEEE/CVF Conference on Computer Vision and Pattern Recognition, CVPR 2020, Seattle, WA, USA, June 13-19, 2020*, pages 1787–1796. Computer Vision Foundation / IEEE.
- [121] Chandan Yeshwanth, Yueh-Cheng Liu, Matthias Nießner, and Angela Dai. 2023. **Scannet++: A high-fidelity dataset of 3d indoor scenes**. In *IEEE/CVF International Conference on Computer Vision, ICCV 2023, Paris, France, October 1-6, 2023*, pages 12–22. IEEE.
- [122] Xianggang Yu, Mutian Xu, Yidan Zhang, Haolin Liu, Chongjie Ye, Yushuang Wu, Zizheng Yan, Chenming Zhu, Zhangyang Xiong, Tianyou Liang, and 1 others. 2023. Mvimagnet: A large-scale dataset of multi-view images. In *Proceedings of the IEEE/CVF conference on computer vision and pattern recognition*, pages 9150–9161.
- [123] Shuai Yuan, Yantai Yang, Xiaotian Yang, Xupeng Zhang, Zhonghao Zhao, Lingming Zhang, and Zhipeng Zhang. 2026. Infinitevgt: Visual geometry grounded transformer for endless streams.
- [124] Amir R Zamir, Alexander Sax, William Shen, Leonidas J Guibas, Jitendra Malik, and Silvio Savarese. 2018. Taskonomy: Disentangling task transfer learning. In *Proceedings of the IEEE conference on computer vision and pattern recognition*, pages 3712–3722.
- [125] Junyi Zhang, Charles Herrmann, Junhwa Hur, Varun Jampani, Trevor Darrell, Forrester Cole, Deqing Sun, and Ming-Hsuan Yang. 2025. **Monst3r: A simple approach for estimating geometry in the presence of motion**. In *The Thirteenth International Conference on Learning Representations, ICLR 2025, Singapore, April 24-28, 2025*. OpenReview.net.
- [126] Junyi Zhang, Charles Herrmann, Junhwa Hur, Chen Sun, Ming-Hsuan Yang, Forrester Cole, Trevor Darrell, and Deqing Sun. 2026. Loger: Long-context geometric reconstruction with hybrid memory. *arXiv preprint arXiv:2603.03269*.
- [127] Yibo Zhang, Li Zhang, Rui Ma, and Nan Cao. 2025. Texverse: A universe of 3d objects with high-resolution textures. *arXiv preprint arXiv:2508.10868*.
- [128] Zhengshen Zhang, Hao Li, Yalun Dai, Zhengbang Zhu, Lei Zhou, Chenchen Liu, Dong Wang, Francis EH Tay, Sijin Chen, Ziwei Liu, and 1 others. 2025. From spatial to actions: Grounding vision-language-action model in spatial foundation priors. *arXiv preprint arXiv:2510.17439*.
- [129] Jia Zheng, Junfei Zhang, Jing Li, Rui Tang, Shenghua Gao, and Zihan Zhou. 2020. Structured3d: A large photo-realistic dataset for structured 3d modeling. In *European Conference on Computer Vision*, pages 519–535. Springer.
- [130] Ruijie Zheng, Dantong Niu, Yuqi Xie, Jing Wang, Mengda Xu, Yunfan Jiang, Fernando Castañeda, Fengyuan Hu, You Liang Tan, Letian Fu, and 1 others. 2026. Egoscale: Scaling dexterous manipulation with diverse egocentric human data. *arXiv preprint arXiv:2602.16710*.

- [131] Yang Zheng, Adam W Harley, Bokui Shen, Gordon Wetzstein, and Leonidas J Guibas. 2023. Pointodyssey: A large-scale synthetic dataset for long-term point tracking. In *Proceedings of the IEEE/CVF International Conference on Computer Vision*, pages 19855–19865.
- [132] Bolei Zhou, Hang Zhao, Xavier Puig, Tete Xiao, Sanja Fidler, Adela Barriuso, and Antonio Torralba. 2019. Semantic understanding of scenes through the ade20k dataset. *International Journal of Computer Vision*, 127(3):302–321.
- [133] Kaichen Zhou, Yuhan Wang, Grace Chen, Xinhai Chang, Gaspard Beaudouin, Fangneng Zhan, Paul Pu Liang, and Mengyu Wang. 2025. Page-4d: Disentangled pose and geometry estimation for 4d perception. *arXiv e-prints*, pages arXiv–2510.
- [134] Tinghui Zhou, Richard Tucker, John Flynn, Graham Fyffe, and Noah Snavely. 2018. Stereo magnification: Learning view synthesis using multiplane images. *arXiv preprint arXiv:1805.09817*.
- [135] Yang Zhou, Yifan Wang, Jianjun Zhou, Wenzheng Chang, Haoyu Guo, Zizun Li, Kaijing Ma, Xinyue Li, Yating Wang, Haoyi Zhu, and 1 others. 2025. Omniworld: A multi-domain and multi-modal dataset for 4d world modeling. *arXiv preprint arXiv:2509.12201*.
- [136] Dong Zhuo, Wenzhao Zheng, Jiahe Guo, Yuqi Wu, Jie Zhou, and Jiwen Lu. 2025. Streaming 4d visual geometry transformer. *arXiv preprint arXiv:2507.11539*.

Appendix Contents

A SpatialBench Data Curation Pipeline	25
A.1 DROID Curation Pipeline	25
A.2 Xperience Curation Pipeline	26
A.3 Other Data Collection	26
A.4 Depth Map Post-Processing Pipeline	26
B Benchmark Details	27
B.1 Benchmark Composition	27
B.2 Multi-density Evaluation Regime Details	27
B.3 General Setting of the Benchmark	29
B.4 Evaluation Metrics	29
B.4.1 Camera Pose Estimation	29
B.4.2 Camera Trajectory Estimation	30
B.4.3 Depth Estimation	31
B.4.4 Dense-View Reconstruction	31
B.5 Evaluated Models Details	32
B.5.1 Optimization-based Methods	33
B.5.2 End-to-End Feed-Forward Methods	33
B.5.3 Online / Streaming Methods	34
B.5.4 Chunk-based Methods	35
B.5.5 SLAM-based Methods	35
B.5.6 Test-Time Training Methods	36
B.6 SpatialBench Visualizations	36
B.7 Evaluated Models and Training Datasets in SpatialBench	36
C The Collection of DA-Next-5M	46
D Detail of DA-Next	47
D.1 Model Architecture	47
D.2 Training Objective	47
D.3 Camera Conditioning Training	49
D.4 Training Datasets	49
D.5 Frame Sampling Strategy	50
D.6 Training Configuration	50
E Additional Findings	51
E.1 Do More Input Frames Always Lead to Better Results?	51
E.2 How to Select the Right Spatial Foundation Model for Your Task?	51
F The Complete SpatialBench Results	57
G Limitations	81

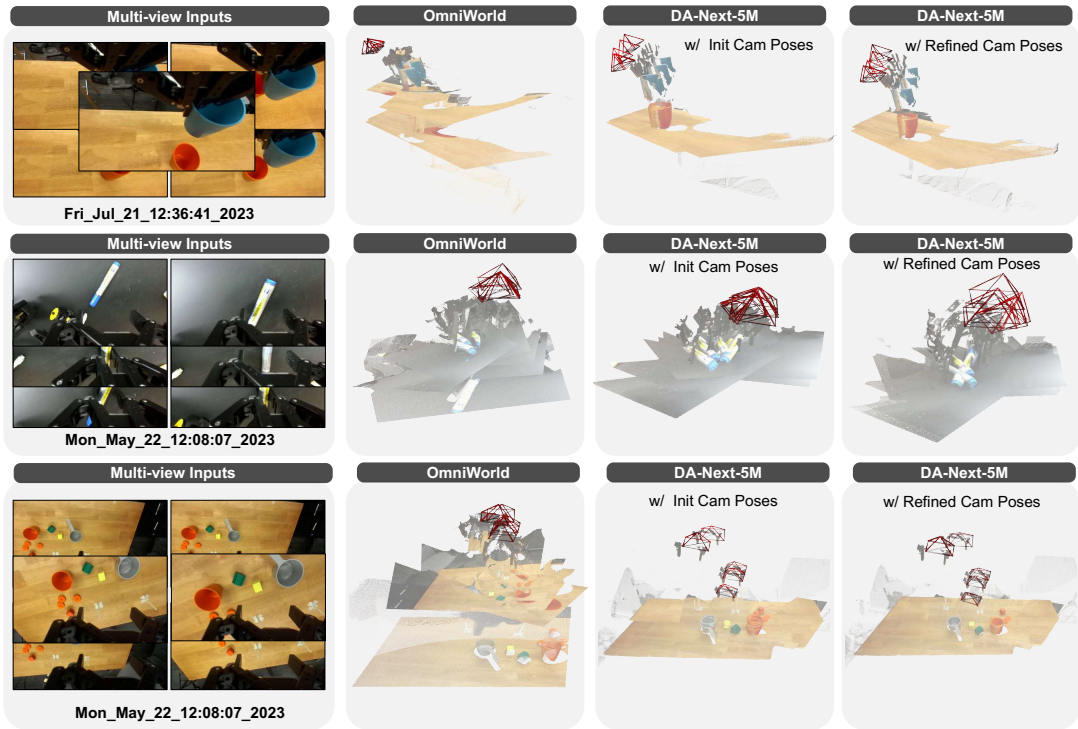


Figure 11 | **Visual comparison on the DROID dataset.** We compare the annotations from OmniWorld against our reconstructed point clouds using initial poses and refined poses, respectively.

A. SpatialBench Data Curation Pipeline

In this section, we detail the data processing pipeline in SpatialBench, covering the post-processing pipelines for Xperience (Sec. A.2), DROID (Sec. A.1), and our collected simulation datasets (Sec. A.3), as well as a unified depth map post-processing pipeline (Sec. A.4) applied to selected datasets to ensure annotation quality.

A.1. DROID Curation Pipeline

Accurate geometric annotations are critical for reliable benchmark evaluation. However, the raw DROID [43] data is highly noisy with unreliable camera calibration, precluding direct use of the original annotations. We first investigate learning-based annotation solutions, including Mega-SaM [51] and VIPE [33] for visual SLAM, and Camera Depth Model [58], PriorDA [103], Lingbot-Depth [88], and PromptDA [55] for depth completion. However, none of these methods are trained on wrist-view domains, and we observe significant failure cases under the close-range, high-motion conditions characteristic of this setting.

Since DROID provides synchronized stereo pairs, we turn to stereo-based depth estimation as a more reliable annotation source. We test S^2M^2 [65], FoundationStereo [104], IGEV [114], DynamicStereo [40], and WAFT-Stereo [102], ultimately selecting S^2M^2 for its superior performance on wrist-view sequences. Specifically, we randomly select a subset of DROID sequences and feed the left-right stereo image pairs from each wrist-view sequence into S^2M^2 to obtain disparity maps. Metric depth maps for the left eye are then computed using the ZED camera intrinsics and baseline, with a confidence threshold of 0.999 applied to mask out unreliable depth predictions. The masked depth maps and camera intrinsics are subsequently injected as priors into MapAnything [42] to obtain initial camera poses. We then employ SAM3 [10] to annotate

masks for moving objects on selected keyframes, which are propagated to the full sequence. Finally, leveraging the initial camera poses, RGB images, and propagated masks, we perform Bundle Adjustment with both depth and photometric losses to refine the camera parameters and obtain globally aligned point clouds. Sequences with poor temporal depth consistency are filtered out by computing the mean per-pixel reprojection depth error between adjacent frames. Fig. 11 presents a comparison between our DROID data curation pipeline and the OmniWorld data processing approach. OmniWorld annotates wrist-view depth using FoundationStereo and relies on the dataset’s original inaccurate camera poses, resulting in unreliable depth estimates and misaligned point clouds across frames (*e.g.*, incorrect depth on the marker pen on the table in Mon_May_22_12:08:07_2023). In contrast, our annotation pipeline produces temporally consistent depth estimates with well-preserved cross-frame continuity.

We also provide a gallery of the DROID [43] dataset we processed in Fig. 12 and 13. For each scene, we visualize the first frame of the RGB sequence overlaid with the SAM3 segmentation mask (top-left), the corresponding depth map (bottom-left), and the reconstructed point cloud (right).

A.2. Xperience Curation Pipeline

Xperience [78] consists of egocentric sequences captured via a head-mounted device during human activity, recorded by four fisheye cameras. We randomly sample a subset of the original data for processing. We obtain camera poses using a SLAM system built upon VIPE [33], and estimate metric depth maps and their confidence maps from rectified stereo image pairs using FoundationStereo [104]. Fig. 14 presents sample visualizations of Xperience sequences included in SpatialBench.

A.3. Other Data Collection

We collect robot manipulation sequences from four simulators: RLBench [36], Robo Colosseum [72], RoboTwin [14], and RoboLab [118]. We refer the reader to Sec. C for details on the data collection procedure.

A.4. Depth Map Post-Processing Pipeline

Raw depth maps collected from sensors or simulation engines often contain systematic artifacts that degrade geometric evaluation quality. We apply a unified five-stage cleaning pipeline to all real-world datasets in SpatialBench, producing a per-frame binary validity mask that downstream evaluation uses to ignore unreliable pixels.

Stage 1: Depth Range Clipping. Depth values are first converted to meters and then clipped to a scene-appropriate valid range $[d_{\min}, d_{\max}]$. Pixels falling outside this range, including near-field sensor noise and far-field sensor dropout are marked invalid. The range bounds are set per dataset according to the typical operating distance of the capture platform (*e.g.*, $[0.05\text{m}, 5\text{m}]$ for egocentric indoor scenes and $[0\text{m}, 3\text{m}]$ for close-range wrist-view sequences).

Stage 2: Flying Point Removal. Flying points are erroneous depth values that appear at depth discontinuity boundaries, caused by stereo mismatches or sensor mixed-pixel effects. We detect them by computing the spatial gradient of the depth map and identifying pixels where the gradient magnitude is disproportionately large relative to the local depth value, which indicates a sharp, physically implausible depth jump. Detected discontinuity pixels and a small surrounding neighborhood (controlled by an erosion radius) are masked out, preventing

boundary artifacts from contaminating geometric metrics.

Stage 3: Edge-Aware Bilateral Filtering. Surviving valid pixels are smoothed using a joint bilateral filter guided by the corresponding RGB image. The filter suppresses high-frequency depth noise while preserving genuine depth edges aligned with visible object boundaries. Only already-valid pixels are updated; no hole-filling is performed, ensuring that masked regions remain invalid after filtering.

Stage 4: Small Isolated Region Removal. After filtering, the valid-pixel mask may contain small, disconnected clusters of surviving pixels that are physically implausible as independent surface patches. We apply connected-component analysis on the binary valid mask and remove any component whose area falls below a minimum threshold, eliminating residual noise fragments that escaped the earlier stages.

Stage 5: Sky Mask. For outdoor datasets (*e.g.*, OmniWorld [135], Lingbot-Depth [88]), depth sensors and stereo algorithms systematically fail on sky regions, producing either missing values or extreme outliers at near-infinite range. We generate a per-frame sky mask using a pretrained semantic segmentation model (SegFormer [112] fine-tuned on ADE20K [132]) and set all sky-classified pixels to invalid regardless of their depth values. This prevents sky regions from inflating depth error metrics or introducing spurious points at the horizon in point cloud evaluation.

B. Benchmark Details

In this section, we provide a comprehensive description of SpatialBench. We first detail the composition of our dataset collection (Sec. B.2), covering the 19 source datasets and the three multi-density evaluation regimes (*Sparse*, *Medium*, and *Dense*). We then describe the hardware configuration and general experimental settings (Sec. B.4), followed by the complete mathematical definitions of all evaluation metrics used to assess camera pose estimation and depth prediction quality. Next, we report the implementation details and hyperparameters for each evaluated method, organized by category: optimization-based, feed-forward, streaming, chunk-based, SLAM-based, and test-time training approaches. Finally, we present qualitative visualizations of prior-enhanced models and summarize the training datasets used by all compared methods.

B.1. Benchmark Composition

Our benchmark aggregates 19 publicly available source datasets, spanning indoor and outdoor scenes, static reconstructions and dynamic sequences, and three viewpoint regimes (third-person, egocentric, and wrist-mounted), captured from both real sensors and simulation. A complete summary of these datasets, together with their per-scene attribute tags, the supported input regimes (Single Frame, Sparse, Medium, Dense), and the number of evaluated scenes and frames, is provided in Table 4. In total, the benchmark contains 546 scenes and 72,540 evaluation frames.

B.2. Multi-density Evaluation Regime Details

SPARSE REGIME. Sparse-view selection is implemented as a deterministic set-cover procedure. Let \mathcal{V} denote the voxel support of a scene and \mathcal{F} the set of candidate frames. Each frame $f \in \mathcal{F}$

Table 4 | **Source Datasets and Scene Attributes Used in Our Benchmark.** We summarize the datasets together with their per-dataset attribute tags. The four *#Scenes* sub-columns report the number of scenes evaluated under each input regime (*Single Frame*, *Sparse*, *Medium*, *Dense*); “–” marks regimes in which a dataset does not participate. *#Frames* is the total frame count actually consumed across all regimes.

#	Dataset	Environment	Dynamics	View Type	Source	#Scenes				#Frames
						Single	Sparse	Medium	Dense	
1	7-Scenes [83]	Indoor	Static	Normal	Real	7	7	7	7	7,242
2	ADT [69]	Indoor	Dynamic	Egocentric	Simulation	4	4	4	4	2,112
3	DROID [43]	Indoor	Dynamic	Wrist	Real	16	16	16	16	3,440
4	DTU [37]	Indoor	Static	Normal	Real	13	13	13	–	431
5	ETH3D [80]	Both	Static	Normal	Real	8	8	8	–	150
6	Hiroom [54]	Indoor	Static	Normal	Simulation	6	6	6	–	90
7	KITTI-Odometry [26]	Outdoor	Dynamic	Normal	Real	–	–	–	11	12,973
8	LingBot-Depth [88]	Both	Static	Mixed	Mixed	50	–	–	–	50
9	NRGBD [4]	Indoor	Static	Normal	Real	8	8	8	8	10,945
10	OmniWorld [135]	Outdoor	Dynamic	Normal	Simulation	5	5	5	4	2,033
11	RLBench [36]	Indoor	Dynamic	Wrist	Simulation	10	10	10	8	1,887
12	RoboLab [118]	Indoor	Dynamic	Wrist	Simulation	8	8	8	8	9,360
13	RoboTwin [14]	Indoor	Dynamic	Wrist	Simulation	8	8	8	7	1,695
14	ScanNet++ [121]	Indoor	Static	Normal	Real	11	11	11	11	4,137
15	Tanks and Temples [44]	Both	Static	Normal	Real	4	4	4	4	934
16	TUM [86]	Indoor	Dynamic	Normal	Real	6	6	6	6	6,657
17	V-KITTI [8]	Outdoor	Dynamic	Normal	Simulation	5	5	5	5	2,851
18	Waymo [87]	Outdoor	Dynamic	Normal	Real	8	8	8	8	2,464
19	Xperience [78]	Indoor	Dynamic	Egocentric	Real	2	2	2	2	3,089
Total						179	129	129	109	72,540

covers a subset of voxels $V_f \subseteq \mathcal{V}$. Given a frame budget K , the selected frame set is defined as

$$\mathcal{S} = \arg \max_{S \subseteq \mathcal{F}, |S| \leq K} \left| \bigcup_{f \in S} V_f \right|.$$

In practice, we optimize this objective greedily by repeatedly selecting the frame that provides the largest marginal increase in voxel coverage.

MEDIUM REGIME. The medium regime uses the same coverage objective but applies a length-adaptive frame budget. For a scene with N frames, the selected set satisfies

$$\mathcal{S} = \arg \max_{S \subseteq \mathcal{F}, F_{\min}(N) \leq |S| \leq F_{\max}(N)} \left| \bigcup_{f \in S} V_f \right|,$$

where $F_{\min}(N)$ and $F_{\max}(N)$ define the admissible range of selected frames. This prevents over-pruning short sequences and over-sampling long ones while preserving moderate view overlap.

DENSE REGIME. For dense evaluation, the goal is to preserve temporal continuity while bounding evaluation cost. Given a scene with N frames and a target maximum budget of $T = 500$ frames, we retain all frames when $N \leq T$. Otherwise, we subsample the trajectory with a stride

$$s = \left\lceil \frac{N}{T} \right\rceil,$$

which yields approximately T evenly spaced frames per scene. Datasets with too few valid frames or too few eligible trajectories after filtering are not included in the DENSE regime. Accordingly, missing dense entries in the per-dataset results tables indicate unavailable evaluation indices rather than failed method runs.

B.3. General Setting of the Benchmark

All experiments are run on a single workstation with the following configuration: 2× Intel Xeon Platinum 8580 processors (60 cores / 120 threads per socket, 240 logical cores in total), 2 TB of system memory, and 8× NVIDIA H200 GPUs, each with 141 GB of memory and pairwise connected through 18-link NVLink (NV18). The system runs Ubuntu 22.04 with CUDA 12.8 and NVIDIA driver 570.148.08. For all methods, we prioritize using the resolution recommended by each method for inference. Specifically, for methods that only support a fixed resolution (e.g., Spann3R at 224×224), we resize the image such that the width matches the target resolution while preserving the original aspect ratio, followed by a center crop. For all other methods, inference is performed at a resolution of 512 or 518 pixels, depending on each model’s patch stride (16 or 14, respectively).

B.4. Evaluation Metrics

We provide the complete mathematical definitions of all evaluation metrics used in Spatial-Bench. Throughout, N denotes the number of input frames in a scene, indexed by $i \in \{1, \dots, N\}$. Each camera pose $G_i \in SE(3)$ is a *world-to-camera* transformation, decomposed as $G_i = [R_i \mid t_i]$ with rotation $R_i \in SO(3)$ and translation $t_i \in \mathbb{R}^3$, so that the camera centre in world coordinates is $\mathbf{c}_i = -R_i^\top t_i$. Ground-truth quantities carry a superscript star (e.g. $R_i^*, t_i^*, \mathbf{c}_i^* = -R_i^{*\top} t_i^*$) and predicted quantities carry a hat (e.g. $\hat{R}_i, \hat{t}_i, \hat{\mathbf{c}}_i = -\hat{R}_i^\top \hat{t}_i$). D_p and \hat{D}_p denote the ground-truth and predicted depth at pixel p , and $\mathbf{P}_p, \hat{\mathbf{P}}_p$ the corresponding 3D world points.

B.4.1. Camera Pose Estimation

Camera pose estimation is evaluated via pairwise relative geometry across all $|\mathcal{P}|$ ordered pairs $\mathcal{P} = \{(i, j) \mid 1 \leq i < j \leq N\}$.

Relative rotation error. The relative rotation from camera i to camera j is

$$R_{ij}^* = R_j^* R_i^{*\top}, \quad \hat{R}_{ij} = \hat{R}_j \hat{R}_i^\top. \quad (1)$$

The pairwise rotation error is the geodesic distance on $SO(3)$:

$$e_{ij}^R = \arccos\left(\frac{\text{tr}(R_{ij}^{*\top} \hat{R}_{ij}) - 1}{2}\right) \in [0^\circ, 180^\circ]. \quad (2)$$

The *Relative Rotation Accuracy* (RAcc) at threshold x is the fraction of pairs whose rotation error falls below x :

$$\text{RAcc}_x = \frac{1}{|\mathcal{P}|} \sum_{(i,j) \in \mathcal{P}} \mathbf{1}[e_{ij}^R < x]. \quad (3)$$

Relative translation error. Since the predicted trajectory may carry an arbitrary global scale, translation quality is measured by the *angular deviation* between the translation components of the predicted and ground-truth pairwise relative poses, with the 180° direction ambiguity folded out. Let

$$t_{ij}^* = [(G_i^*)^{-1} G_j^*]_{\text{trans}} = R_i^{*\top} (t_j^* - t_i^*), \quad \hat{t}_{ij} = [\hat{G}_i^{-1} \hat{G}_j]_{\text{trans}} = \hat{R}_i^\top (\hat{t}_j - \hat{t}_i) \quad (4)$$

denote the translation components of the relative $SE(3)$ poses, expressed in camera i ’s local frame, with corresponding unit directions

$$\tau_{ij}^* = \frac{t_{ij}^*}{\|t_{ij}^*\|_2}, \quad \hat{\tau}_{ij} = \frac{\hat{t}_{ij}}{\|\hat{t}_{ij}\|_2}. \quad (5)$$

The pairwise translation error is

$$e_{ij}^t = \arccos\left(|\tau_{ij}^* \cdot \hat{\tau}_{ij}|\right) \in [0^\circ, 90^\circ], \quad (6)$$

where the absolute value absorbs the inherent 180° direction ambiguity under unknown global scale. The *Relative Translation Accuracy* (TAcc) at threshold x is

$$\text{TAcc}_x = \frac{1}{|\mathcal{P}|} \sum_{(i,j) \in \mathcal{P}} \mathbf{1}\left[e_{ij}^t < x\right]. \quad (7)$$

AUC. The joint accuracy curve measures the fraction of pairs for which *both* rotation and translation errors are below threshold x :

$$\text{Acc}_x = \frac{1}{|\mathcal{P}|} \sum_{(i,j) \in \mathcal{P}} \mathbf{1}\left[\max\left(e_{ij}^R, e_{ij}^t\right) < x\right]. \quad (8)$$

The *Area Under the Curve* up to a maximum threshold x_{\max} is

$$\text{AUC}_{x_{\max}} = \frac{1}{x_{\max}} \int_0^{x_{\max}} \text{Acc}_x \, dx, \quad (9)$$

approximated in practice by linear interpolation over a uniform grid of thresholds $x \in [0^\circ, x_{\max}]$.

B.4.2. Camera Trajectory Estimation

For continuous image sequences (medium and dense regimes), the predicted trajectory $\{\hat{R}_i, \hat{\mathbf{c}}_i\}_{i=1}^N$ is first aligned to the ground truth $\{R_i^*, \mathbf{c}_i^*\}_{i=1}^N$ via a global Sim(3) transformation. Specifically, we solve for scale $s^* > 0$, rotation $\bar{R}^* \in SO(3)$, and translation $\bar{\mathbf{t}}^* \in \mathbb{R}^3$ by minimising

$$\min_{s, \bar{R}, \bar{\mathbf{t}}} \sum_{i=1}^N \left\| s \bar{R} \hat{\mathbf{c}}_i + \bar{\mathbf{t}} - \mathbf{c}_i^* \right\|_2^2, \quad (10)$$

yielding scale-aligned camera centres $\tilde{\mathbf{c}}_i = s^* \bar{R}^* \hat{\mathbf{c}}_i + \bar{\mathbf{t}}^*$ and correspondingly aligned rotations $\tilde{R}_i = \bar{R}^* \hat{R}_i$. Let $\tilde{T}_i \in SE(3)$ denote the resulting aligned camera pose.

Absolute Trajectory Error (ATE).

$$\text{ATE} = \sqrt{\frac{1}{N} \sum_{i=1}^N \left\| \tilde{\mathbf{c}}_i - \mathbf{c}_i^* \right\|_2^2}. \quad (11)$$

Relative Pose Error. For consecutive frame pairs with temporal displacement $\Delta = 1$, the ground-truth and aligned-predicted relative SE(3) motions are

$$\delta T_i^* = (G_i^*)^{-1} G_{i+1}^*, \quad \delta \tilde{T}_i = \tilde{T}_i^{-1} \tilde{T}_{i+1}, \quad (12)$$

$$\delta R_i^* = R_{i+1}^* R_i^{*\top}, \quad \delta \tilde{R}_i = \tilde{R}_{i+1} \tilde{R}_i^\top, \quad (13)$$

and the per-step pose-error matrix is $E_i = (\delta T_i^*)^{-1} \delta \tilde{T}_i \in SE(3)$. The *Relative Translation Error* and *Relative Rotation Error*, each averaged over all $N-1$ consecutive windows, are

$$\text{RPE}_t = \frac{1}{N-1} \sum_{i=1}^{N-1} \left\| [E_i]_{\text{trans}} \right\|_2, \quad (14)$$

$$\text{RPE}_r = \frac{1}{N-1} \sum_{i=1}^{N-1} \arccos\left(\frac{\text{tr}(\delta R_i^{*\top} \delta \tilde{R}_i) - 1}{2}\right), \quad (15)$$

where $[E_i]_{\text{trans}}$ denotes the translation component of E_i . This follows the standard evo-library RPE definition adopted by the DROID-SLAM evaluation protocol. ATE and RPE_t are reported in metres; RPE_r is in degrees.

B.4.3. Depth Estimation

Let $\Omega_D = \{p \mid D_p > 0\}$ denote the set of pixels with valid ground-truth depth in a given frame. For models that do not produce metric-scale output, the predicted depth \hat{D}_p is first rescaled by the per-frame *median alignment*:

$$\hat{D}_p \leftarrow s \cdot \hat{D}_p, \quad s = \text{median}_{p \in \Omega_D} \left(\frac{D_p}{\hat{D}_p} \right). \quad (16)$$

All depth metrics reported in this paper are computed after median-scale alignment, unless otherwise specified.

Absolute Relative Error (AbsRel).

$$\text{AbsRel} = \frac{1}{|\Omega_D|} \sum_{p \in \Omega_D} \frac{|D_p - \hat{D}_p|}{D_p}. \quad (17)$$

Squared Relative Error (SqRel).

$$\text{SqRel} = \frac{1}{|\Omega_D|} \sum_{p \in \Omega_D} \frac{(D_p - \hat{D}_p)^2}{D_p}. \quad (18)$$

Root Mean Squared Error (RMSE).

$$\text{RMSE} = \sqrt{\frac{1}{|\Omega_D|} \sum_{p \in \Omega_D} (D_p - \hat{D}_p)^2}. \quad (19)$$

Log-scale RMSE (LogRMSE).

$$\text{LogRMSE} = \sqrt{\frac{1}{|\Omega_D|} \sum_{p \in \Omega_D} (\log D_p - \log \hat{D}_p)^2}. \quad (20)$$

Threshold Inlier Ratio (δ_τ).

$$\delta_\tau = \frac{1}{|\Omega_D|} \left| \left\{ p \in \Omega_D \mid \max \left(\frac{D_p}{\hat{D}_p}, \frac{\hat{D}_p}{D_p} \right) < \tau \right\} \right|. \quad (21)$$

We report $\delta_{1.03}$, $\delta_{1.05}$, and $\delta_{1.10}$, following the RMVD evaluation protocol of Schröppel et al. [81]. For AbsRel, SqRel, RMSE, and LogRMSE, lower is better; for δ_τ , higher is better.

B.4.4. Dense-View Reconstruction

Scene-level reconstruction quality is evaluated by comparing the predicted and ground-truth point clouds on ScanNet++ [121], NRGBD [4], DTU [37], HIRoom [54], and 7-Scenes [83], following the protocol of DA3-Bench [54].

The ground-truth point cloud \mathcal{P}^* is obtained by uniformly sampling 10^6 points from the GT mesh, which is reconstructed via offline TSDF fusion of all available RGB-D frames. The predicted point cloud $\hat{\mathcal{P}}$ is obtained via online TSDF fusion of the model’s per-frame predicted depth maps and camera poses, from which a triangle mesh is extracted and uniformly resampled to 10^6 points.

Before computing metrics, both point clouds undergo dataset-specific preprocessing. For ScanNet++, NRGBD, and DTU, $\hat{\mathcal{P}}$ is cropped to the axis-aligned bounding box of \mathcal{P}^* inflated by 0.1 m to exclude out-of-range predictions. No cropping is applied for 7-Scenes and Hroom. Both point clouds are then voxel-downsampled with dataset-specific voxel sizes: 0.02 m for ScanNet++ and NRGBD, 0.01 m for DTU, and 4/512 m (≈ 7.8 mm) for 7-Scenes and Hroom.

We report two complementary families of Chamfer-based metrics.

Threshold-based Precision and Recall.

$$\text{Precision} = \frac{1}{|\hat{\mathcal{P}}|} \sum_{\hat{\mathbf{P}}_m \in \hat{\mathcal{P}}} \mathbf{1} \left[\min_{\mathbf{P}_n^* \in \mathcal{P}^*} \|\hat{\mathbf{P}}_m - \mathbf{P}_n^*\|_2 < d_\tau \right], \quad (22)$$

$$\text{Recall} = \frac{1}{|\mathcal{P}^*|} \sum_{\mathbf{P}_n^* \in \mathcal{P}^*} \mathbf{1} \left[\min_{\hat{\mathbf{P}}_m \in \hat{\mathcal{P}}} \|\mathbf{P}_n^* - \hat{\mathbf{P}}_m\|_2 < d_\tau \right]. \quad (23)$$

Precision is the fraction of predicted points within d_τ of any GT point. Recall is the fraction of GT points covered by the prediction within d_τ . Both are reported as percentages.

Mean Chamfer Accuracy and Completeness (metres).

$$\overline{\text{Acc}} = \frac{1}{|\hat{\mathcal{P}}|} \sum_{\hat{\mathbf{P}}_m \in \hat{\mathcal{P}}} \min_{\mathbf{P}_n^* \in \mathcal{P}^*} \|\hat{\mathbf{P}}_m - \mathbf{P}_n^*\|_2, \quad (24)$$

$$\overline{\text{Comp}} = \frac{1}{|\mathcal{P}^*|} \sum_{\mathbf{P}_n^* \in \mathcal{P}^*} \min_{\hat{\mathbf{P}}_m \in \hat{\mathcal{P}}} \|\mathbf{P}_n^* - \hat{\mathbf{P}}_m\|_2, \quad (25)$$

which measures the mean nearest-neighbor distances in metres.

F-score and Overall.

$$\text{F-score} = \frac{2 \cdot \text{Precision} \cdot \text{Recall}}{\text{Precision} + \text{Recall}} \quad (\%), \quad (26)$$

$$\text{Overall} = \frac{\overline{\text{Acc}} + \overline{\text{Comp}}}{2} \quad (\text{m}). \quad (27)$$

F-score is the harmonic mean of threshold-based precision and recall. Overall is the mean of the two Chamfer distances, reported in metres. The distance threshold is set to $d_\tau = 0.05$ m across all datasets.

B.5. Evaluated Models Details

We group the 32 methods (41 variants) into six paradigms. For each model, we briefly summarize its core idea, and then list the key inference-time configuration adopted in our benchmark. Unless otherwise noted, every model is driven by a unified `ModelAdapter` interface that feeds a complete scene (RGB tensors, GT intrinsics used only for evaluation) to the model and collects `pred_depth`, `pred_pose` (cam-to-world), and optionally `pred_pointcloud/pred_confidence`; depth is aligned to GT by median scaling before computing metrics unless the model produces metric depth.

B.5.1. Optimization-based Methods

DUST3R [99] regresses per-pair dense point maps in a canonical coordinate frame, and recovers a globally consistent reconstruction by a gradient-based global alignment over all image pairs. In our benchmark, the ViT-Large 512 checkpoint (naver/DUST3R_ViT_Large_BaseDecoder_512_dpt) is used, with `niter=300`, `schedule=cosine`, `lr=0.01` for the global aligner, and inputs resized to width 512 aligned to a stride of 16.

MASt3R [48] extends DUST3R with a dense matching head that produces robust 2D correspondences, enabling metric-scale recovery through a sparse global optimizer. We use the metric checkpoint naver/MASt3R_ViT_Large_BaseDecoder_512_catmlpdpt_metric with `niter=300`, `schedule=linear`, `lr=0.01`, input width 512 (align 16), and median depth scaling for final evaluation.

B.5.2. End-to-End Feed-Forward Methods

VGGT [94] is a single forward model using a unified transformer that jointly predicts camera poses, depth maps, and point clouds for an arbitrary set of views. We run facebook/VGGT-1B at the native 518-pixel resolution; no extra iterative refinement is applied.

VGGT-Omega [95] We use official implementation code and VGGT-Omega-1B-512 checkpoint and run VGGT-Omega-1B at the native 512-pixel resolution.

Fast3R [116] performs one-shot multi-view prediction for up to a thousand views, using factorized global attention to scale VGGT-style reconstruction to long sequences. We use jedyang97/Fast3R_ViT_Large_512 with input width 512 (align 16) and `niter_PnP=100` for the auxiliary PnP-RANSAC pose estimation.

FastVGGT [82] accelerates VGGT by a training-free token-merging scheme that drops redundant cross-view tokens inside the transformer. In our runs (checkpoint checkpoints/fastvggt/model_tracker_fixed_e20.pt) we set `merging=0` (baseline layer) with `merge_ratio=0.9` and `enable_point=false` to save memory.

MUST3R [9] couples DUST3R-style pair prediction with a multi-view registrar that produces a single globally aligned reconstruction without per-scene optimization. We use MUST3R_512.pth at width 512 (align 16), with `preserve_gpu_mem=true` and `num_refinements_iterations=1`.

MapAnything [42] is a universal feed-forward reconstructor that can ingest any combination of images, poses, intrinsics and depth priors and output metric-scale dense geometry. We evaluate MapAnything on the facebook/map-anything checkpoint with `memory_efficient_inference=true` and `use_amp=true`.

OmniVGGT [71] augments VGGT with a Geo-Adapter so that any subset of camera poses with intrinsics and depths can be injected as priors. We run Livioni/OmniVGGT in its prior-free configuration for the main comparison, and additionally use its prior-injection branch in Table 3.

Pi3 (π^3) [101] removes the reference-frame bias of VGGT-style models with a permutation-equivariant design, predicting depth and cameras in a symmetric manner across views. We evaluate yyfz233/Pi3 and its metric variant yyfz233/Pi3X. Pi3X additionally predicts metric-scale depth and is evaluated without scale alignment. Pi3X also supports causal prior information injection, which is also used in Table 3.

AMB3R [93] introduces an attention-based multi-branch backbone that outputs metric-

scale depth and poses in one forward pass. We use checkpoints/amb3r/amb3r.pt with depth_alignment=none and data_type=bf16.

Depth Anything 3 (DA3) [54] is a scalable 3D foundation model based on transformers trained on large-scale data. We benchmark four sizes: **DA3-Small** (depth-anything/DA3-SMALL), **DA3-Base** (depth-anything/DA3-BASE), **DA3-Large 1.1** (depth-anything/DA3-LARGE-1.1) and **DA3-Giant 1.1** (depth-anything/DA3-GIANT-1.1), all with reference-view strategy ref_view_strategy=first for fair comparison. The two-branch variant **DA3Nested** (depth-anything/DA3NESTED-GIANT-LARGE-1.1) outputs metric-scale depth by combining an anyview Giant branch with a metric Large branch.

WorldMirror [59] is a unified feed-forward reconstruction model that can flexibly condition on (pose, depth, intrinsic) priors. We use tencent/HunyuanWorld-Mirror with cond_flags=[0,0,0] (no prior) for the main benchmark.

B.5.3. Online / Streaming Methods

Spann3R [92] builds an external spatial memory on top of DUST3R so that each incoming frame can be incrementally fused into a shared canonical frame. We use spann3r_101.pth at a resolution of 224 (align 16) with inference_mode=online, use_feat=false and focal_mode=weiszfeld.

CUT3R [98] performs continuous updating of a persistent internal scene state, regressing dense geometry frame-by-frame. We use the default CUT3R checkpoint at width 512 (align 16) with focal_mode=weiszfeld for focal estimation.

MonST3R [125] specializes DUST3R for dynamic scenes by injecting temporal smoothness, optical-flow, and translation losses into the global optimizer. We use Junyi42/MonST3R_PO-TA-S-W_ViTLarge_BaseDecoder_512_dpt at width 512 (align 16) with niter=300, schedule=linear, lr=0.01, batch_size=16, winsize=5, scenegraph_type=swinstride, flow_loss_weight=0.01, flow_loss_threshold=25, flow_loss_start_iter=0.1, sam2_mask_refine=true, batchify=true (temporal_smoothing_weight=0.01, translation_weight=1.0, shared_focal=true).

Point3R [107] maintains an explicit online 3D point memory that grows as new frames arrive, enabling streaming reconstruction with constant-time per-frame cost. We use point3r_512.pth at width 512 (align 16) with focal_mode=weiszfeld.

Stream3R [46] formulates multi-view reconstruction as causal next-token prediction over pointmaps, enabling an efficient StreamVGGT-style decoder. We use yslan/Stream3R checkpoint and implement stream and window variants using default settings.

StreamVGGT [136] is a streaming counterpart of VGGT with temporally causal cross-view attention and KV-caching. We use lch01/StreamVGGT in the default online mode.

PAGE4D [133] extends VGGT to 4D reconstruction by modeling both static scene geometry and dynamic motion components. We use checkpoints/page4d/checkpoint_nomask.pt in its default configuration.

InfiniteVGGT [123] augments StreamVGGT with a rolling KV-cache, so that arbitrarily long sequences can be processed with bounded memory. We use lch01/StreamVGGT as the backbone, image width 518 (align 14) and total_budget=1,200,000 KV-tokens.

WinT3R [52] employs a sliding-window transformer with a camera-token pool

to capture long-range geometry cheaply. We use lizizun/WinT3R at width 512 (align 16) with `inference_mode=online`, `window_size=4`, `state_size=1024` and `ret_first_pred=false`.

LongStream [17] builds on a VGGT backbone with a keyframe-driven long-context memory module to target long-horizon streaming reconstruction. We use NicolasCC/LongStream at width 518 (align 14) under `streaming_mode=causal` with `keyframe_stride=8`, `keyframe_mode=fixed` and `rel_pose_num_iterations=4`, and evaluate two inference variants: *batch-refresh* and *streaming-refresh* with a sliding window of size 48. The `refresh` parameter is set to 3 for *batch-refresh* and 7 for *streaming-refresh*. In addition, we disable the scale token prediction of LongStream, as we observe that enabling metric scale prediction introduces erroneous outliers in depth estimation metrics on our benchmark, despite the model natively supporting metric-scale output.

LingBot-Map [13] is an online mapping model designed for streaming data, supporting both per-frame streaming and window-based inference with KV-cache sliding windows. We evaluate two variants: **LingBot-Map (windowed)** with `mode>windowed`, `window_size=64`, `overlap_size=16`, `num_scale_frames=8`, `kv_cache_sliding_window=64` and `camera_num_iterations=4`; and **LingBot-Map (streaming)** with adaptive `keyframe_interval`, `kv_cache_sliding_window=64`, `kv_cache_scale_frames=8` and SDPA attention (`use_sdpa=false`, `enable_3d_rope=true`). Both variants use `image_size=518`, `patch_size=14` and `enable_point=false`. The medium regime runs use the long-context checkpoint `lingbot-map-long.pt`, while the sparse and single-frame settings use the short-context `lingbot-map.pt` checkpoint.

B.5.4. Chunk-based Methods

VGGT-Long [23] scales VGGT to long sequences by overlapping-chunk inference and cross-chunk Sim(3) alignment. We use facebook/VGGT-1B as the backbone with `chunk_size=60` and `overlap=30`. The chunked streaming variant **DA3-Streaming** uses backbone `depth-anything/DA3-GIANT-1.1` with `chunk_size=60`, `overlap=30` and `ref_view_strategy=first` for long sequences. The long-sequence variant **Pi-Long** (built on the Pi3 backbone) also uses `chunk_size=60`, `overlap=30`.

B.5.5. SLAM-based Methods

MASt3R-SLAM [66] integrates MASt3R’s metric dense matcher into a SLAM pipeline that jointly estimates camera trajectory and metric geometry. We use `MASt3R_ViTLarge_BaseDecoder_512_catmlpdppt_metric.pth` in uncalibrated mode (`use_calib=false`), with explicit overrides `img_size=512` and `c_conf_threshold=1.5` (point-cloud filtering); the remaining tracking hyper-parameters use the official `config/base.yaml` defaults (`C_conf=0.0`, `Q_conf=1.5`, `min_match_frac=0.05`, `max_iters=50`).

VGGT-SLAM [61] turns VGGT into a SLAM system by constructing overlapping submaps and performing Sim(3) cross-submap alignment with loop closures. We use facebook/VGGT-1B with `submap_size=32`, `overlapping_window_size=3`, `max_loops=0` (no loop closure), `conf_threshold=25.0`, `lc_thres=0.95` and `use_optical_flow=true`.

B.5.6. Test-Time Training Methods

TTT3R [16] performs per-sequence test-time training on top of a CUT3R-style backbone, fine-tuning a small set of parameters to adapt to each scene. We use `cut3r_512_dpt_4_64.pth` at width 512 (align 16) with `focal_mode=weiszfeld`.

Scal3R [113] introduces a scalable pipeline that processes long videos in blocks with loop-level test-time refinement. We use `xbillowy/Scal3R` at width 518 (align 14) with `block_size=60`, `overlap_size=30` (20 for dense), `loop_size=20`, `use_xyz_align=1` and `test_use_amp=false`.

LoGeR [126] is a long-context hybrid-memory geometry model that combines test-time training with sliding-window attention. We evaluate the LoGeR and LoGeR* variants from Junyi42/LoGeR at width 518 (align 14) with `window_size=32`, `overlap_size=3` and `reset_every=1` (TTT-state reset across windows). For LoGeR we set `se3=false`, `sim3=false`; for LoGeR* we set `se3=true`, `sim3=false`.

B.6. SpatialBench Visualizations

Qualitative Comparison on Representative SpatialBench Cases. Fig. 15 visualizes four representative cases from SpatialBench, covering short indoor reconstruction, dense outdoor driving, dense indoor long-horizon reconstruction, and wrist-view out-of-distribution input. Each case shows the sampled input views, point-cloud reconstructions from representative methods, and the corresponding depth and camera metrics.

Qualitative Comparison on Prior-Enhanced Models. Fig. 16, Fig. 17, and Fig. 18 present qualitative comparisons of prior-aware models under joint camera and depth prior injection, camera-only prior injection, and depth-only prior injection settings, respectively.

Bad Cases For Prior-Enhanced Models. Fig. 19 illustrates representative failure cases of prior-aware models under challenging conditions, including object-centric scenes, extreme no-overlap view, and out-of-distribution wrist-view sequences. MapAnything fails on object-centric scenes when GT camera priors are injected. WorldMirror fails on out-of-distribution scenes such as wrist-view sequences, even with both camera and depth priors provided. OmniVGGT breaks down under extreme no-overlap conditions.

B.7. Evaluated Models and Training Datasets in SpatialBench

In this subsection, we summarize the training data and annotations used by all evaluated methods. Tab. 5 presents the training datasets of all compared methods, excluding training-free and chunk-wise methods, as they do not involve explicit training. Evaluation-only, qualitative-only, and runtime benchmark datasets are not marked. ✓ indicates datasets directly used for model training. ✓ indicates that the method is initialized from a pretrained checkpoint whose backbone has been trained on the corresponding dataset. Tab. 6 presents the properties of each dataset, including scene type, real-world vs. synthetic domain, the presence of dynamic content, and public license information.

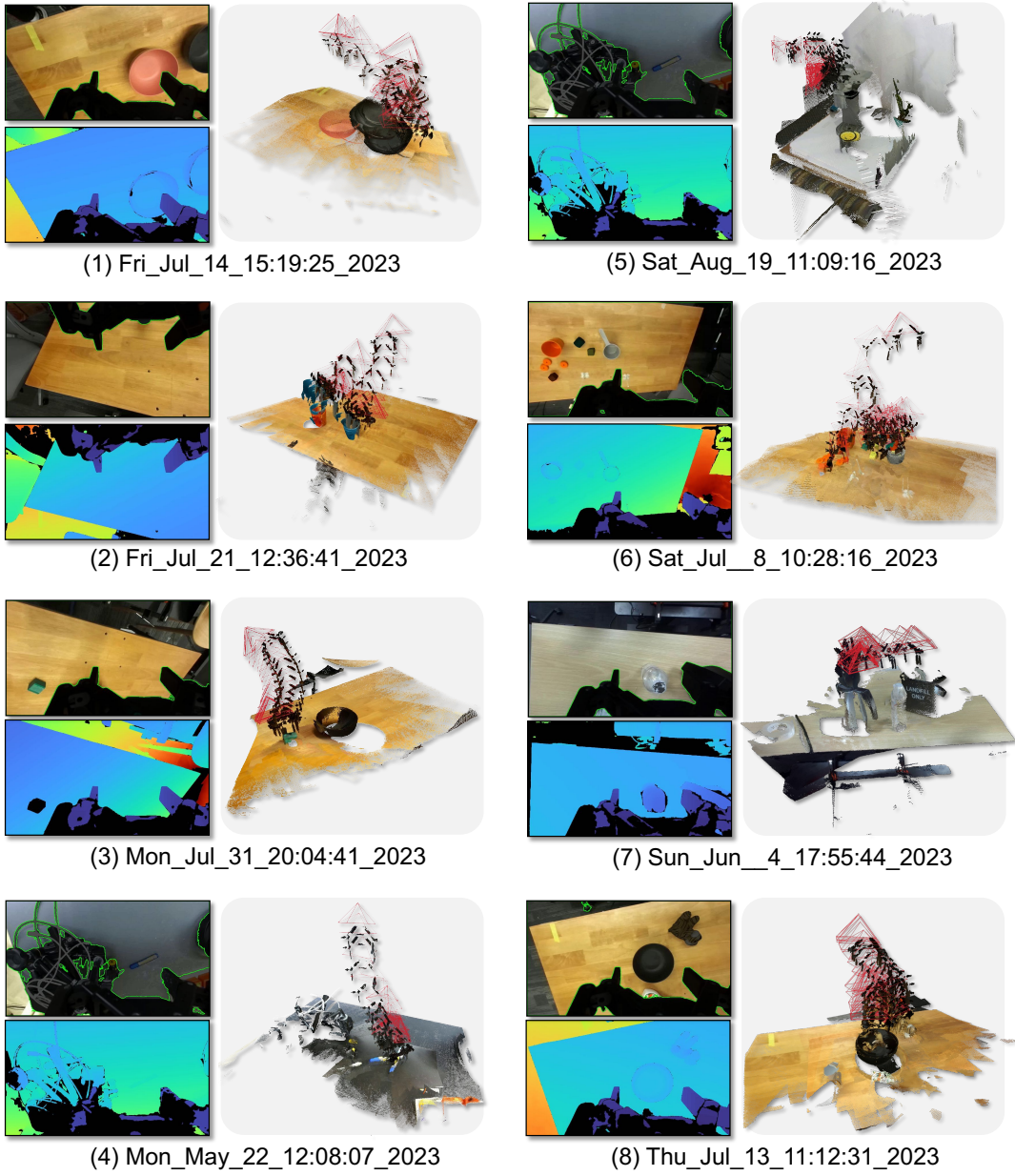


Figure 12 | DROID Gallery 1.

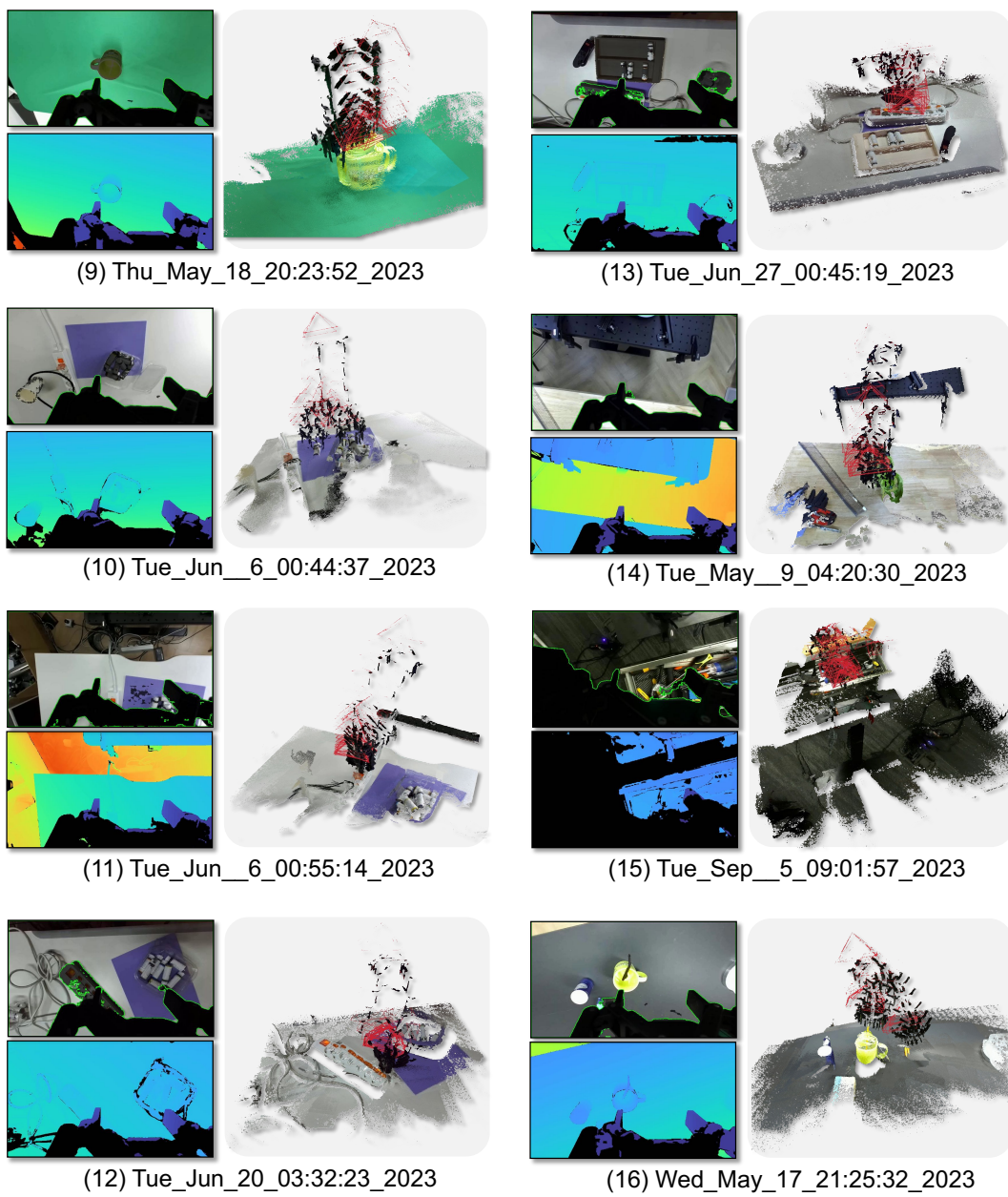


Figure 13 | DROID Gallery 2.

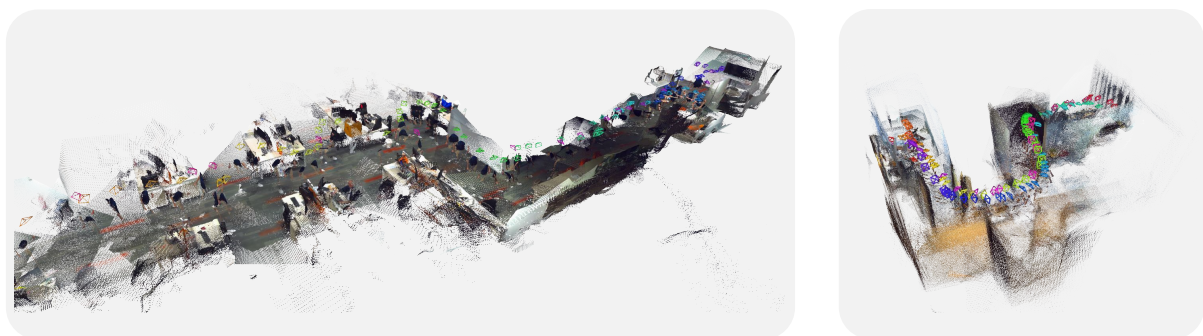


Figure 14 | Visualization of Xperience Samples.

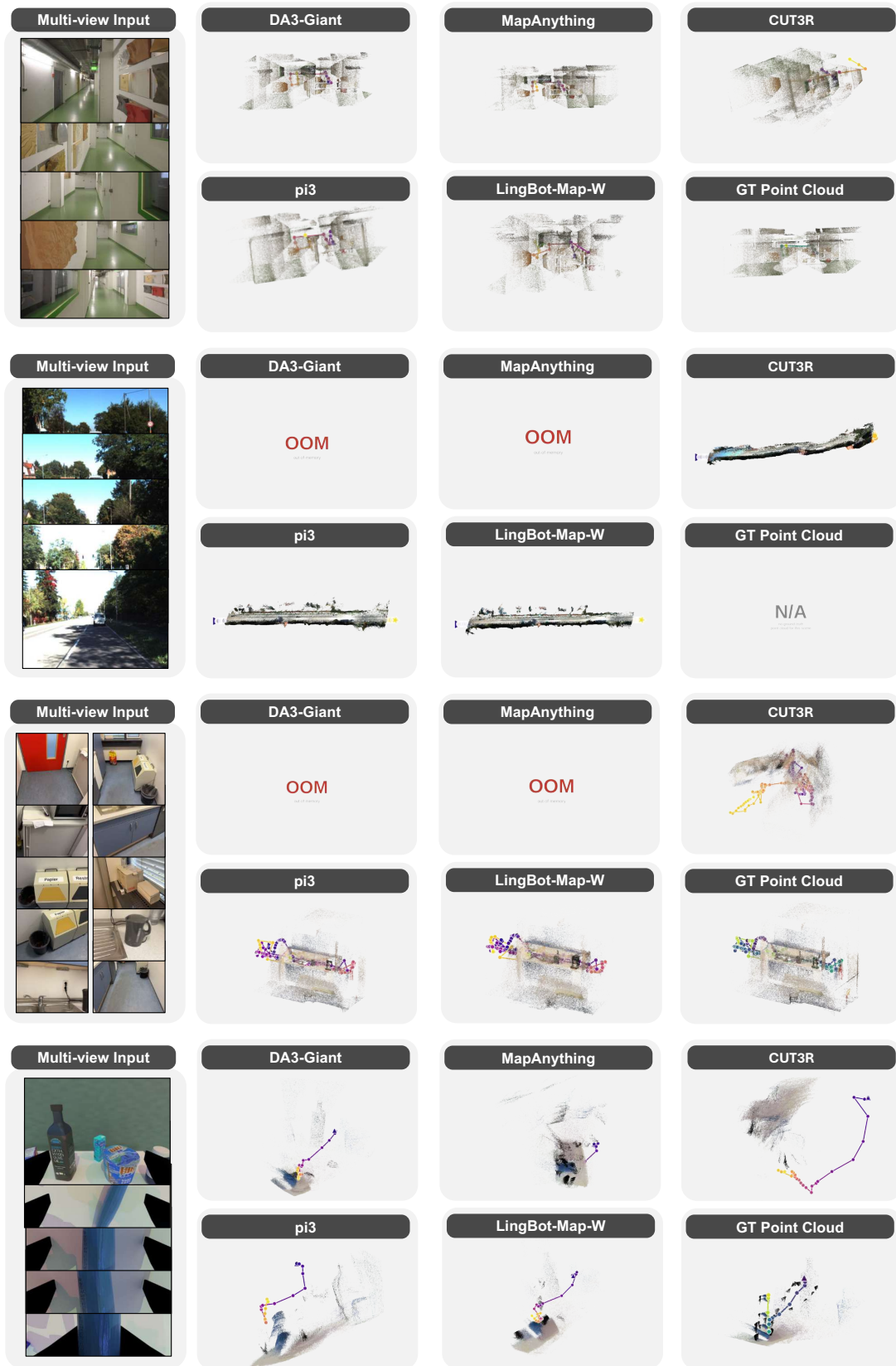


Figure 15 | **Representative benchmark cases.** We show input views, per-method point-cloud reconstructions, and depth/camera metrics for four representative scenes spanning short indoor reconstruction, dense outdoor driving, dense indoor long-horizon reconstruction, and wrist-view OOD input.

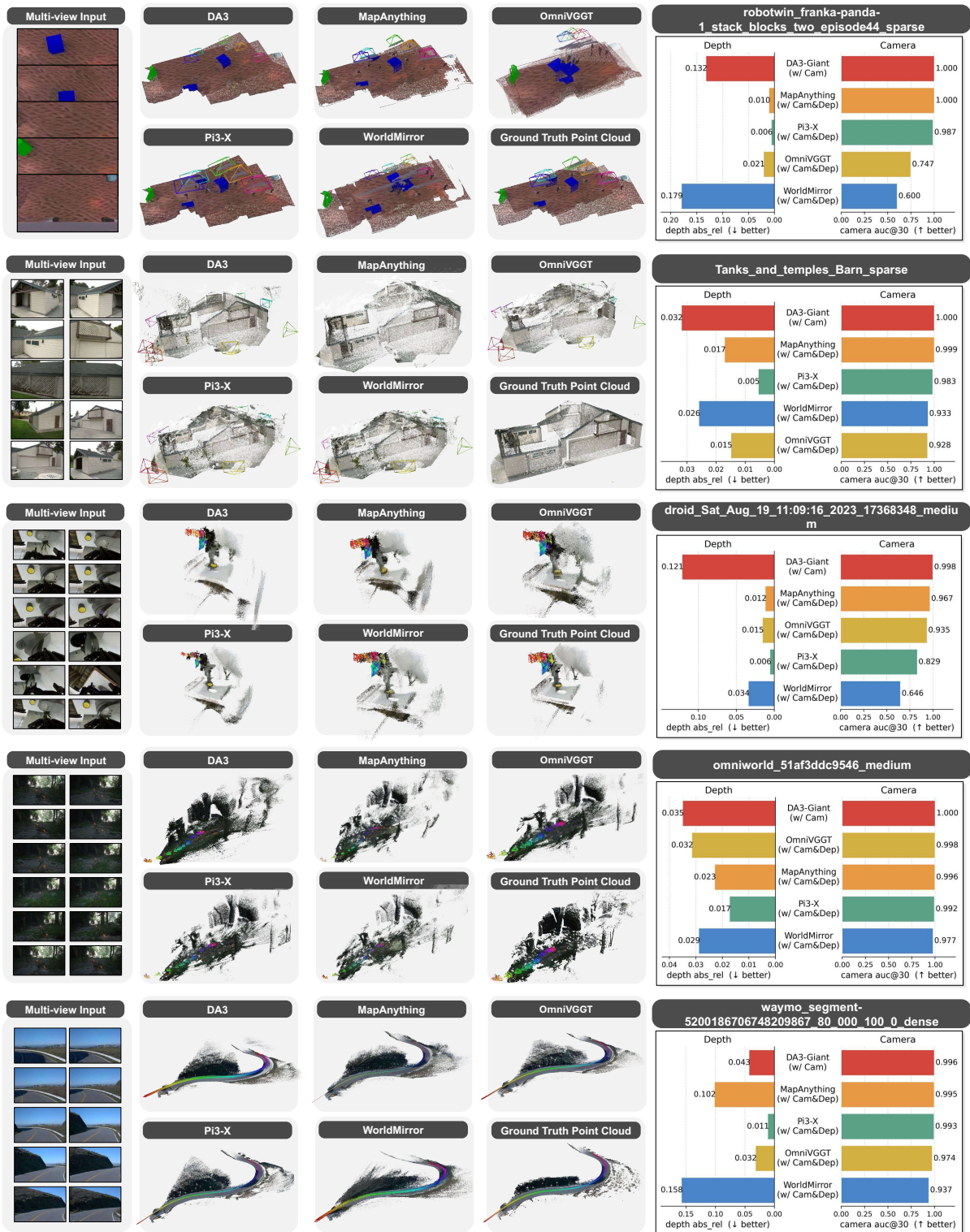


Figure 16 | **Qualitative Comparison on Prior-Enhanced Models with Auxiliary Camera and Depth Information.** We visualize the reconstruction quality of DA3-Giant, MapAnything, OmniVGGT, Pi3, and WorldMirror under the setting where both camera and depth prior information are provided as auxiliary inputs. For each scene, the right panel reports the depth AbsRel and camera AUC@30 metrics for each method.

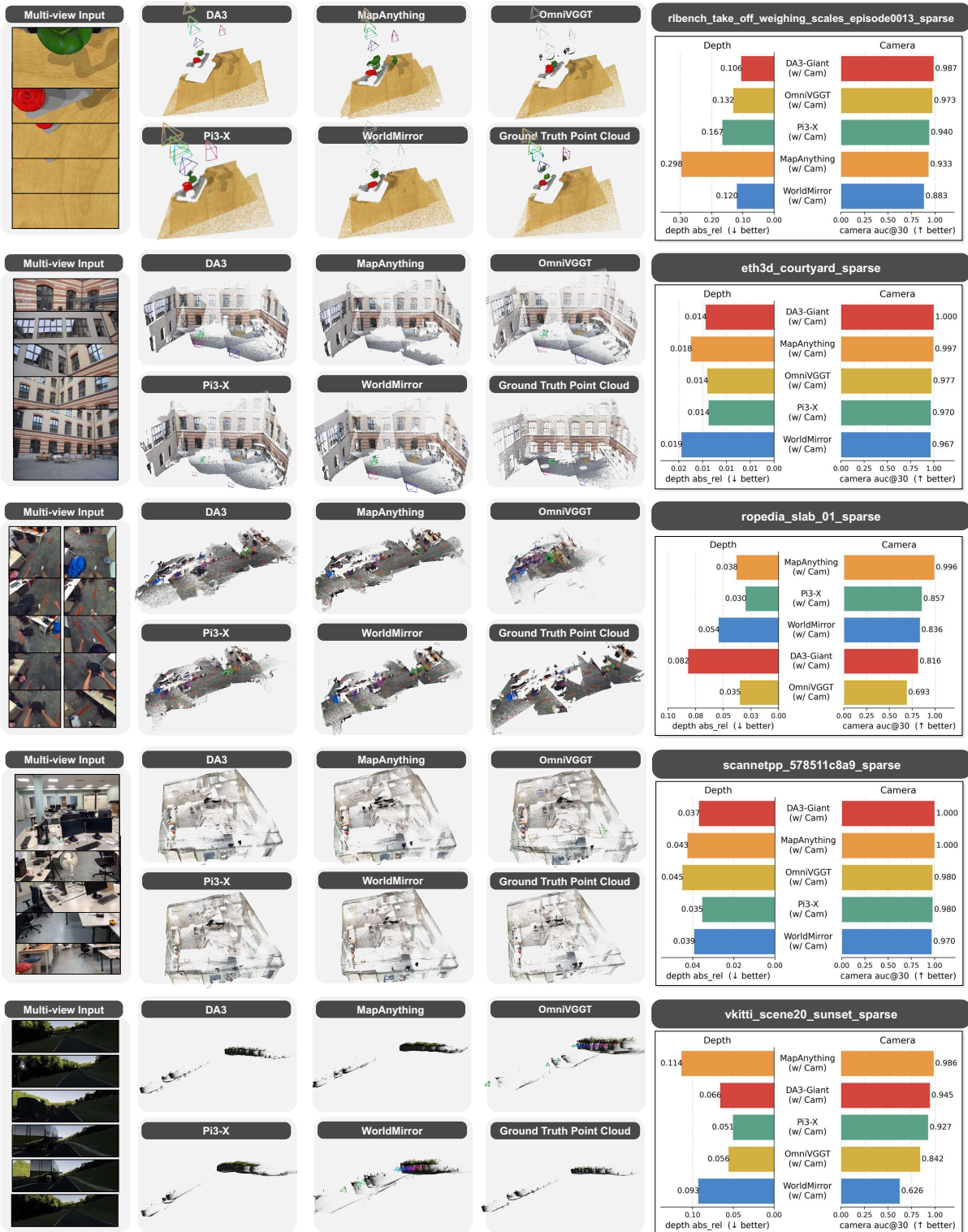


Figure 17 | **Qualitative Comparison on Prior-Enhanced Models with Auxiliary Camera Information.** We visualize the reconstruction quality of DA3-Giant, MapAnything, OmniVGGT, Pi3, and WorldMirror under the setting where camera prior information is provided as auxiliary inputs. For each scene, the right panel reports the depth AbsRel and camera AUC@30 metrics for each method.

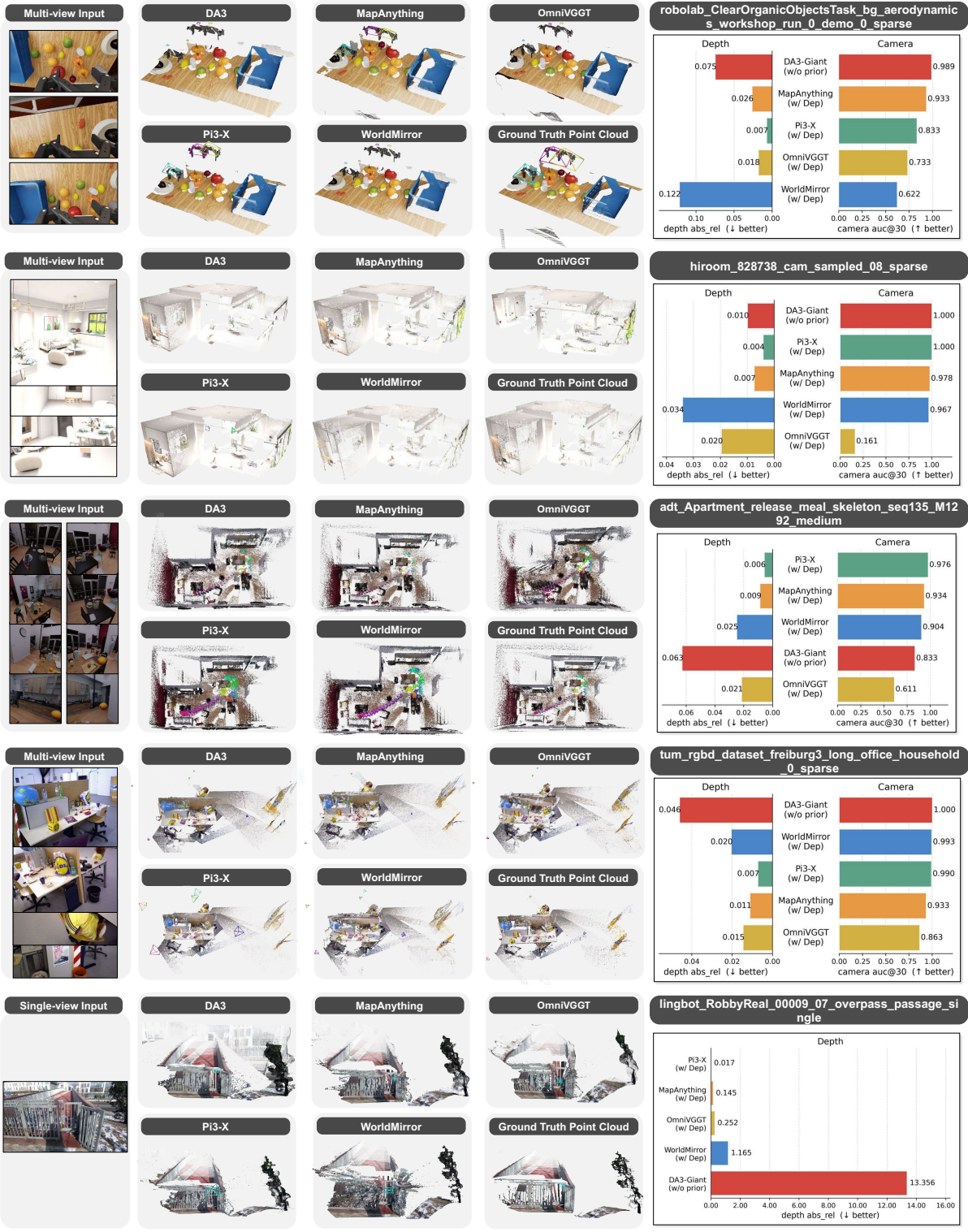


Figure 18 | **Qualitative Comparison on Prior-Enhanced Models with Auxiliary Depth Information.** We visualize the reconstruction quality of DA3-Giant, MapAnything, OmniVGGT, Pi3, and WorldMirror under the setting where depth prior information is provided as auxiliary inputs. For each scene, the right panel reports the depth AbsRel and camera AUC@30 metrics for each method.

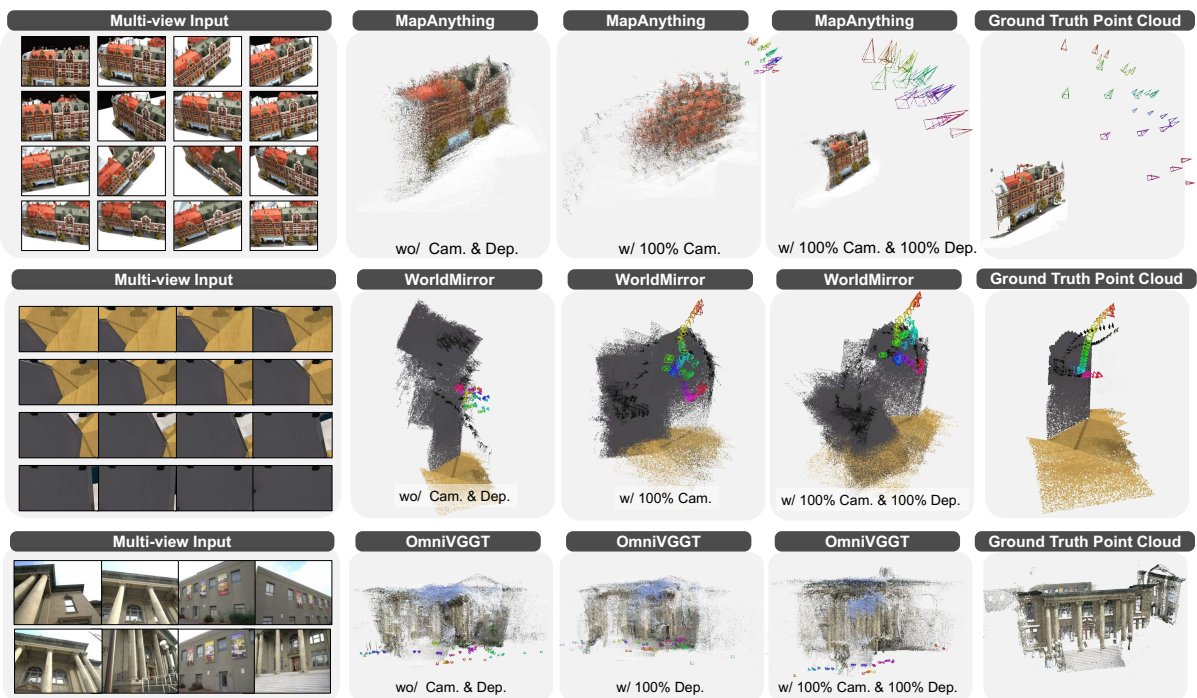


Figure 19 | **Failure Cases on Challenging Scenes.** We visualize failure cases of MapAnything, WorldMirror, and OmniVGGT across three challenging scenes.

Table 5 | **Dataset usage across all methods.** ✓ indicates datasets directly used for model training, fine-tuning, or teacher/student training; ✓ indicates datasets inherited from a pretrained checkpoint whose backbone has been trained on the corresponding dataset. The last row reports total used (trained): the first number counts all datasets either directly used by the method or inherited through its pretrained checkpoint, while the number in parentheses counts only datasets used to train or fine-tune the method itself. Identical values, e.g., 42 (42), indicate that no additional datasets are inherited. Evaluation-only, qualitative-only, and runtime benchmark datasets are not marked.

Dataset	End-to-end											Online / streaming							Test-Time Training					
	AMg3R	D43	DUS3R	Fuse3R	MapAnything	MAS3R	MUS3R	OmniVCGT	π^3	VCGT	WorldMerge	CUT3R	Lingbo-map	LongStream	Mono3R	PAC3D	Point3R	Span3R	Stream3R	StreamVCGT	WDT3R	TIT3R	Scal3R	LoCar
CO3D [75]	✓	✓	✓	✓		✓	✓	✓	✓	✓	✓	✓	✓	✓	✓	✓	✓	✓	✓	✓	✓	✓	✓	✓
RealEstate10K [134]																								
ScanNet [21]	✓	✓	✓	✓		✓	✓	✓	✓	✓	✓	✓	✓	✓	✓	✓	✓	✓	✓	✓	✓	✓	✓	✓
ScanNet++ [121]	✓	✓	✓	✓	✓	✓	✓	✓	✓	✓	✓	✓	✓	✓	✓	✓	✓	✓	✓	✓	✓	✓	✓	✓
ARKitScenes [5]	✓	✓	✓	✓		✓	✓	✓	✓	✓	✓	✓	✓	✓	✓	✓	✓	✓	✓	✓	✓	✓	✓	✓
Habitat [79]	✓	✓	✓	✓		✓	✓	✓	✓	✓	✓	✓	✓	✓	✓	✓	✓	✓	✓	✓	✓	✓	✓	✓
BlendedMVS [120]	✓	✓	✓	✓		✓	✓	✓	✓	✓	✓	✓	✓	✓	✓	✓	✓	✓	✓	✓	✓	✓	✓	✓
MegaDepth [50]	✓	✓	✓	✓		✓	✓	✓	✓	✓	✓	✓	✓	✓	✓	✓	✓	✓	✓	✓	✓	✓	✓	✓
DL3DV [57]	✓	✓	✓	✓	✓	✓	✓	✓	✓	✓	✓	✓	✓	✓	✓	✓	✓	✓	✓	✓	✓	✓	✓	✓
MapFree [2]	✓	✓	✓	✓		✓	✓	✓	✓	✓	✓	✓	✓	✓	✓	✓	✓	✓	✓	✓	✓	✓	✓	✓
WildRGBD [109]	✓	✓	✓	✓		✓	✓	✓	✓	✓	✓	✓	✓	✓	✓	✓	✓	✓	✓	✓	✓	✓	✓	✓
Waymo [87]	✓	✓	✓	✓		✓	✓	✓	✓	✓	✓	✓	✓	✓	✓	✓	✓	✓	✓	✓	✓	✓	✓	✓
VirtualKITTI [8]	✓	✓	✓	✓		✓	✓	✓	✓	✓	✓	✓	✓	✓	✓	✓	✓	✓	✓	✓	✓	✓	✓	✓
TartanAir [100]	✓	✓	✓	✓		✓	✓	✓	✓	✓	✓	✓	✓	✓	✓	✓	✓	✓	✓	✓	✓	✓	✓	✓
Unreal4K [90]	✓	✓	✓	✓		✓	✓	✓	✓	✓	✓	✓	✓	✓	✓	✓	✓	✓	✓	✓	✓	✓	✓	✓
MVS-Synth [34]	✓	✓	✓	✓		✓	✓	✓	✓	✓	✓	✓	✓	✓	✓	✓	✓	✓	✓	✓	✓	✓	✓	✓
HyperSim [76]	✓	✓	✓	✓		✓	✓	✓	✓	✓	✓	✓	✓	✓	✓	✓	✓	✓	✓	✓	✓	✓	✓	✓
Mapillary [1]	✓	✓	✓	✓		✓	✓	✓	✓	✓	✓	✓	✓	✓	✓	✓	✓	✓	✓	✓	✓	✓	✓	✓
ASE [3]	✓	✓	✓	✓		✓	✓	✓	✓	✓	✓	✓	✓	✓	✓	✓	✓	✓	✓	✓	✓	✓	✓	✓
ADT [69]	✓	✓	✓	✓		✓	✓	✓	✓	✓	✓	✓	✓	✓	✓	✓	✓	✓	✓	✓	✓	✓	✓	✓
PointOdyssey [131]	✓	✓	✓	✓		✓	✓	✓	✓	✓	✓	✓	✓	✓	✓	✓	✓	✓	✓	✓	✓	✓	✓	✓
Spring [64]	✓	✓	✓	✓		✓	✓	✓	✓	✓	✓	✓	✓	✓	✓	✓	✓	✓	✓	✓	✓	✓	✓	✓
Dynamic Replica [40]					✓																			
ParallelDomain-4D [91]					✓																			
SAIL-VOS 3D [32]					✓																			
OmniObject3D [106]	✓	✓	✓	✓		✓	✓				✓													
StaticThings3D [81]															✓		✓				✓			
TartanGround [70]												✓												✓
Matterport3D [11]								✓			✓		✓									✓		
BEDLAM [7]												✓										✓		
UASOL [6]								✓														✓		
MVImgNet [122]																						✓		
CoP3D [84]																						✓		
EDEN [47]																						✓		
IRS [97]																						✓		
Synscapes [105]																						✓		
3D Ken Burns [67]																						✓		
SmartPortraits [45]																						✓		
UrbanSyn [28]																						✓		
HO4D [60]																						✓		
Kubric [29]	✓	✓	✓	✓				✓	✓	✓	✓	✓	✓	✓	✓	✓	✓	✓	✓	✓	✓	✓	✓	✓
Replica [85]	✓	✓	✓	✓				✓	✓	✓	✓	✓	✓	✓	✓	✓	✓	✓	✓	✓	✓	✓	✓	✓
Objaverse [22]	✓	✓	✓	✓				✓	✓	✓	✓	✓	✓	✓	✓	✓	✓	✓	✓	✓	✓	✓	✓	✓
Texverse [127]																								
GTA-SfM [96]	✓	✓	✓	✓				✓	✓	✓	✓	✓	✓	✓	✓	✓	✓	✓	✓	✓	✓	✓	✓	✓
SceneNet RGB-D [63]																								
MatrixCity [49]																								
Mid-Air [24]																								
KITTI-360 [53]																								
Gibson [108]																								
HM3D [74]																								
Taskonomy [124]																								
MegaSynth [38]																								
OmniWorld [135]																								
Trellis [110]																								
TauAgent [27]																								
Structured3D [129]																								
DIML Outdoor [18]																								
DDAD [30]																								
Argoverse [12]																								
Lyft [31]																								
PandaSet [111]																								
DSEC [25]																								
Driving Stereo [115]																								
Cityscapes [20]																								

#Datasets: total used (trained) 22 (11) 42 (42) 8 (8) 10 (8) 13 (13) 14 (14) 13 (13) 27 (19) 24 (14) 17 (17) 23 (15) 32 (32) 30 (30) 19 (18) 11 (4) 20 (6) 16 (14) 9 (6) 36 (29) 21 (13) 15 (12) 32 (0) 18 (18) 29 (13)

Table 6 | **Dataset licenses and basic properties.** We summarize the scene type, real/synthetic domain, dynamic content, and public license or access terms for each dataset. “Non-Commercial” denotes non-commercial use, “Terms” denotes dataset-specific access terms, and “Not specified” indicates that no clear standalone public dataset license was identified.

Idx.	Dataset	Scene Type	Real/Synth.	Dynamic	License / Access Terms
1	CO3D [75]	Object	Real	Static	CC BY-NC 4.0
2	RealEstate10K [134]	Indoor+Outdoor	Real	Static	CC BY 4.0
3	ScanNet [21]	Indoor	Real	Static	Non-Commercial
4	ScanNet++ [121]	Indoor	Real	Static	Non-Commercial
5	ARKitScenes [5]	Indoor	Real	Static	Non-Commercial
6	Habitat [79]	Indoor	Real	Static	Habitat dataset-specific terms
7	BlendedMVS [120]	Indoor+Outdoor	Synth.	Static	CC BY 4.0
8	MegaDepth [50]	Outdoor	Real	Static	CC BY 4.0 + source image licenses
9	DL3DV [57]	Indoor+Outdoor	Real	Mostly Static	DL3DV Terms
10	MapFree [2]	Outdoor	Real	Static	Non-Commercial
11	WildRGBD [109]	Object	Real	Static	MIT
12	Waymo [87]	Outdoor	Real	Dynamic	Non-Commercial
13	VirtualKITTI [8]	Outdoor	Synth.	Dynamic	CC BY-NC-SA 3.0
14	TartanAir [100]	Indoor+Outdoor	Synth.	Dynamic	CC BY 4.0
15	Unreal4K [90]	Indoor+Outdoor	Synth.	Static	MIT
16	MVS-Synth [34]	Outdoor	Synth.	Mostly Static	Non-Commercial
17	HyperSim [76]	Indoor	Synth.	Static	CC BY-SA 3.0
18	Mapillary [1]	Outdoor	Real	Static	CC BY-NC-SA
19	ASE [3]	Indoor	Synth.	Static	Non-Commercial
20	ADT [69]	Indoor	Real	Dynamic	Non-Commercial
21	PointOdyssey [131]	Indoor+Outdoor	Synth.	Dynamic	CC BY-NC-SA 4.0
22	Spring [64]	Outdoor	Synth.	Dynamic	CC BY 4.0
23	Dynamic Replica [40]	Indoor	Synth.	Dynamic	Non-Commercial
24	ParallelDomain-4D [91]	Outdoor	Synth.	Dynamic	CC BY-NC 4.0
25	SAIL-VOS 3D [32]	Indoor+Outdoor	Synth.	Dynamic	Non-Commercial
26	OmniObject3D [106]	Object	Real	Static	CC BY 4.0
27	StaticThings3D [81]	Object	Synth.	Static	Non-Commercial
28	TartanGround [70]	Outdoor	Synth.	Static	CC BY 4.0
29	Matterport3D [11]	Indoor	Real	Static	Non-Commercial
30	BEDLAM [7]	Human-centric	Synth.	Dynamic	Non-Commercial
31	UASOL [6]	Outdoor	Real	Static	CC BY-NC-SA 3.0
32	MVImgNet [122]	Object	Real	Static	MVImgNet Terms
33	CoP3D [84]	Object	Real	Dynamic	CC BY-NC 4.0
34	EDEN [47]	Outdoor	Synth.	Static	Research Use
35	IRS [97]	Indoor	Synth.	Static	Apache 2.0
36	Synscapes [105]	Outdoor	Synth.	Dynamic	Non-Commercial
37	3D Ken Burns [67]	Indoor+Outdoor	Synth.	Static	CC BY-NC-SA 4.0
38	SmartPortraits [45]	Human-centric	Real	Dynamic	Academic Use
39	UrbanSyn [28]	Outdoor	Synth.	Dynamic	CC BY-SA 4.0
40	HOI4D [60]	Indoor	Real	Dynamic	CC BY-NC 4.0
41	Kubric [29]	Object	Synth.	Dynamic	Apache 2.0
42	Replica [85]	Indoor	Real	Static	Research Use
43	Objaverse [22]	Object	Synth.	Static	Per-object CC licenses
44	TexVerse [127]	Object	Synth.	Static	Per-object CC licenses
45	GTA-SfM [96]	Outdoor	Synth.	Static	Not specified
46	SceneNet RGB-D [63]	Indoor	Synth.	Static	Non-Commercial
47	MatrixCity [49]	Outdoor	Synth.	Static	CC BY-NC 4.0
48	Mid-Air [24]	Outdoor	Synth.	Static	CC BY-NC-SA 4.0
49	KITTI-360 [53]	Outdoor	Real	Dynamic	CC BY-NC-SA 3.0
50	Gibson [108]	Indoor	Real	Static	Non-Commercial
51	HM3D [74]	Indoor	Real	Static	Non-Commercial
52	Taskonomy [124]	Indoor	Real	Static	Non-Commercial
53	MegaSynth [38]	Indoor	Synth.	Static	CC BY-NC-SA 4.0
54	OmniWorld [135]	Outdoor	Synth.	Dynamic	CC BY-NC-SA 4.0
55	Trellis [110]	Object	Synth.	Static	MIT
56	TauAgent [27]	Indoor+Outdoor	Synth.	Dynamic	Not specified
57	Structured3D [129]	Indoor	Synth.	Static	Structured3D Terms
58	DIML Outdoor [18]	Outdoor	Real	Mostly Static	Non-Commercial
59	DDAD [30]	Outdoor	Real	Dynamic	CC BY-NC-SA 4.0
60	Argoverse [12]	Outdoor	Real	Dynamic	CC BY-NC-SA 4.0
61	Lyft [31]	Outdoor	Real	Dynamic	CC BY-NC-SA 4.0
62	PandaSet [111]	Outdoor	Real	Dynamic	CC BY 4.0
63	DSEC [25]	Outdoor	Real	Dynamic	CC BY-SA 4.0
64	Driving Stereo [115]	Outdoor	Real	Dynamic	MIT
65	Cityscapes [20]	Outdoor	Real	Dynamic	Non-Commercial

C. The Collection of DA-Next-5M

This section details the data collection pipeline of DA-Next-5M. DA-Next-5M consists of 22K sequences with 5.5M frames in total. Each scene in the dataset contains an image sequence $\mathbf{I} \in \mathbb{R}^{N \times H \times W \times 3}$, depth maps $\mathbf{D} \in \mathbb{R}^{H \times W \times N}$, camera intrinsics $\mathbf{K} \in \mathbb{R}^{3 \times 3}$, and camera extrinsics $\mathbf{G}_{c2w} \in \text{SE}(3)$ for each frame. Fig. 4 showcases data samples from DA-Next-5M. Note that all evaluation scenes in SpatialBench are held out from the training splits of their respective datasets.

Table 7 | DA-Next-5M dataset statistics.

Id	Dataset	View	R/S	Fr.	Sc.
1	Xperience [78]	Ego	Real	400K	100
2	Aria Digital Twin [69]	Ego	Syn.	86K	232
3	Colosseum [72]	Wrist	Syn.	334K	1,837
4	HOI4D [60]	Ego	Real	739K	2,466
5	RLBench [36]	Wrist	Syn.	1.2M	5,120
6	Robolab [118]	Wrist	Syn.	158K	132
7	RoboTwin [14]	Wrist	Syn.	2.6M	11,923

Aria Digital Twin (ADT). ADT [69] is an egocentric RGB-D dataset captured with Meta Project Aria smart glasses in two instrumented indoor environments. It comprises 200 sequences of natural daily activities performed by 9 participants interacting with 398 object instances (344 static, 74 dynamic). We process the raw data into 232 sequences with 86K frames in total at a resolution of 512×512 using official preprocessing scripts. We observe scattered outlier points along object boundaries in scene visualizations and apply a unified depth post-processing step to refine the depth maps accordingly.

HOI4D. HOI4D [60] is a large-scale 4D egocentric dataset for category-level human-object interaction, containing 2.4M RGB-D frames across 4,000 sequences collected by 9 participants interacting with 800 object instances from 16 categories in 610 distinct indoor rooms. Each frame provides RGB and depth from a head-mounted RGBD camera with a resolution of 1920×1080 , together with camera 6-DoF poses, 3D hand poses, category-level object poses, panoptic segmentation, and reconstructed scene point clouds. We directly use a subset of the raw HOI4D data (2.5K scenes and 739K frames) with only depth post-processing filtering (Appendix A.4) applied.

RLBench. RLBench [36] is a large-scale robot learning benchmark and simulation environment built on CoppeliaSim [77], featuring more than 100 distinct hand-designed manipulation tasks ranging from simple reaching to long-horizon multi-stage operations. Each task provides an unlimited supply of expert demonstrations via built-in motion planners. Visual observations include RGB, depth, and segmentation from both an over-the-shoulder stereo camera and an eye-in-hand monocular camera, with pixel-accurate synthetic depth and ground-truth 6-DoF camera poses available at every frame. Since the original simulation’s wrist-view camera does not capture the gripper, we adjust the wrist camera pose relative to the end-effector and increase the resolution to 1280×720 to broaden the field of view. We collect around 50 episodes per task using motion planners with random seeds across 103 tasks to form our dataset, with 1.2M frames in total.

Robo Colosseum. The Robo Colosseum [72] is a robotic manipulation benchmark built on top of RLBench that introduces systematic environmental perturbations for evaluating generalization. It provides 20 diverse manipulation tasks evaluated across 14 perturbation axes, including object color, texture, and size, background and tabletop appearance, lighting conditions, number of distractors, physical properties, and camera pose, with each perturbation applied independently and in combination. RGB, depth, and camera pose annotations are identical in format to RLBench. We similarly adjust the initial wrist camera placement and set the rendering resolution to 1280×720 . We collect 100 episodes per task

with random seeds across 19 tasks, which is 1.8K episodes with 334K frames. Domain randomization is configured as follows: the number of distractor objects is set to 5–8; camera pose perturbations follow `euler_range = [[-0.05, -0.05, -0.05], [0.05, 0.05, 0.05]]` and `position_range = [[0, 0, 0], [0, 0, 0.3]]`; surface colors (e.g., table and objects) are randomized within `color_range = [[0.25, 0.25, 0.25], [1.0, 1.0, 1.0]]`; lighting color is randomized within `[[0, 0, 0], [0.5, 0.5, 0.5]]`; object scale is perturbed in the range [0.8, 1.0]; and texture randomization is enabled for objects, the table surface, and the background.

RoboTwin. RoboTwin [14] is a large-scale simulation-based dataset and benchmark for bimanual robotic manipulation, built on top of the RoboTwin Object Dataset (RoboTwin-OD) comprising 731 object instances across 147 categories with rich manipulation annotations (grasp points, functional points, object axes) and diverse language descriptions. It spans 50 dual-arm collaborative manipulation tasks executed across 5 heterogeneous robot embodiments. For DA-Next-5M, we collect data using five robot embodiments: Aloha-AgileX, ARX-X5, Franka, Piper, and UR5 across 50 bimanual tasks, which is 11K scenes with 2.6M frames in total. The wrist camera resolution is set to 1280×720 with a field of view of 60° , and approximately 25 episodes are collected per task. Domain randomization is enabled with random backgrounds, cluttered table setups, a clean background rate of 0.2, random table height variation of 0.1, and random lighting. The wrist camera position is randomly switched between two fixed placements across episodes. For each episode, the image sequence from either the left or right arm is randomly selected for collection. The RoboTwin dataset has 12K episodes, comprising 2.6M frames in total.

Robolab. Robolab [118] is a high-fidelity simulation benchmarking framework for task-generalist robotic policies, developed by NVIDIA and built on Isaac Sim. It introduces the Robolab-120 benchmark comprising 120 tasks organized along three competency axes: *visual*, *procedural*, and *relational*, each at three difficulty levels, with LLM-enabled generation of novel scenes and tasks. Scenes feature photorealistic assets and physically accurate simulation, with ground-truth RGB, depth, and 6-DoF camera poses from wrist-mounted and external cameras. For DA-Next-5M, we use $\pi_{0.5}$ [35] as the trajectory generator to collect data across 108 tasks under 2 background settings, yielding a total of 158K frames at a resolution of 1280×720 .

D. Detail of DA-Next

D.1. Model Architecture

DA-Next is built upon the Giant variant of Depth-Anything-3 [54]. The backbone adopts the DINOv2 [68] ViT-Giant (vitg) architecture, in which Alternating Attention, QK-Norm, and Rotary Position Embedding (RoPE) are enabled starting from the 13th layer, while the `cat_token` and `scale_token` are retained. Multi-scale features are extracted from the 19th, 27th, 33rd, and 39th layers. The depth and ray prediction heads are instantiated as a DualDPT module with an input dimension of 3072, a feature dimension of 256, output channels of [256, 512, 1024, 1024], and an output dimension of 2. The Scale Head is implemented as a 3-layer MLP (input 1536, hidden 1024, ReLU activation, Softplus output), and the Camera Encoder has an output dimension of 1536. All weights are initialized from the officially released `da3-giant-1.1` checkpoint.

D.2. Training Objective

In DA-Next, all input images $\mathbf{I} = \{I_i\}_{i=1}^N$, together with the available camera parameters $\mathbf{C} = \{C_i\}_{i=1}^N = \{K_i, G_i\}_{i=1}^N$ (if provided), are fed into the network \mathcal{G} , which predicts the complete

ray maps $\hat{\mathbf{R}}$, depth maps $\hat{\mathbf{D}}$, scale \hat{S} , and their corresponding confidence maps $\hat{\mathbf{Y}}_d, \hat{\mathbf{Y}}_r$ in an end-to-end manner:

$$\mathcal{G}(\mathbf{I}, \mathbf{C}) = (\hat{\mathbf{R}}, \hat{\mathbf{D}}, \hat{\mathbf{Y}}_d, \hat{\mathbf{Y}}_r, \hat{S}). \quad (28)$$

The total training objective is a weighted sum of five task-specific ℓ_1 terms,

$$\mathcal{L} = \mathcal{L}_{\text{depth}} + \alpha \mathcal{L}_{\text{grad}} + \mathcal{L}_{\text{ray}} + \mathcal{L}_{\text{pmap}} + \mathcal{L}_{\text{scale}}, \quad (29)$$

with $\alpha = 1$. Let $m_p \in \{0, 1\}$ denote the per-pixel validity mask of the ground truth and $\Omega = \{p \mid m_p = 1\}$ the set of valid pixels across all N views, with $|\Omega|$ its cardinality. We detail each term below.

Confidence-weighted regression. Following Wang et al. [99], Leroy et al. [48], each dense prediction is supervised with a confidence-weighted ℓ_1 regression term. Given a prediction \hat{x} , its confidence \hat{y} , and the ground truth x , the per-pixel regression and confidence terms are

$$\ell_{\text{reg}}(\hat{x}, x; p) = \|\hat{x}_p - x_p\|_1, \quad \ell_{\text{conf}}(\hat{x}, x, \hat{y}; p) = \gamma \hat{y}_p \ell_{\text{reg}}(\hat{x}, x; p) - \beta \log \hat{y}_p, \quad (30)$$

where γ and β balance the data term and the confidence regularizer that prevents $\hat{y} \rightarrow 0$.

Depth loss. For the predicted depth map $\hat{\mathbf{D}}$ with confidence $\hat{\mathbf{Y}}_d$, the depth term aggregates the confidence-weighted and plain ℓ_1 terms over valid pixels:

$$\mathcal{L}_{\text{depth}}(\hat{\mathbf{D}}, \mathbf{D}; \hat{\mathbf{Y}}_d) = \frac{1}{|\Omega|} \sum_{p \in \Omega} \left(\gamma \hat{Y}_{d,p} |\hat{D}_p - D_p| - \beta \log \hat{Y}_{d,p} + |\hat{D}_p - D_p| \right). \quad (31)$$

Depth-gradient loss. To preserve sharp edges while enforcing smoothness on planar regions, we penalize the discrepancy between the depth gradients of the prediction and the ground truth:

$$\mathcal{L}_{\text{grad}}(\hat{\mathbf{D}}, \mathbf{D}) = \|\nabla_x \hat{\mathbf{D}} - \nabla_x \mathbf{D}\|_1 + \|\nabla_y \hat{\mathbf{D}} - \nabla_y \mathbf{D}\|_1, \quad (32)$$

where ∇_x and ∇_y are the horizontal and vertical finite difference operators. In practice, this term is evaluated in a multi-scale manner over J dyadic scales (stride 2^j , $j = 0, \dots, J-1$) and averaged.

Ray loss. The ray map $\hat{\mathbf{R}} \in \mathbb{R}^{N \times H \times W \times 6}$ encodes per-pixel camera origins $\hat{\mathbf{o}}$ and viewing directions $\hat{\mathbf{d}}$. With its confidence $\hat{\mathbf{Y}}_r$, the ray loss mirrors the depth term:

$$\mathcal{L}_{\text{ray}}(\hat{\mathbf{R}}, \mathbf{R}; \hat{\mathbf{Y}}_r) = \frac{1}{|\Omega|} \sum_{p \in \Omega} \left(\gamma \hat{Y}_{r,p} \|\hat{\mathbf{R}}_p - \mathbf{R}_p\|_1 - \beta \log \hat{Y}_{r,p} + \|\hat{\mathbf{R}}_p - \mathbf{R}_p\|_1 \right). \quad (33)$$

Point-map loss. We recover the 3D world points by back-projecting depth along the predicted rays, $\hat{\mathbf{P}} = \hat{\mathbf{D}} \odot \hat{\mathbf{d}} + \hat{\mathbf{o}}$, and supervise them with a masked ℓ_1 against the ground-truth world points \mathbf{P} :

$$\mathcal{L}_{\text{pmap}}(\hat{\mathbf{D}} \odot \hat{\mathbf{d}} + \hat{\mathbf{o}}, \mathbf{P}) = \frac{1}{|\Omega|} \sum_{p \in \Omega} \|\hat{\mathbf{P}}_p - \mathbf{P}_p\|_1. \quad (34)$$

Scale loss. The predicted global scale \hat{S} is supervised against the ground-truth scale factor S via a log-space ℓ_1 term,

$$\mathcal{L}_{\text{scale}}(\hat{S}, S) = \|f_{\log}(\hat{S}) - f_{\log}(S)\|_1, \quad f_{\log} : \mathbf{x} \mapsto \frac{\mathbf{x}}{\|\mathbf{x}\|} \log(1 + \|\mathbf{x}\|), \quad (35)$$

which compresses the dynamic range of absolute scale and yields stable gradients across scenes of drastically different sizes.

Ground-truth preprocessing and scale target. To remove the inherent scene-scale ambiguity across heterogeneous training data and keep the magnitudes of different modalities consistent, all ground-truth signals are canonicalized in a two-step procedure before loss computation. (i) *Coordinate canonicalization.* The first frame is taken as the reference: we apply the cam-to-world transform of the first camera to all extrinsics, and accordingly transform the ground-truth world points \mathbf{P} into the first-camera coordinate frame. (ii) *Scale normalization.* We then compute the per-scene scale factor as the mean ℓ_2 norm of the valid reprojected world points,

$$S = \frac{1}{|\Omega|} \sum_{p \in \Omega} \|\mathbf{P}_p\|_2, \quad (36)$$

and divide the ground-truth world points, depths and camera translations by S :

$$\mathbf{P} \leftarrow \mathbf{P}/S, \quad \mathbf{D} \leftarrow \mathbf{D}/S, \quad \mathbf{t} \leftarrow \mathbf{t}/S. \quad (37)$$

The resulting scalar S is also kept as the regression target of the scale head, so that \hat{S} in $\mathcal{L}_{\text{scale}}$ learns to recover the absolute metric scale that the other dense predictions are invariant to. During inference, the predicted \hat{S} is multiplied back to lift the normalized geometry into its metric space. We set $\gamma = 1.0$ and $\beta = 0.2$ for all confidence-weighted terms, use $J = 3$ scales for the multi-scale gradient loss, and apply quantile filtering with $\tau = 0.98$ to suppress outliers.

D.3. Camera Conditioning Training

We adopt a *stochastic pose-conditioning* scheme at training time: for each mini-batch we flip a Bernoulli coin with probability $p \in [0, 1]$, and inject the ground-truth camera as an auxiliary input only when the coin turns up, i.e.

$$u \sim \text{Bernoulli}(p), \quad (\hat{\mathbf{R}}, \hat{\mathbf{D}}, \hat{\mathbf{Y}}_d, \hat{\mathbf{Y}}_r, \hat{S}) = \begin{cases} \mathcal{G}(\mathbf{I}, \tilde{\mathbf{G}}, \mathbf{K}), & u = 1, \\ \mathcal{G}(\mathbf{I}), & u = 0, \end{cases} \quad (38)$$

where $\tilde{\mathbf{G}}$ denotes the canonicalized ground-truth extrinsics described below, and $\mathbf{K} = \{\mathbf{K}_i\}_{i=1}^N$ the intrinsics. When $u = 0$, the encoder instead receives a learnable placeholder camera token \mathbf{e}_c ; when $u = 1$, $(\tilde{\mathbf{G}}, \mathbf{K})$ is tokenized and replaces \mathbf{e}_c , so that the encoder attends to geometrically grounded pose cues.

Extrinsic Normalization for Conditioning. The extrinsics fed into the network are preprocessed independently from the supervision pipeline of Eq. (36), so as to remain agnostic to the absolute metric scale. Specifically, given the world-to-camera matrices $\{G_i\}_{i=1}^N$, we (i) right-multiply by G_1^{-1} so that the first view becomes the canonical frame, and (ii) divide the translation components by the median camera-centre distance \bar{d} :

$$\tilde{G}_i = G_i G_1^{-1}, \quad \tilde{G}_i[:3, 3] \leftarrow \tilde{G}_i[:3, 3] / \max(\bar{d}, \epsilon), \quad (39)$$

with $\bar{d} = \text{median}_i \|\mathbf{c}_i\|_2$ and \mathbf{c}_i the camera centre extracted from \tilde{G}_i^{-1} . This keeps the conditioning signal in a scale-invariant canonical frame and prevents trivial leakage of the ground-truth scale through the pose input (which is instead supervised via $\mathcal{L}_{\text{scale}}$).

D.4. Training Datasets

We train DA-Next model using images from 18 datasets, including: DA-Next-5M (7 datasets in total), HyperSim [76], Infinigen [73], Spring [64], MapFree [2], Matterport 3D [74], MVS-Synth [34], ScanNet++ [121], TartanAir [100], Unreal 4K [90], Virtual KITTI [8], Waymo [87].

Table 8 | **Training Datasets Statistics.** Each training epoch is composed of 18 datasets, and their dataset mixture ratios are reported as the training prob.

Cat.	Id.	Dataset	Scene	R/S	Dyn.	# Fr.	Met.	Prob.
General 3D Datasets	1	HyperSim [76]	Indoor	Syn.	Stat.	70K	✓	2.8
	2	Infinigen [73]	Indoor	Syn.	Stat.	142K	✓	2.5
	3	MapFree [2]	Outdoor	Real	Stat.	2.6M	✓	6.5
	4	Matterport 3D [74]	Indoor	Real	Stat.	1.9M	✓	7.3
	5	MVS-Synth [34]	Outdoor	Syn.	Stat.	12K	✓	0.4
	6	ScanNet++ [121]	Indoor	Real	Stat.	7.8M	✓	4.1
	7	Spring [64]	Outdoor	Syn.	Dyn.	5K	✓	2.3
	8	Tartanair [100]	Mixed	Syn.	Stat.	3M	✓	6.8
	9	Unreal 4K [90]	Outdoor	Syn.	Stat.	16K	✓	0.4
	10	Vkitti [8]	Outdoor	Syn.	Dyn.	42K	✓	1.5
	11	Waymo [87]	Outdoor	Real	Dyn.	7.9M	✓	5.1
DA-Next-5M	12	Aria Digital Twin [69]	Indoor	Syn.	Dyn.	87K	✓	8.0
	13	Colosseum [72]	Indoor	Syn.	Dyn.	334K	✓	5.5
	14	HOI4D [60]	Indoor	Real	Dyn.	739K	✓	11.1
	15	RLBench [36]	Indoor	Syn.	Dyn.	1.2M	✓	5.5
	16	Robolab [118]	Indoor	Syn.	Dyn.	158K	✓	11.1
	17	RoboTwin [14]	Indoor	Syn.	Dyn.	1.8M	✓	11.1
	18	Xperience [78]	Mixed	Real	Dyn.	400K	✓	8.0

These datasets cover normal, egocentric, and wrist view perspectives, both synthetic and real-world content, indoor and outdoor environments, as well as static and dynamic scenes. Such a diverse composition preserves a strong generalization capability for DA-Next. Table 8 summarizes the statistics of the datasets we used. In each epoch, we sample a fixed total number of samples from the training datasets, with their mixture ratio indicated by the “Training Prob” column in the table.

D.5. Frame Sampling Strategy

For every batch, we select between 2 and 18 frames from multiple random training scenes while maintaining a constant total of 18 frames within each batch. We sample each batch of images based on the Euclidean distance to the camera pose. For each frame, all other frames are ranked according to their pose distance, and the top N (N depends on the frame density in each dataset) closest frames are selected as its valid range. Then, for each sequence, we randomly choose one frame as the anchor frame and sample the remaining frames from its valid range.

D.6. Training Configuration

Our DA-Next architecture follows DA3-Giant [54] with $L = 40$ Transformer blocks and is initialized by pre-trained weights. During training, each batch incorporates ground-truth camera information as auxiliary input with probability $p = 20\%$. The training runs end-to-end on 4 NVIDIA H200 GPUs over seven days. Training is conducted in BF16 mixed precision with a fixed random seed of 42 for 10 epochs in total. The per-device batch size is 18 frames, and gradient accumulation is performed every 2 steps. During training, the backbone, depth and ray prediction head, camera encoder, and scale head are jointly optimized, whereas the camera decoder is kept frozen (we use the ray map branch). Since the 3D Gaussian Splatting branch is not involved in this work, its corresponding GS Head is also frozen. Gradient checkpointing is further enabled to reduce GPU memory consumption. We employ the AdamW optimizer with $\beta_1 = 0.9$, $\beta_2 = 0.95$, $\epsilon = 1 \times 10^{-8}$, and a weight decay of 0.01. A layer-wise learning rate scheme is adopted: 1×10^{-5} for the backbone, 2×10^{-5} for the prediction head, camera encoder. The learning rate follows a cosine decay schedule with linear warm-up, where the warm-up stage

lasts 5,000 steps and the minimum learning rate factor is 0.1. Gradient clipping is applied with a maximum norm of 1.0. To enhance robustness across varying aspect ratios, multi-scale training is performed over 17 resolutions, where the width is fixed at 504 and the height ranges from 280 to 504 with a step of 14.

E. Additional Findings

E.1. Do More Input Frames Always Lead to Better Results?

A natural assumption in 3D reconstruction is that more input frames yield better geometric estimates. However, Tab. 1 reveals a more nuanced picture. Under the sparse regime, where inputs consist of only a few frames with large inter-frame baselines and limited overlap, most models struggle with geometric estimation due to insufficient visual correspondence. Increasing the number of input frames from sparse to medium consistently improves both depth and camera pose metrics across paradigms, confirming that a moderate level of multi-view overlap is beneficial. However, further extending to the dense regime does not uniformly bring additional gains. For many feed-forward models, dense inputs introduce redundant or near-duplicate frames that add memory pressure without providing useful new geometric constraints, leading to stagnating or even degraded performance on reconstruction. This non-monotonic behavior suggests that the relationship between input density and reconstruction quality is task- and model-dependent, rather than strictly increasing.

Takeaway: *For bounded 3D reconstruction tasks, there exists an optimal input density range that maximizes reconstruction quality. Too few frames leave geometric constraints underspecified, while excessive inputs can introduce redundancy and hurt performance, making careful input density selection as important as model choice.*

E.2. How to Select the Right Spatial Foundation Model for Your Task?

Fig. 20 presents the overall ranking of the best-performing methods from each paradigm (Feed-Forward, Chunk-wise, Online, and TTT) across different domain subsets of SpatialBench. The overall ranking is computed from the weighted Average column of each per-domain sub-table, aggregating four complementary metrics: AbsRel, AUC@30, ATE, and F-Score. We partition SpatialBench into five domain groups: G1: Indoor, G2: Outdoor, G3: Driving, G4: Wrist-view, and G5: Ego-view. The colored cells report the ranking of each method on each domain, while the scatter points indicate whether the method’s training data includes in-domain samples from the corresponding group. Fig. 21, Fig. 22, and Fig. 23 present the per-domain ranking breakdowns under the sparse, medium, and dense input settings, respectively.

Fig. 20 reveals that model rankings are highly inconsistent across domain groups and input density settings. This inconsistency stems from two factors: the training data coverage of each method, and their architectural design choices that favor different operating regimes (e.g., long-sequence streaming methods naturally excel on dense, extended trajectories but may underperform on sparse multi-view inputs). This finding gives a guideline for downstream deployment: selecting a spatial foundation model for a target application requires verifying not only its general benchmark performance, but also whether its training mixture covers the relevant domain. Furthermore, for practitioners preparing fine-tuning datasets, these results suggest that domain match matters more than dataset volume: prioritizing data from the target domain, even in modest quantities, is likely to yield greater gains than simply increasing the total number of training scenes from unrelated distributions.

Takeaway: *No single model dominates across all domains and input regimes. Domain coverage in training data is the primary predictor of per-domain ranking, and should be the first consideration when selecting or fine-tuning a spatial foundation model for a specific downstream application.*

Dataset	Feed Forward	Feed Forward	Feed Forward	Chunk	Chunk	Online	Online	TTT	TTT
	VGGT	π^1	DA3-Giant	DA3-Streaming	π^1 -Long	StreamVGGT	LingBot-Map	LoGeR	ScalaBR
G1 — INDOOR (N=28)									
7-Scenes	2	9	1	3	5	6	4	7	8
DTU	1	6	3	4	6	5	9	8	2
HRSom	7	3	1	1	3	9	8	6	5
NeuralRGBD	2	9	1	3	6	7	4	5	8
ScanNet++	3	2	1	5	6	9	4	7	8
TUM-Dynamic	1	8	2	4	6	7	3	5	9
AriaSyntheticENV	•		•	•			•		•
ARKitScenes		•	•	•	•			•	
Bonn						•			
CO3Dv2	•	•	•	•	•	•	•		•
Gibson							•		
Habitat	•	•			•				
HM3D							•		
HyperSim	•	•	•	•	•	•	•	•	•
Matterport3D							•		
MegaSynth			•	•					
NYU-v2						•			
Objaverse	•		•	•			•		
OmniObject			•	•					
Replica	•		•	•			•		•
ScanNet	•	•			•	•	•	•	
SceneNetRGBD			•	•					•
SceneRGBD							•		
SyntheticAssets	•								
Taskonomy		•			•				•
Texverse							•		
Trellis			•	•					
WildRGBD	•	•	•	•	•		•		•
G2 — OUTDOOR (N=20)									
ETH3D	7	4	1	1	4	9	8	3	6
Tanks&Temples	1	2	4	9	3	8	5	7	6
BlendedMVS	•	•	•	•	•	•	•	•	•
DL3DV	•		•	•		•		•	•
DynamicInternal		•			•		•		
GTA-SIM		•			•		•		
Kubric	•						•		
Mapfree			•	•			•		•
Mapillary	•						•		•
MatrixCity		•			•		•		•
MegaDepth	•	•			•	•	•	•	•
MidAir		•			•		•		
MVSSynth	•		•	•			•		•
PointOdyssey	•		•	•			•		
Sintel						•			
Spring								•	
TartanAir		•	•	•	•	•	•	•	•
TartanAirGround							•		
TartanAirV2							•	•	
Unreal4K							•	•	
G3 — AUTONOMOUS DRIVING (N=5)									
OmniWorld	8	2	1	3	6	9	5	4	7
VirtuaIKITTI	1	4	8	5	7	9	2	6	3
Waymo	7	3	1	1	3	9	8	5	6
KITTI						•			
KITTI-360							•		
G4 — WRIST-VIEW (N=4)									
DROID	4	2	1	3	5	9	8	6	7
RLBench	8	1	2	6	3	9	7	4	5
RoboLab	3	2	1	4	5	8	6	9	7
RoboTwin	7	1	2	4	3	8	9	6	5
G5 — EGO-VIEW (N=2)									
AriaDigitalTwin	5	1	4	7	3	9	2	6	8
Xperience-10M	6	7	2	5	4	9	1	3	8

Figure 20 | **Training Data Domain Coverage vs. Overall Ranking Across Domain Groups.** We compare the best-performing methods from each paradigm on five domain groups in SpatialBench: *Indoor*, *Outdoor*, *Autonomous Driving*, *Wrist-view*, and *Ego-view*, where N denotes the number of datasets in each group. Colored cells report the per-domain ranking of each method, while scatter points indicate whether the corresponding training set includes in-domain data from that group.

Dataset	Feed Forward	Feed Forward	Feed Forward	Chunk	Chunk	Online	Online	TTT	TTT
	VGGT	π^1	DA3-Giant	DA3-Streaming	π^3 -Long	StreamVGGT	LingBot-Map	LoGeR	ScalBR
G1 — INDOOR (N=28)									
7-Scenes	7	3	1	1	3	9	8	5	6
DTU	7	3	1	1	3	9	8	5	6
HRSom	7	3	1	1	3	9	8	5	6
NeuralRGBD	7	3	1	1	3	9	8	5	6
ScanNet++	7	3	1	1	3	9	8	5	6
TUM-Dynamic	7	3	1	1	3	9	8	5	6
AriaSyntheticENV	•		•	•			•		•
ARKitScenes		•	•	•	•			•	
Bonn						•			
CO3Dv2	•	•	•	•	•	•	•		•
Gibson							•		
Habitat	•	•			•				
HM3D							•		
HyperSim	•	•	•	•	•	•	•	•	•
Matterport3D							•		
MegaSynth			•	•					
NYU-v2						•			
Objaverse	•		•	•			•		
OmniObject			•	•					
Replica	•		•	•			•		•
ScanNet	•	•			•	•	•	•	
SceneNetRGBD			•	•					•
SceneRGBD							•		
SyntheticAssets	•								
Taskonomy		•			•				•
Texverse							•		
Trellis			•	•					
WildRGBD	•	•	•	•	•		•		•
G2 — OUTDOOR (N=20)									
ETH3D	7	3	1	1	3	9	8	5	6
Tanks&Temples	7	3	1	1	3	9	8	5	6
BlendedMVS	•	•	•	•	•	•	•	•	•
DL3DV	•		•	•		•		•	•
DynamicInternal		•			•		•		
GTA-SIM		•			•		•		
Kubric	•						•		
Mapfree			•	•			•		•
Mapillary	•								•
MatrixCity		•			•		•		•
MegaDepth	•	•			•	•	•	•	•
MidAir		•			•		•		
MVSSynth	•		•	•			•		•
PointOdyssey	•		•	•			•		
Sintel						•			
Spring								•	
TartanAir		•	•	•	•	•	•	•	•
TartanAirGround							•		
TartanAirV2							•	•	
Unreal4K							•	•	
G3 — AUTONOMOUS DRIVING (N=5)									
OmniWorld	7	3	1	1	3	9	8	5	6
VirtuaIKITTI	7	3	1	1	3	9	8	5	6
Waymo	7	3	1	1	3	9	8	5	6
KITTI						•			
KITTI-360							•		
G4 — WRIST-VIEW (N=4)									
DROID	7	3	1	1	3	9	8	5	6
RLBench	7	3	1	1	3	9	8	5	6
RoboLab	7	3	1	1	3	9	8	5	6
RoboTwin	7	3	1	1	3	9	8	5	6
G5 — EGO-VIEW (N=2)									
AriaDigitalTwin	7	3	1	1	3	9	8	5	6
Xperience-10M	7	3	1	1	3	9	8	5	6

Figure 21 | Training Data Domain Coverage vs. Overall Ranking Across Domain Groups (Sparse). We compare the best-performing methods from each paradigm on five domain groups in SpatialBench under the sparse regime, where N denotes the number of datasets in each group. Colored cells report the per-domain ranking of each method, while scatter points indicate whether the corresponding training set includes in-domain data from that group.

Dataset	Feed Forward	Feed Forward	Feed Forward	Chunk	Chunk	Online	Online	TTT	TTT
	VGGT	π^1	DA3-Giant	DA3-Streaming	π^1 -Long	StreamVGGT	LingBot-Map	LoGeR	ScalBR
G1 — INDOOR (N=28)									
7-Scenes	5	3	1	2	4	9	8	7	6
DTU	5	3	1	2	4	9	8	7	6
HRSom	5	3	1	2	4	9	8	7	6
NeuralRGBD	5	3	1	2	4	9	8	7	6
ScanNet++	5	3	1	2	4	9	8	7	6
TUM-Dynamic	5	3	1	2	4	9	8	7	6
AriaSyntheticENV	•		•	•			•		•
ARKitScenes		•	•	•	•			•	
Bonn						•			
CO3Dv2	•	•	•	•	•	•	•		•
Gibson							•		
Habitat	•	•			•				
HM3D							•		
HyperSim	•	•	•	•	•	•	•	•	•
Matterport3D							•		
MegaSynth			•	•					
NYU-v2						•			
Objaverse	•		•	•			•		
OmniObject			•	•					
Replica	•		•	•			•		•
ScanNet	•	•			•	•	•	•	
SceneNetRGBD			•	•					•
SceneRGBD							•		
SyntheticAssets	•								
Taskonomy		•			•				•
Texverse							•		
Trellis			•	•					
WildRGBD	•	•	•	•	•		•		•
G2 — OUTDOOR (N=20)									
ETH3D	5	3	1	2	4	9	8	7	6
Tanks&Temples	5	3	1	2	4	9	8	7	6
BlendedMVS	•	•	•	•	•	•	•	•	•
DL3DV	•		•	•		•		•	•
DynamicInternal		•			•		•		
GTA-SIM		•			•		•		
Kubric	•						•		
Mapfree			•	•			•		•
Mapillary	•								•
MatrixCity		•			•		•		•
MegaDepth	•	•			•	•	•	•	•
MidAir		•			•		•		
MVSSynth	•		•	•			•		•
PointOdyssey	•		•	•			•		
Sintel						•			
Spring								•	
TartanAir		•	•	•	•	•	•	•	•
TartanAirGround							•		
TartanAirV2							•	•	
Unreal4K							•	•	
G3 — AUTONOMOUS DRIVING (N=5)									
OmniWorld	5	3	1	2	4	9	8	7	6
VirtuaIKITTI	5	3	1	2	4	9	8	7	6
Waymo	5	3	1	2	4	9	8	7	6
KITTI						•			
KITTI-360							•		
G4 — WRIST-VIEW (N=4)									
DROID	5	3	1	2	4	9	8	7	6
RLBench	5	3	1	2	4	9	8	7	6
RoboLab	5	3	1	2	4	9	8	7	6
RoboTwin	5	3	1	2	4	9	8	7	6
G5 — EGO-VIEW (N=2)									
AriaDigitalTwin	5	3	1	2	4	9	8	7	6
Xperience-10M	5	3	1	2	4	9	8	7	6

Figure 22 | Training Data Domain Coverage vs. Overall Ranking Across Domain Groups (Medium). We compare the best-performing methods from each paradigm on five domain groups in SpatialBench under the medium regime, where N denotes the number of datasets in each group. Colored cells report the per-domain ranking of each method, while scatter points indicate whether the corresponding training set includes in-domain data from that group.

Dataset	Feed Forward	Feed Forward	Feed Forward	Chunk	Chunk	Online	Online	TTT	TTT
	VGGT	π^1	DA3-Giant	DA3-Streaming	π^1 -Long	StreamVGGT	LingBot-Map	LoGeR	ScalBR
G1 — INDOOR (N=28)									
7-Scenes	☐	3	☐	2	6	7	1	5	4
DTU	☐	3	☐	2	6	7	1	5	4
HRSom	☐	3	☐	2	6	7	1	5	4
NeuralRGBD	☐	3	☐	2	6	7	1	5	4
ScanNet++	☐	3	☐	2	6	7	1	5	4
TUM-Dynamic	☐	3	☐	2	6	7	1	5	4
AriaSyntheticENV	●		●	●			●		●
ARKitScenes		●	●	●	●			●	
Bonn						●			
CO3Dv2	●	●	●	●	●	●	●		●
Gibson							●		
Habitat	●	●			●				
HM3D							●		
HyperSim	●	●	●	●	●	●	●	●	●
Matterport3D							●		
MegaSynth			●	●					
NYU-v2						●			
Objaverse	●		●	●			●		
OmniObject			●	●					
Replica	●		●	●			●		●
ScanNet	●	●		●	●	●	●	●	●
SceneNetRGBD			●	●					●
SceneRGBD							●		
SyntheticAssets	●								
Taskonomy		●			●				●
Texverse							●		
Trellis			●	●					
WildRGBD	●	●	●	●	●		●		●
G2 — OUTDOOR (N=20)									
ETH3D	☐	3	☐	2	6	7	1	5	4
Tanks&Temples	☐	3	☐	2	6	7	1	5	4
BlendedMVS	●	●	●	●	●	●	●	●	●
DL3DV	●		●	●		●	●	●	●
DynamicInternal		●			●		●		
GTA-SIM		●			●		●		
Kubric	●						●		
Mapfree			●	●			●		●
Mapillary	●						●		●
MatrixCity		●			●		●		●
MegaDepth	●	●			●	●	●	●	●
MidAir		●			●		●		
MVSSynth	●		●	●			●		●
PointOdyssey	●		●	●			●		
Sintel						●			
Spring								●	
TartanAir		●	●	●	●	●	●	●	●
TartanAirGround							●		
TartanAirV2							●	●	
Unreal4K							●	●	
G3 — AUTONOMOUS DRIVING (N=5)									
OmniWorld	☐	3	☐	2	6	7	1	5	4
VirtualKITTI	☐	3	☐	2	6	7	1	5	4
Waymo	☐	3	☐	2	6	7	1	5	4
KITTI						●			
KITTI-360							●		
G4 — WRIST-VIEW (N=4)									
DROID	☐	3	☐	2	6	7	1	5	4
RLBench	☐	3	☐	2	6	7	1	5	4
RoboLab	☐	3	☐	2	6	7	1	5	4
RoboTwin	☐	3	☐	2	6	7	1	5	4
G5 — EGO-VIEW (N=2)									
AriaDigitalTwin	☐	3	☐	2	6	7	1	5	4
Xperience-10M	☐	3	☐	2	6	7	1	5	4

Figure 23 | **Training Data Domain Coverage vs. Overall Ranking Across Domain Groups (Dense).** We compare the best-performing methods from each paradigm on five domain groups in SpatialBench under the dense regime, where N denotes the number of datasets in each group. Colored cells report the per-domain ranking of each method, while scatter points indicate whether the corresponding training set includes in-domain data from that group. Empty cells indicate that the method runs out of memory under the corresponding input regime.

F. The Complete SpatialBench Results

Per-regime Breakdowns of the Main Table. We present detailed per-regime results for the single-frame, sparse, medium, and dense input settings in Tab. 9, Tab. 10, Tab. 11, and Tab. 12, respectively, complementing the aggregated results in Tab. 1.

Performance Comparison on Each Dataset. We present per-dataset metric breakdowns for all evaluated methods in this section.

- **7-Scenes.** Per-dataset results on 7-Scenes are reported in Table 13.
- **ADT.** Per-dataset results on Aria Digital Twin (ADT) are reported in Table 14.
- **DROID.** Per-dataset results on DROID are reported in Table 15.
- **DTU.** Per-dataset results on DTU are reported in Table 16.
- **ETH3D.** Per-dataset results on ETH3D are reported in Table 17.
- **HiRoom.** Per-dataset results on HiRoom are reported in Table 18.
- **KITTI Odometry.** Per-dataset results on KITTI Odometry are reported in Table 19.
- **Lingbot-Depth.** Per-dataset results on Lingbot are reported in Table 20.
- **NRGBD.** Per-dataset results on NRGBD are reported in Table 21.
- **OmniWorld.** Per-dataset results on OmniWorld are reported in Table 22.
- **RLBench.** Per-dataset results on RLBench are reported in Table 23.
- **Robolab.** Per-dataset results on Robolab are reported in Table 24.
- **RoboTwin.** Per-dataset results on RoboTwin are reported in Table 25.
- **Xperience.** Per-dataset results on Xperience are reported in Table 26.
- **ScanNet++.** Per-dataset results on ScanNet++ are reported in Table 27.
- **Tanks and Temples.** Per-dataset results on Tanks and Temples are reported in Table 28.
- **TUM RGB-D.** Per-dataset results on TUM RGB-D are reported in Table 29.
- **Virtual KITTI.** Per-dataset results on Virtual KITTI are reported in Table 30.
- **Waymo.** Per-dataset results on Waymo are reported in Table 31.

Metric Depth Evaluation. Tab. 32 compares the native metric-depth prediction quality of all six metric-scale-capable methods on SpatialBench, evaluated without median/scale alignment across single-frame, sparse, and medium input settings.

Table 9 | **Detailed Results on the Single-Frame Setting.** The best, second-best, and third-best results in each column are highlighted in **deep blue**, **medium blue**, and **light blue**, respectively. Out-of-memory cells are shaded **light red**. Within each sub-category, the **bold** value marks the in-group best.

Method	#Params (M)	Depth					
		AbsRel↓	SqRel↓	RMSE↓	$\delta_{1.03}$ ↑	$\delta_{1.05}$ ↑	$\delta_{1.10}$ ↑
Optimization-based							
DUS3R	571.17	0.385	5.337	0.992	0.391	0.524	0.685
MASt3R	688.64	0.456	10.14	0.973	0.373	0.508	0.684
End-to-End Feed-Forward							
VGGT	1256.54	0.184	0.779	0.608	0.517	0.639	0.773
Fast3R	647.55	0.350	3.454	1.139	0.339	0.463	0.631
FastVGGT	1157.94	0.183	0.761	0.608	0.517	0.640	0.773
MUS3R	423.43	0.429	8.637	0.934	0.393	0.524	0.699
MapAnything	1228.49	0.451	11.99	0.854	0.441	0.583	0.747
OmniVGGT	1217.49	0.188	0.795	0.620	0.525	0.649	0.791
π^3	958.70	0.478	16.85	0.983	0.542	0.665	0.794
π^3 -X	1360.03	0.371	8.834	0.631	0.522	0.651	0.802
AMB3R	1563.12	0.466	15.32	0.658	0.544	0.671	0.802
DA3-Small	34.30	0.385	6.358	0.948	0.300	0.431	0.625
DA3-Base	135.37	0.349	5.281	0.842	0.359	0.501	0.691
DA3-Large	410.94	0.333	5.649	0.763	0.449	0.579	0.742
DA3-Giant	1355.67	0.368	7.494	0.724	0.504	0.628	0.771
DA3-Nested	1689.85	0.364	7.358	0.800	0.500	0.633	0.778
WorldMirror	1263.34	0.349	7.695	0.707	0.485	0.619	0.776
VGGT-Omega	1143.81	0.516	20.72	1.086	0.552	0.671	0.812
DANext [†] (Ours)	1303.76	0.166	0.985	0.646	0.511	0.636	0.802
Online							
Spann3r ²²⁴	658.69	0.370	12.39	2.345	0.288	0.417	0.596
CUT3R	793.31	0.247	1.356	0.712	0.409	0.555	0.720
MonST3R	571.17	0.309	2.500	0.999	0.348	0.470	0.633
Point3R	828.01	0.379	6.806	0.783	0.400	0.534	0.703
Stream3R-S	1190.60	0.409	11.3	0.672	0.564	0.691	0.811
Stream3R-W	1190.60	0.409	11.3	0.672	0.564	0.691	0.811
StreamVGGT	1256.54	0.219	1.696	0.583	0.523	0.646	0.784
Page4D	1256.81	0.228	1.977	0.636	0.467	0.606	0.762
InfiniteVGGT	1256.54	0.217	1.643	0.583	0.524	0.645	0.783
Wint3R	749.46	0.619	25.47	1.053	0.434	0.555	0.719
LongStream-B	1190.60	0.523	17.1	0.682	0.458	0.597	0.770
LongStream-S	1190.60	0.523	17.1	0.682	0.458	0.597	0.770
LingbotMap [*] -W	1157.94	0.333	4.470	0.755	0.437	0.572	0.741
LingbotMap [*] -S	1157.94	0.333	4.470	0.755	0.437	0.572	0.741
Chunk-wise							
VGGT-Long	1256.54	0.184	0.779	0.608	0.517	0.639	0.773
π^3 -Long	958.70	0.478	16.85	0.983	0.542	0.665	0.794
DA3-Streaming	1355.67	0.368	7.494	0.724	0.504	0.628	0.771
SLAM-based							
MASt3R-SLAM	688.64	0.348	1.553	1.237	0.165	0.268	0.471
VGGT-SLAM	1256.54	0.184	0.779	0.608	0.517	0.639	0.773
Test-Time Training							
TTT3R	793.31	0.247	1.357	0.712	0.409	0.555	0.720
Scal3R	1266.14	0.227	1.583	0.613	0.519	0.644	0.775
LoGeR	1254.62	0.251	2.718	0.635	0.527	0.666	0.800
LoGeR*	1254.60	0.200	1.320	0.637	0.540	0.668	0.803

Table 10 | **Detailed Results on the Sparse Setting.** The best, second-best, and third-best results in each column are highlighted in **deep blue**, **medium blue**, and **light blue**, respectively. Out-of-memory cells are shaded **light red**. Within each sub-category, the **bold** value marks the in-group best.

Method	#Params (M)	Depth						Camera						
		AbsRel↓	SqRel↓	RMSE↓	$\delta_{1.03}$ ↑	$\delta_{1.05}$ ↑	$\delta_{1.10}$ ↑	RAcc ₃ ↑	RAcc ₅ ↑	TAcc ₃ ↑	TAcc ₅ ↑	AUC@5↑	AUC@15↑	AUC@30↑
Optimization-based														
DUSt3R	571.17	0.257	2.693	1.567	0.295	0.420	0.600	0.527	0.654	0.242	0.350	0.184	0.374	0.498
MASt3R	688.64	0.209	0.606	1.246	0.309	0.456	0.639	0.587	0.701	0.301	0.411	0.244	0.438	0.568
End-to-End Feed-Forward														
VGGT	1256.54	0.105	0.105	0.673	0.498	0.627	0.778	0.734	0.833	0.454	0.550	0.405	0.585	0.700
Fast3R	647.55	0.260	0.760	1.576	0.228	0.340	0.508	0.347	0.486	0.156	0.235	0.109	0.264	0.392
FastVGGT	1157.94	0.113	0.098	0.666	0.457	0.590	0.752	0.642	0.773	0.384	0.472	0.314	0.503	0.631
MUSt3R	423.43	0.165	0.276	0.999	0.366	0.502	0.686	0.622	0.726	0.343	0.435	0.273	0.482	0.614
MapAnything	1228.49	0.153	1.079	1.337	0.361	0.512	0.701	0.608	0.762	0.300	0.423	0.244	0.446	0.579
OmniVGGT	1217.49	0.117	0.119	0.669	0.534	0.671	0.810	0.620	0.746	0.416	0.507	0.332	0.537	0.665
π^3	958.70	0.092	0.258	0.855	0.547	0.686	0.826	0.769	0.854	0.474	0.586	0.412	0.619	0.742
π^3 -X	1360.03	0.084	0.084	0.599	0.576	0.710	0.833	0.756	0.837	0.491	0.595	0.427	0.627	0.741
AMB3R	1563.12	0.088	0.083	0.617	0.534	0.668	0.812	0.743	0.844	0.475	0.591	0.412	0.619	0.739
DA3-Small	34.30	0.191	0.270	1.057	0.308	0.440	0.633	0.392	0.568	0.172	0.300	0.127	0.336	0.476
DA3-Base	135.37	0.159	0.210	0.937	0.386	0.520	0.690	0.528	0.678	0.292	0.399	0.222	0.427	0.566
DA3-Large	410.94	0.128	0.198	0.839	0.470	0.601	0.753	0.662	0.776	0.443	0.528	0.361	0.559	0.688
DA3-Giant	1355.67	0.095	0.107	0.608	0.563	0.689	0.821	0.792	0.871	0.586	0.682	0.525	0.699	0.785
DA3-Nested	1689.85	0.106	0.199	0.805	0.564	0.692	0.814	0.784	0.855	0.577	0.682	0.519	0.691	0.779
WorldMirror	1263.34	0.139	0.162	0.798	0.440	0.583	0.748	0.697	0.793	0.394	0.506	0.320	0.532	0.660
VGGT-Omega	1143.81	0.077	0.362	1.089	0.556	0.702	0.843	0.808	0.892	0.585	0.678	0.504	0.695	0.803
DANext [†] (Ours)	1303.76	0.050	0.073	0.554	0.647	0.772	0.893	0.815	0.900	0.587	0.718	0.518	0.718	0.809
Online														
Spann3r ²²⁴	658.69	0.274	212.3	10.47	0.209	0.317	0.496	0.265	0.423	0.080	0.163	0.052	0.198	0.329
CUT3R	793.31	0.196	0.218	0.917	0.300	0.445	0.638	0.478	0.637	0.223	0.356	0.177	0.388	0.519
MonST3R	571.17	0.227	0.399	1.338	0.220	0.332	0.521	0.243	0.311	0.107	0.177	0.069	0.172	0.269
Point3R	828.01	0.221	0.280	1.044	0.251	0.379	0.559	0.194	0.372	0.058	0.123	0.028	0.177	0.339
Stream3R-S	1190.60	0.114	0.120	0.705	0.450	0.597	0.765	0.618	0.774	0.351	0.437	0.278	0.471	0.603
Stream3R-W	1190.60	0.117	0.131	0.739	0.442	0.584	0.753	0.610	0.762	0.344	0.430	0.272	0.464	0.597
StreamVGGT	1256.54	0.154	0.362	1.243	0.314	0.424	0.609	0.638	0.771	0.339	0.435	0.283	0.472	0.598
Page4D	1256.81	0.112	0.089	0.646	0.438	0.587	0.758	0.551	0.730	0.295	0.428	0.224	0.456	0.608
InfiniteVGGT	1256.54	0.154	0.363	1.245	0.314	0.423	0.610	0.639	0.767	0.346	0.435	0.286	0.471	0.596
Wint3R	749.46	0.157	0.232	0.909	0.399	0.532	0.702	0.438	0.600	0.214	0.334	0.157	0.366	0.499
LongStream-B	1190.60	0.153	0.152	0.771	0.380	0.526	0.712	0.502	0.678	0.263	0.383	0.197	0.417	0.549
LongStream-S	1190.60	0.151	0.144	0.754	0.383	0.531	0.716	0.501	0.677	0.258	0.377	0.196	0.413	0.543
LingbotMap*-W	1157.94	0.138	0.138	0.759	0.376	0.536	0.730	0.696	0.811	0.359	0.469	0.303	0.520	0.650
LingbotMap*-S	1157.94	0.138	0.138	0.759	0.376	0.536	0.730	0.696	0.811	0.359	0.469	0.303	0.520	0.650
Chunk-wise														
VGGT-Long	1256.54	0.105	0.105	0.673	0.498	0.627	0.778	0.734	0.833	0.454	0.550	0.405	0.585	0.700
π^3 -Long	958.70	0.092	0.258	0.855	0.547	0.686	0.826	0.769	0.854	0.474	0.586	0.412	0.619	0.742
DA3-Streaming	1355.67	0.095	0.107	0.608	0.563	0.689	0.821	0.790	0.871	0.588	0.682	0.525	0.699	0.785
SLAM-based														
MASt3R-SLAM	688.64	0.336	1.715	2.282	0.120	0.194	0.347	0.317	0.401	0.066	0.095	0.047	0.118	0.190
VGGT-SLAM	1256.54	0.105	0.105	0.673	0.498	0.627	0.778	0.734	0.833	0.454	0.550	0.405	0.585	0.700
Test-Time Training														
TTT3R	793.31	0.202	0.257	0.966	0.282	0.428	0.628	0.452	0.591	0.197	0.302	0.153	0.342	0.469
Scal3R	1266.14	0.114	0.091	0.593	0.535	0.669	0.810	0.734	0.833	0.484	0.581	0.418	0.610	0.732
LoGeR	1254.62	0.095	0.077	0.569	0.546	0.700	0.833	0.695	0.821	0.411	0.538	0.348	0.564	0.687
LoGeR*	1254.60	0.077	0.071	0.558	0.581	0.725	0.854	0.715	0.824	0.424	0.547	0.353	0.576	0.708

Table 11 | **Detailed Results on the Medium Setting.** The best, second-best, and third-best results in each column are highlighted in **deep blue**, **medium blue**, and **light blue**, respectively. Out-of-memory cells are shaded **light red**. Within each sub-category, the **bold** value marks the in-group best.

Method	#Params (M)	Depth						Camera						Trajectory			PointCloud		
		AbsRel↓	SqRel↓	RMSE↓	$\delta_{1.05} \uparrow$	$\delta_{1.05} \uparrow$	$\delta_{1.10} \uparrow$	RAcc \uparrow	RAcc \uparrow	TAcc \uparrow	TAcc \uparrow	AUC@5 \uparrow	AUC@15 \uparrow	AUC@30 \uparrow	ATE↓	RPE \downarrow	RPE \downarrow	F-Score \uparrow	Overall↓
Optimization-based																			
DUST3R	571.17	0.276	0.860	1.447	0.247	0.361	0.529	0.402	0.543	0.172	0.273	0.130	0.315	0.448	1.691	0.386	4.096	0.343	0.142
MAS3R	688.64	0.259	1.871	1.898	0.259	0.379	0.554	0.477	0.615	0.230	0.344	0.176	0.381	0.522	1.911	0.236	2.997	0.370	0.382
End-to-End Feed-Forward																			
VGGT	1256.54	0.125	0.602	0.688	0.499	0.613	0.747	0.695	0.782	0.484	0.562	0.432	0.586	0.687	0.727	0.216	2.202	0.661	0.087
Fast3R	647.55	0.255	0.567	1.539	0.241	0.344	0.496	0.296	0.422	0.164	0.248	0.117	0.272	0.386	6.582	2.055	13.65	0.300	0.210
FastVGGT	1157.94	0.105	0.086	0.611	0.479	0.597	0.737	0.678	0.771	0.448	0.542	0.379	0.554	0.662	0.738	0.259	3.260	0.576	0.121
MUS3R	423.43	0.162	0.327	0.966	0.388	0.522	0.696	0.618	0.734	0.361	0.475	0.296	0.507	0.643	3.097	0.613	2.686	0.507	0.230
MapAnything	1228.49	0.146	0.490	1.052	0.347	0.491	0.681	0.563	0.702	0.312	0.419	0.254	0.451	0.579	1.737	0.533	2.852	0.420	0.114
OmniVGGT	1217.49	0.111	0.096	0.649	0.518	0.645	0.780	0.609	0.726	0.426	0.527	0.340	0.542	0.665	1.491	0.355	2.768	0.595	0.104
π^3	958.70	0.082	0.229	0.822	0.563	0.689	0.814	0.742	0.830	0.501	0.613	0.433	0.636	0.749	0.565	0.128	1.240	0.649	0.080
π^3 -X	1360.03	0.078	0.061	0.538	0.582	0.712	0.831	0.741	0.827	0.536	0.628	0.463	0.644	0.744	0.369	0.108	1.459	0.658	0.074
AMB3R	1563.12	0.085	0.074	0.580	0.539	0.661	0.795	0.704	0.799	0.496	0.588	0.429	0.613	0.727	0.645	0.223	1.881	0.554	0.123
DA3-Small	34.30	0.176	0.226	1.008	0.312	0.435	0.617	0.370	0.535	0.192	0.301	0.136	0.338	0.479	4.850	1.356	5.534	0.432	0.123
DA3-Base	135.37	0.142	0.171	0.884	0.395	0.521	0.683	0.494	0.626	0.289	0.407	0.227	0.430	0.562	3.865	0.976	3.928	0.515	0.100
DA3-Large	410.94	0.105	0.155	0.779	0.498	0.618	0.767	0.655	0.758	0.487	0.575	0.411	0.588	0.701	2.722	0.460	2.800	0.626	0.130
DA3-Giant	1355.67	0.086	0.088	0.578	0.572	0.686	0.812	0.749	0.834	0.587	0.663	0.532	0.684	0.776	1.161	0.285	2.253	0.742	0.073
DA3-Nested	1689.85	0.086	0.182	0.801	0.577	0.690	0.810	0.742	0.833	0.569	0.658	0.510	0.676	0.770	1.980	0.394	2.708	0.737	0.073
WorldMirror	1263.34	0.118	0.126	0.741	0.445	0.573	0.721	0.674	0.775	0.417	0.533	0.352	0.556	0.674	1.357	0.347	2.056	0.575	0.090
VGGT-Omega	1143.81	0.067	0.304	1.049	0.589	0.721	0.845	0.787	0.870	0.589	0.692	0.512	0.700	0.795	0.659	0.160	1.369	0.706	0.078
DANext [†] (Ours)	1303.76	0.035	0.062	0.520	0.715	0.830	0.928	0.806	0.880	0.630	0.733	0.553	0.733	0.819	1.442	0.251	1.602	0.727	0.072
Online																			
Spann3r ²²⁴	658.69	0.252	145	9.194	0.208	0.315	0.486	0.198	0.358	0.085	0.160	0.049	0.205	0.361	4.312	1.118	6.784	0.254	0.249
CUT3R	793.31	0.189	0.423	1.095	0.271	0.396	0.576	0.335	0.506	0.160	0.273	0.110	0.316	0.469	2.676	0.373	4.271	0.286	0.385
MonST3R	571.17	0.241	0.595	1.551	0.162	0.252	0.413	0.161	0.221	0.037	0.078	0.026	0.100	0.195	2.234	0.526	12.99	0.081	0.502
Point3R	828.01	0.228	0.261	1.044	0.247	0.368	0.551	0.178	0.340	0.055	0.116	0.027	0.161	0.303	6.512	0.847	8.545	0.211	0.213
Stream3R-S	1190.60	0.204	0.725	1.414	0.295	0.395	0.544	0.392	0.514	0.223	0.299	0.178	0.317	0.427	5.717	0.621	5.650	0.348	0.594
Stream3R-W	1190.60	0.240	1.099	1.717	0.260	0.350	0.500	0.330	0.441	0.173	0.251	0.136	0.265	0.364	6.756	0.896	7.827	0.323	0.565
StreamVGGT	1256.54	0.171	0.509	1.458	0.271	0.372	0.539	0.566	0.679	0.305	0.405	0.251	0.437	0.562	4.940	0.526	3.820	0.397	0.154
Page4D	1256.81	0.107	0.079	0.613	0.454	0.589	0.748	0.531	0.712	0.334	0.464	0.246	0.479	0.618	0.855	0.255	2.574	0.423	0.118
InfiniteVGGT	1256.54	0.170	0.504	1.453	0.271	0.372	0.539	0.566	0.679	0.304	0.407	0.251	0.439	0.563	4.964	0.536	3.908	0.402	0.151
Wint3R	749.46	0.144	0.174	0.856	0.356	0.494	0.677	0.336	0.508	0.157	0.267	0.108	0.303	0.444	3.944	0.625	3.351	0.401	0.201
LongStream-B	1190.60	0.224	0.182	0.854	0.213	0.324	0.504	0.376	0.550	0.165	0.270	0.118	0.315	0.455	0.925	0.282	4.074	0.135	0.303
LongStream-S	1190.60	0.166	0.147	0.796	0.288	0.418	0.609	0.266	0.412	0.128	0.217	0.085	0.249	0.385	1.188	0.345	4.945	0.126	0.345
LingbotMap [†] -W	1157.94	0.114	0.177	0.799	0.385	0.535	0.725	0.610	0.745	0.349	0.471	0.290	0.502	0.641	0.509	0.176	1.896	0.362	0.196
LingbotMap [†] -S	1157.94	0.114	0.179	0.807	0.405	0.549	0.730	0.621	0.753	0.369	0.479	0.304	0.511	0.647	0.508	0.193	2.025	0.411	0.175
Chunk-wise																			
VGGT-Long	1256.54	0.131	0.601	0.679	0.479	0.593	0.735	0.673	0.773	0.465	0.548	0.410	0.573	0.679	0.512	0.164	2.199	0.633	0.090
π^3 -Long	958.70	0.097	0.248	0.897	0.446	0.583	0.742	0.734	0.825	0.501	0.609	0.426	0.626	0.740	0.465	0.106	1.149	0.590	0.087
DA3-Streaming	1355.67	0.091	0.110	0.618	0.560	0.674	0.794	0.743	0.828	0.578	0.656	0.520	0.675	0.767	0.563	0.135	1.922	0.725	0.074
SLAM-based																			
MAS3R-SLAM	688.64	0.348	1.504	2.278	0.102	0.169	0.312	0.321	0.438	0.084	0.135	0.064	0.168	0.262	6.075	0.682	10.98	0.130	0.870
VGGT-SLAM	1256.54	0.129	0.212	0.691	0.448	0.562	0.703	0.617	0.723	0.416	0.502	0.363	0.531	0.645	0.686	0.145	2.186	0.610	0.091
Test-Time Training																			
TTT3R	793.31	0.179	0.242	0.970	0.295	0.424	0.604	0.412	0.573	0.188	0.307	0.142	0.351	0.493	2.343	0.462	5.740	0.294	0.373
Scal3R	1266.14	0.147	0.170	0.818	0.327	0.423	0.602	0.629	0.753	0.435	0.535	0.349	0.546	0.670	0.400	0.154	1.713	0.671	0.201
LoGeR	1254.62	0.113	0.065	0.542	0.435	0.576	0.741	0.690	0.793	0.405	0.540	0.340	0.564	0.693	0.591	0.123	1.254	0.504	0.096
LoGeR*	1254.60	0.083	0.057	0.515	0.523	0.667	0.799	0.704	0.801	0.452	0.569	0.373	0.589	0.714	0.566	0.097	1.080	0.574	0.086

Table 12 | **Detailed Results on the Dense Regime.** The best, second-best, and third-best results in each column are highlighted in **deep blue**, **medium blue**, and **light blue**, respectively. Out-of-memory (OOM) and Timeout (T.O) cells are shaded **light red**. Within each sub-category, the **bold** value marks the in-group best.

Method	#Params (M)	Depth						Camera						Trajectory			PointCloud		
		AbsRel↓	SqRel↓	RMSE↓	$\delta_{1.03}$ ↑	$\delta_{1.05}$ ↑	$\delta_{1.10}$ ↑	RAcc3↑	RAcc5↑	TAcc3↑	TAcc5↑	AUC@5↑	AUC@15↑	AUC@30↑	ATE↓	RPE _r ↓	RPE _t ↓	F-Score↑	Overall↓
Optimization-based																			
DUS3R	571.17	OOM	OOM	OOM	OOM	OOM	OOM	OOM	OOM	OOM	OOM	OOM	OOM	OOM	OOM	OOM	OOM	OOM	OOM
MAS3R	688.64	OOM	OOM	OOM	OOM	OOM	OOM	OOM	OOM	OOM	OOM	OOM	OOM	OOM	OOM	OOM	OOM	OOM	OOM
End-to-End Feed-Forward																			
VGGT	1256.54	OOM	OOM	OOM	OOM	OOM	OOM	OOM	OOM	OOM	OOM	OOM	OOM	OOM	OOM	OOM	OOM	OOM	OOM
Fast3R	647.55	0.331	0.814	2.162	0.152	0.232	0.376	0.191	0.304	0.071	0.116	0.047	0.135	0.232	13.68	3.064	12.04	0.224	0.289
FastVGGT	1157.94	0.120	0.102	0.685	0.421	0.552	0.704	0.609	0.716	0.368	0.456	0.306	0.473	0.588	19.23	1.145	1.899	0.479	0.185
MUS3R	423.43	T.O	T.O	T.O	T.O	T.O	T.O	T.O	T.O	T.O	T.O	T.O	T.O	T.O	T.O	T.O	T.O	T.O	T.O
MapAnything	1228.49	OOM	OOM	OOM	OOM	OOM	OOM	OOM	OOM	OOM	OOM	OOM	OOM	OOM	OOM	OOM	OOM	OOM	OOM
OmniVGGT	1217.49	OOM	OOM	OOM	OOM	OOM	OOM	OOM	OOM	OOM	OOM	OOM	OOM	OOM	OOM	OOM	OOM	OOM	OOM
π^3	958.70	0.109	0.268	1.008	0.403	0.553	0.738	0.528	0.627	0.300	0.379	0.254	0.410	0.524	16.39	1.132	2.237	0.332	0.757
π^3 -X	1360.03	OOM	OOM	OOM	OOM	OOM	OOM	OOM	OOM	OOM	OOM	OOM	OOM	OOM	OOM	OOM	OOM	OOM	OOM
AMB3R	1563.12	OOM	OOM	OOM	OOM	OOM	OOM	OOM	OOM	OOM	OOM	OOM	OOM	OOM	OOM	OOM	OOM	OOM	OOM
DA3-Small	34.30	0.208	0.280	1.226	0.249	0.368	0.556	0.297	0.435	0.130	0.215	0.088	0.243	0.368	28.12	3.996	5.154	0.325	0.187
DA3-Base	135.37	0.166	0.220	1.093	0.327	0.454	0.632	0.378	0.509	0.198	0.285	0.151	0.310	0.436	26.35	3.818	6.089	0.399	0.146
DA3-Large	410.94	OOM	OOM	OOM	OOM	OOM	OOM	OOM	OOM	OOM	OOM	OOM	OOM	OOM	OOM	OOM	OOM	OOM	OOM
DA3-Giant	1355.67	OOM	OOM	OOM	OOM	OOM	OOM	OOM	OOM	OOM	OOM	OOM	OOM	OOM	OOM	OOM	OOM	OOM	OOM
DA3-Nested	1689.85	OOM	OOM	OOM	OOM	OOM	OOM	OOM	OOM	OOM	OOM	OOM	OOM	OOM	OOM	OOM	OOM	OOM	OOM
WorldMirror	1263.34	OOM	OOM	OOM	OOM	OOM	OOM	OOM	OOM	OOM	OOM	OOM	OOM	OOM	OOM	OOM	OOM	OOM	OOM
DA-Next	1303.76	OOM	OOM	OOM	OOM	OOM	OOM	OOM	OOM	OOM	OOM	OOM	OOM	OOM	OOM	OOM	OOM	OOM	OOM
Online																			
Spann3r	658.69	0.315	97.78	5.152	0.136	0.217	0.373	0.143	0.260	0.050	0.099	0.023	0.125	0.246	26.48	3.257	5.064	0.159	0.322
CUT3R	793.31	0.260	0.497	1.346	0.192	0.290	0.458	0.130	0.200	0.043	0.079	0.023	0.080	0.165	25.54	4.484	1.180	0.109	0.497
MonST3R	571.17	OOM	OOM	OOM	OOM	OOM	OOM	OOM	OOM	OOM	OOM	OOM	OOM	OOM	OOM	OOM	OOM	OOM	OOM
Point3R	828.01	0.285	1.066	1.450	0.230	0.339	0.504	0.148	0.263	0.035	0.080	0.015	0.104	0.212	28.09	1.286	3.057	0.139	0.299
Stream3R-S	1190.60	OOM	OOM	OOM	OOM	OOM	OOM	OOM	OOM	OOM	OOM	OOM	OOM	OOM	OOM	OOM	OOM	OOM	OOM
Stream3R-W	1190.60	OOM	OOM	OOM	OOM	OOM	OOM	OOM	OOM	OOM	OOM	OOM	OOM	OOM	OOM	OOM	OOM	OOM	OOM
StreamVGGT	1256.54	0.198	0.590	1.715	0.179	0.279	0.460	0.414	0.565	0.152	0.244	0.111	0.278	0.413	26.9	1.719	1.785	0.251	0.197
Page4D	1256.81	OOM	OOM	OOM	OOM	OOM	OOM	OOM	OOM	OOM	OOM	OOM	OOM	OOM	OOM	OOM	OOM	OOM	OOM
InfiniteVGGT	1256.54	0.197	0.585	1.703	0.179	0.280	0.461	0.416	0.566	0.154	0.246	0.112	0.280	0.416	27.01	1.717	1.750	0.254	0.197
Wint3R	749.46	0.234	0.280	1.215	0.179	0.278	0.466	0.167	0.262	0.042	0.083	0.021	0.098	0.202	27.8	0.874	1.213	0.114	0.475
LongStream-B	1190.60	0.269	0.225	1.013	0.158	0.245	0.411	0.165	0.273	0.097	0.158	0.039	0.149	0.294	5.766	0.105	0.702	0.083	0.410
LongStream-S	1190.60	0.279	0.230	0.998	0.170	0.261	0.426	0.130	0.210	0.076	0.126	0.026	0.107	0.218	10.08	0.186	1.038	0.083	0.438
LingbotMap ⁻ -W	1157.94	0.167	0.211	0.976	0.265	0.392	0.572	0.524	0.678	0.294	0.393	0.229	0.414	0.553	4.694	0.098	0.502	0.352	0.383
LingbotMap ⁻ -S	1157.94	0.139	0.209	0.958	0.384	0.516	0.677	0.602	0.724	0.382	0.477	0.308	0.496	0.627	3.470	0.328	0.749	0.472	0.296
Chunk-wise																			
VGGT-Long	1256.54	0.222	1.006	0.986	0.310	0.428	0.582	0.464	0.593	0.257	0.347	0.211	0.379	0.507	8.467	0.149	0.693	0.467	0.142
π^3 -Long	958.70	0.216	0.375	1.464	0.121	0.203	0.363	0.595	0.741	0.321	0.437	0.253	0.469	0.614	4.021	0.093	0.396	0.251	0.223
DA3-Streaming	1355.67	0.245	22.56	2.475	0.379	0.502	0.666	0.513	0.625	0.331	0.405	0.277	0.427	0.546	8.575	0.119	0.588	0.516	0.162
SLAM-based																			
MAS3R-SLAM	688.64	0.404	2.171	2.920	0.086	0.140	0.265	0.357	0.475	0.117	0.180	0.088	0.207	0.311	25.7	0.413	1.983	0.121	0.493
VGGT-SLAM	1256.54	0.211	0.366	1.051	0.266	0.373	0.530	0.381	0.510	0.206	0.284	0.159	0.309	0.441	9.069	0.152	0.626	0.384	0.160
Test-Time Training																			
TTT3R	793.31	0.222	0.353	1.222	0.220	0.331	0.507	0.221	0.351	0.102	0.172	0.064	0.193	0.321	21.07	0.569	1.234	0.173	0.283
Scal3R	1266.14	0.244	0.280	1.127	0.124	0.197	0.353	0.407	0.552	0.247	0.335	0.161	0.328	0.480	2.396	0.111	0.864	0.498	0.142
LoGeR	1254.62	0.197	0.112	0.741	0.225	0.345	0.524	0.535	0.677	0.249	0.345	0.197	0.391	0.552	5.217	0.090	0.385	0.335	0.165
LoGeR*	1254.60	0.156	0.086	0.684	0.304	0.435	0.611	0.590	0.725	0.317	0.411	0.256	0.446	0.598	4.598	0.077	0.347	0.421	0.145

Table 13 | **Per-Dataset Results on 7Scenes**. Performance across different input regimes: *Single Frame*, *Sparse*, *Medium*, *Dense*, and *Average*. The best, second-best, and third-best results in each column are highlighted in **deep blue**, **medium blue**, and **light blue**, respectively. Out-of-memory (OOM) and Timeout (T.O) cells are shaded **light red**; *Average* values for those rows are wrapped in parentheses and excluded from per-column ranking. Within each sub-category, the **bold** value marks the in-group best. Note that DA-Next (Ours) is excluded from the per-column rankings.

Method	#Params (M)	Single Frame	Sparse		Medium			Dense			Average					
		AbsRel↓	AbsRel↓	AUC@30↑	AbsRel↓	AUC@30↑	ATE↓	F-Score↑	AbsRel↓	AUC@30↑	ATE↓	F-Score↑	AbsRel↓	AUC@30↑	ATE↓	F-Score↑
Optimization-based																
DUS3R	571.2	0.084	0.075	0.641	0.083	0.591	0.107	0.281	OOM	OOM	OOM	OOM	(0.079)	(0.616)	(0.107)	(0.281)
MAS3R	688.6	0.111	0.085	0.591	0.105	0.614	0.121	0.294	OOM	OOM	OOM	OOM	(0.095)	(0.603)	(0.121)	(0.294)
End-to-End Feed-Forward																
VGGT	1257	0.074	0.068	0.715	0.064	0.777	0.070	0.463	OOM	OOM	OOM	OOM	(0.066)	(0.746)	(0.070)	(0.463)
Fast3R	647.5	0.104	0.218	0.428	0.087	0.603	0.201	0.216	0.124	0.341	0.321	0.075	0.143	0.457	0.261	0.146
FastVGGT	1158	0.075	0.072	0.604	0.062	0.771	0.071	0.431	0.066	0.732	0.115	0.401	0.067	0.703	0.093	0.416
MUS3R	423.4	0.072	0.077	0.557	0.063	0.748	0.077	0.383	T.O	T.O	T.O	T.O	(0.070)	(0.652)	(0.077)	(0.383)
MapAnything	1228	0.076	0.073	0.642	0.066	0.732	0.072	0.378	OOM	OOM	OOM	OOM	(0.070)	(0.687)	(0.072)	(0.378)
OmniVGGT	1217	0.062	0.063	0.673	0.058	0.753	0.081	0.469	OOM	OOM	OOM	OOM	(0.061)	(0.713)	(0.081)	(0.469)
π^3	958.7	0.065	0.063	0.663	0.059	0.769	0.063	0.393	0.074	0.161	0.427	0.052	0.065	0.531	0.245	0.222
π^3 -X	1360	0.069	0.064	0.693	0.061	0.776	0.063	0.442	OOM	OOM	OOM	OOM	(0.062)	(0.735)	(0.063)	(0.442)
AMB3R	1563	0.063	0.060	0.680	0.058	0.782	0.063	0.490	OOM	OOM	OOM	OOM	(0.059)	(0.731)	(0.063)	(0.490)
DA3-Small	34.3	0.090	0.082	0.549	0.067	0.699	0.096	0.404	0.070	0.671	0.103	0.399	0.073	0.640	0.099	0.401
DA3-Base	135.4	0.088	0.075	0.675	0.061	0.743	0.079	0.395	0.060	0.735	0.086	0.405	0.065	0.718	0.082	0.400
DA3-Large	410.9	0.077	0.074	0.760	0.059	0.789	0.062	0.464	OOM	OOM	OOM	OOM	(0.066)	(0.774)	(0.062)	(0.464)
DA3-Giant	1356	0.066	0.066	0.780	0.058	0.790	0.059	0.439	OOM	OOM	OOM	OOM	(0.062)	(0.785)	(0.059)	(0.439)
DA3-Nested	1690	0.067	0.064	0.784	0.058	0.790	0.060	0.435	OOM	OOM	OOM	OOM	(0.061)	(0.787)	(0.060)	(0.435)
WorldMirror	1263	0.068	0.066	0.695	0.059	0.770	0.068	0.463	OOM	OOM	OOM	OOM	(0.063)	(0.733)	(0.068)	(0.463)
VGGT-Omega	1144	0.059	0.056	0.808	0.049	0.858	0.035	0.582	-	-	-	-	(0.052)	(0.833)	(0.035)	(0.582)
DA-Next (Ours)	1304	0.066	0.063	0.744	0.059	0.790	0.063	0.446	OOM	OOM	OOM	OOM	(0.063)	(0.767)	(0.063)	(0.446)
Online																
Spann3r ²²⁴	658.7	0.076	0.096	0.429	0.086	0.477	0.195	0.147	0.102	0.452	0.224	0.138	0.095	0.452	0.209	0.143
CUT3R	793.3	0.072	0.073	0.640	0.081	0.648	0.123	0.318	0.105	0.069	0.498	0.055	0.087	0.452	0.311	0.187
MonST3R	571.2	0.104	0.097	0.270	0.092	0.345	0.192	0.151	OOM	OOM	OOM	OOM	(0.095)	(0.307)	(0.192)	(0.151)
Point3R	828	0.072	0.080	0.537	0.083	0.588	0.120	0.225	0.093	0.427	0.239	0.094	0.086	0.517	0.179	0.159
Stream3R-S	1191	0.079	0.078	0.614	0.437	0.236	0.499	0.040	OOM	OOM	OOM	OOM	(0.257)	(0.425)	(0.499)	(0.040)
Stream3R-W	1191	0.079	0.078	0.614	0.308	0.214	0.537	0.048	OOM	OOM	OOM	OOM	(0.193)	(0.414)	(0.537)	(0.048)
StreamVGGT	1257	0.069	0.081	0.598	0.073	0.740	0.086	0.307	0.085	0.659	0.130	0.278	0.080	0.666	0.108	0.292
Page4D	1257	0.069	0.065	0.632	0.062	0.743	0.079	0.373	OOM	OOM	OOM	OOM	(0.064)	(0.687)	(0.079)	(0.373)
InfiniteVGGT	1257	0.069	0.081	0.600	0.073	0.741	0.086	0.310	0.085	0.658	0.131	0.283	0.080	0.666	0.109	0.297
Wint3R	749.5	0.070	0.075	0.598	0.065	0.676	0.097	0.358	0.106	0.241	0.318	0.054	0.082	0.505	0.207	0.206
LongStream-B	1191	0.057	0.067	0.605	0.087	0.683	0.094	0.100	0.087	0.362	0.151	0.060	0.081	0.550	0.123	0.080
LongStream-S	1191	0.057	0.067	0.605	0.071	0.442	0.150	0.040	0.085	0.293	0.180	0.042	0.075	0.447	0.165	0.041
LingbotMap*-W	1158	0.076	0.069	0.702	0.085	0.758	0.070	0.340	0.111	0.674	0.107	0.220	0.088	0.711	0.088	0.280
LingbotMap*-S	1158	0.076	0.069	0.702	0.081	0.770	0.068	0.375	0.092	0.769	0.069	0.300	0.081	0.747	0.069	0.337
Chunk-wise																
VGGT-Long	1257	0.074	0.068	0.715	0.065	0.777	0.063	0.420	0.078	0.645	0.101	0.332	0.070	0.712	0.082	0.376
π^3 -Long	958.7	0.065	0.063	0.663	0.078	0.782	0.058	0.310	0.118	0.679	0.091	0.213	0.086	0.708	0.074	0.261
DA3-Streaming	1356	0.066	0.066	0.780	0.058	0.788	0.059	0.439	0.066	0.675	0.084	0.336	0.063	0.748	0.071	0.388
SLAM-based																
MAS3R-SLAM	688.6	0.141	0.185	0.193	0.181	0.662	0.095	0.209	0.196	0.648	0.099	0.178	0.187	0.501	0.097	0.194
VGGT-SLAM	1257	0.074	0.068	0.715	0.069	0.733	0.075	0.382	0.084	0.576	0.125	0.270	0.074	0.675	0.100	0.326
Test-Time Training																
TTT3R	793.3	0.072	0.077	0.552	0.070	0.701	0.097	0.339	0.097	0.304	0.333	0.151	0.081	0.519	0.215	0.245
Scal3R	1266	0.073	0.069	0.668	0.133	0.688	0.068	0.402	0.140	0.531	0.097	0.288	0.114	0.629	0.083	0.345
LoGeR	1255	0.066	0.062	0.686	0.081	0.758	0.079	0.282	0.106	0.651	0.116	0.238	0.083	0.698	0.097	0.260
LoGeR*	1255	0.070	0.060	0.735	0.061	0.765	0.063	0.455	0.079	0.701	0.074	0.370	0.067	0.734	0.069	0.413

Table 14 | **Per-Dataset Results on ADT**. Performance across different input regimes: *Single Frame*, *Sparse*, *Medium*, *Dense*, and the *Average*. The best, second-best, and third-best results in each column are highlighted in **deep blue**, **medium blue**, and **light blue**, respectively. Out-of-memory (OOM) and Timeout (T.O) cells are shaded **light red**; *Average* values for those rows are wrapped in parentheses and excluded from per-column ranking. Within each sub-category, the **bold** value marks the in-group best. Note that DA-Next (Ours) is excluded from the per-column rankings.

Method	#Params (M)	Single Frame	Sparse		Medium			Dense			Average		
		AbsRel↓	AbsRel↓	AUC@30↑	AbsRel↓	AUC@30↑	ATE↓	AbsRel↓	AUC@30↑	ATE↓	AbsRel↓	AUC@30↑	ATE↓
Optimization-based													
DUS3R	571.2	0.160	0.117	0.882	0.120	0.762	0.117	OOM	OOM	OOM	(0.119)	(0.822)	(0.117)
MAS3R	688.6	0.155	0.079	0.905	0.103	0.861	0.065	OOM	OOM	OOM	(0.091)	(0.883)	(0.065)
End-to-End Feed-Forward													
VGGT	1257	0.133	0.072	0.787	0.073	0.840	0.122	OOM	OOM	OOM	(0.072)	(0.813)	(0.122)
Fast3R	647.5	0.172	0.147	0.597	0.189	0.611	0.710	0.220	0.380	1.032	0.185	0.529	0.871
FastVGGT	1158	0.133	0.064	0.776	0.068	0.873	0.097	0.065	0.825	0.083	0.066	0.825	0.090
MUS3R	423.4	0.168	0.074	0.915	0.126	0.941	0.029	T.O	T.O	T.O	(0.100)	(0.928)	(0.029)
MapAnything	1228	0.108	0.066	0.833	0.073	0.867	0.093	OOM	OOM	OOM	(0.069)	(0.850)	(0.093)
OmniVGGT	1217	0.114	0.078	0.741	0.081	0.742	0.254	OOM	OOM	OOM	(0.080)	(0.741)	(0.254)
π^3	958.7	0.048	0.045	0.954	0.041	0.957	0.025	0.042	0.877	0.042	0.043	0.929	0.033
π^3 -X	1360	0.080	0.046	0.954	0.041	0.965	0.021	OOM	OOM	OOM	(0.044)	(0.959)	(0.021)
AMB3R	1563	0.081	0.045	0.905	0.045	0.934	0.035	OOM	OOM	OOM	(0.045)	(0.920)	(0.035)
DA3-Small	34.3	0.135	0.105	0.571	0.097	0.598	0.326	0.092	0.640	0.255	0.098	0.603	0.290
DA3-Base	135.4	0.159	0.090	0.583	0.092	0.632	0.275	0.091	0.661	0.242	0.091	0.625	0.259
DA3-Large	410.9	0.127	0.072	0.726	0.059	0.783	0.130	OOM	OOM	OOM	(0.066)	(0.755)	(0.130)
DA3-Giant	1356	0.095	0.063	0.775	0.057	0.851	0.101	OOM	OOM	OOM	(0.060)	(0.813)	(0.101)
DA3-Nested	1690	0.089	0.064	0.754	0.059	0.850	0.098	OOM	OOM	OOM	(0.061)	(0.802)	(0.098)
WorldMirror	1263	0.105	0.078	0.807	0.089	0.871	0.078	OOM	OOM	OOM	(0.084)	(0.839)	(0.078)
VGGT-Omega	1144	0.081	0.064	0.851	0.042	0.937	0.039	-	-	-	(0.053)	(0.894)	(0.039)
DA-Next (Ours)	1304	0.010	0.017	0.963	0.013	0.980	0.013	OOM	OOM	OOM	(0.013)	(0.972)	(0.013)
Online													
Spann3r ²²⁴	658.7	0.230	0.110	0.731	0.095	0.807	0.122	0.116	0.699	0.202	0.107	0.746	0.162
CUT3R	793.3	0.130	0.106	0.657	0.131	0.576	0.272	0.159	0.255	0.968	0.132	0.496	0.620
MonST3R	571.2	0.212	0.153	0.146	0.182	0.093	0.631	OOM	OOM	OOM	(0.168)	(0.119)	(0.631)
Point3R	828	0.142	0.140	0.421	0.143	0.494	0.320	0.159	0.397	0.420	0.147	0.437	0.370
Stream3R-S	1191	0.112	0.075	0.732	0.449	0.060	1.494	OOM	OOM	OOM	(0.262)	(0.396)	(1.494)
Stream3R-W	1191	0.112	0.078	0.720	0.655	0.054	1.512	OOM	OOM	OOM	(0.367)	(0.387)	(1.512)
StreamVGGT	1257	0.124	0.117	0.722	0.100	0.779	0.208	0.113	0.672	0.229	0.110	0.725	0.219
Page4D	1257	0.163	0.091	0.657	0.079	0.677	0.199	OOM	OOM	OOM	(0.085)	(0.667)	(0.199)
InfiniteVGGT	1257	0.124	0.117	0.719	0.100	0.779	0.209	0.114	0.673	0.229	0.111	0.724	0.219
Wint3R	749.5	0.136	0.089	0.529	0.079	0.731	0.137	0.094	0.496	0.375	0.087	0.585	0.256
LongStream-B	1191	0.056	0.068	0.776	0.148	0.529	0.266	0.138	0.327	0.281	0.118	0.544	0.274
LongStream-S	1191	0.056	0.068	0.776	0.141	0.238	0.512	0.152	0.145	0.565	0.120	0.386	0.539
LingbotMap*-W	1158	0.199	0.070	0.915	0.071	0.909	0.046	0.068	0.728	0.069	0.069	0.851	0.057
LingbotMap*-S	1158	0.199	0.070	0.915	0.067	0.919	0.038	0.058	0.835	0.044	0.065	0.890	0.041
Chunk-wise													
VGGT-Long	1257	0.133	0.072	0.787	0.079	0.792	0.139	0.109	0.574	0.219	0.087	0.718	0.179
π^3 -Long	958.7	0.048	0.045	0.954	0.115	0.953	0.022	0.135	0.835	0.045	0.098	0.914	0.033
DA3-Streaming	1356	0.095	0.063	0.775	0.059	0.837	0.102	0.071	0.633	0.162	0.064	0.748	0.132
SLAM-based													
MAS3R-SLAM	688.6	0.425	0.319	0.118	0.354	0.481	0.544	0.371	0.747	0.076	0.348	0.449	0.310
VGGT-SLAM	1257	0.133	0.072	0.787	0.103	0.653	0.208	0.111	0.529	0.233	0.095	0.656	0.221
Test-Time Training													
TTT3R	793.3	0.130	0.130	0.531	0.121	0.589	0.445	0.136	0.481	0.383	0.129	0.534	0.414
Scal3R	1266	0.114	0.072	0.903	0.168	0.784	0.027	0.178	0.589	0.042	0.139	0.759	0.035
LoGeR	1255	0.095	0.053	0.904	0.101	0.831	0.095	0.106	0.682	0.111	0.087	0.806	0.103
LoGeR*	1255	0.069	0.046	0.933	0.054	0.904	0.045	0.065	0.816	0.039	0.055	0.884	0.042

Table 15 | **Per-Dataset Results on DROID**. Performance across different input regimes: *Single Frame*, *Sparse*, *Medium*, *Dense*, and the *Average*. The best, second-best, and third-best results in each column are highlighted in **deep blue**, **medium blue**, and **light blue**, respectively. Out-of-memory (OOM) and Timeout (T.O) cells are shaded **light red**; *Average* values for those rows are wrapped in parentheses and excluded from per-column ranking. Within each sub-category, the **bold** value marks the in-group best. Note that DA-Next (Ours) is excluded from the per-column rankings.

Method	#Params (M)	Single Frame	Sparse		Medium			Dense			Average		
		AbsRel↓	AbsRel↓	AUC@30↑	AbsRel↓	AUC@30↑	ATE↓	AbsRel↓	AUC@30↑	ATE↓	AbsRel↓	AUC@30↑	ATE↓
Optimization-based													
DUS3R	571.2	0.218	0.301	0.177	0.305	0.124	0.080	OOM	OOM	OOM	(0.303)	(0.151)	(0.080)
MAS3R	688.6	0.167	0.203	0.269	0.244	0.188	0.072	OOM	OOM	OOM	(0.224)	(0.229)	(0.072)
End-to-End Feed-Forward													
VGGT	1257	0.121	0.111	0.525	0.131	0.450	0.025	OOM	OOM	OOM	(0.121)	(0.487)	(0.025)
Fast3R	647.5	0.199	0.320	0.200	0.282	0.150	0.074	0.303	0.134	0.076	0.301	0.161	0.075
FastVGGT	1158	0.121	0.123	0.506	0.125	0.443	0.028	0.129	0.447	0.026	0.126	0.465	0.027
MUS3R	423.4	0.185	0.190	0.412	0.176	0.389	0.037	T.O	T.O	T.O	(0.183)	(0.401)	(0.037)
MapAnything	1228	0.100	0.167	0.266	0.144	0.272	0.044	OOM	OOM	OOM	(0.155)	(0.269)	(0.044)
OmniVGGT	1217	0.136	0.262	0.551	0.121	0.509	0.020	OOM	OOM	OOM	(0.192)	(0.530)	(0.020)
π^3	958.7	0.106	0.151	0.534	0.105	0.522	0.022	0.105	0.508	0.022	0.120	0.521	0.022
π^3 -X	1360	0.100	0.103	0.607	0.094	0.563	0.019	OOM	OOM	OOM	(0.099)	(0.585)	(0.019)
AMB3R	1563	0.098	0.091	0.561	0.080	0.481	0.024	OOM	OOM	OOM	(0.085)	(0.521)	(0.024)
DA3-Small	34.3	0.198	0.238	0.168	0.219	0.185	0.052	0.224	0.162	0.058	0.227	0.172	0.055
DA3-Base	135.4	0.158	0.190	0.294	0.159	0.252	0.040	0.161	0.237	0.042	0.170	0.261	0.041
DA3-Large	410.9	0.136	0.162	0.523	0.095	0.477	0.020	OOM	OOM	OOM	(0.129)	(0.500)	(0.020)
DA3-Giant	1356	0.114	0.125	0.642	0.092	0.593	0.016	OOM	OOM	OOM	(0.108)	(0.618)	(0.016)
DA3-Nested	1690	0.123	0.146	0.675	0.110	0.578	0.018	OOM	OOM	OOM	(0.128)	(0.627)	(0.018)
WorldMirror	1263	0.125	0.256	0.539	0.125	0.477	0.026	OOM	OOM	OOM	(0.190)	(0.508)	(0.026)
VGGT-Omega	1144	0.073	0.091	0.621	0.059	0.533	0.021	-	-	-	(0.075)	(0.577)	(0.021)
DA-Next (Ours)	1304	0.098	0.090	0.627	0.044	0.582	0.018	OOM	OOM	OOM	(0.077)	(0.605)	(0.018)
Online													
Spann3r ²²⁴	658.7	0.189	0.246	0.087	0.259	0.103	0.076	0.326	0.077	0.091	0.277	0.089	0.084
CUT3R	793.3	0.190	0.253	0.305	0.294	0.199	0.057	0.399	0.066	0.086	0.315	0.190	0.071
MonST3R	571.2	0.195	0.204	0.183	0.269	0.168	0.073	OOM	OOM	OOM	(0.237)	(0.176)	(0.073)
Point3R	828	0.213	0.369	0.167	0.353	0.094	0.081	0.348	0.077	0.082	0.357	0.113	0.081
Stream3R-S	1191	0.093	0.112	0.467	0.139	0.339	0.050	OOM	OOM	OOM	(0.125)	(0.403)	(0.050)
Stream3R-W	1191	0.093	0.112	0.467	0.220	0.217	0.086	OOM	OOM	OOM	(0.166)	(0.342)	(0.086)
StreamVGGT	1257	0.105	0.130	0.488	0.161	0.380	0.038	0.177	0.327	0.048	0.156	0.398	0.043
Page4D	1257	0.135	0.127	0.322	0.113	0.345	0.028	OOM	OOM	OOM	(0.120)	(0.334)	(0.028)
InfiniteVGGT	1257	0.105	0.131	0.491	0.162	0.379	0.038	0.178	0.328	0.048	0.157	0.400	0.043
Wint3R	749.5	0.189	0.187	0.262	0.179	0.159	0.059	0.321	0.058	0.084	0.229	0.160	0.072
LongStream-B	1191	0.176	0.306	0.367	0.559	0.174	0.070	0.481	0.204	0.067	0.449	0.249	0.069
LongStream-S	1191	0.176	0.306	0.368	0.302	0.217	0.061	0.512	0.167	0.062	0.373	0.251	0.062
LingbotMap*-W	1158	0.142	0.176	0.308	0.145	0.391	0.033	0.209	0.269	0.048	0.177	0.322	0.041
LingbotMap*-S	1158	0.142	0.176	0.308	0.145	0.376	0.035	0.163	0.323	0.036	0.161	0.336	0.036
Chunk-wise													
VGGT-Long	1257	0.121	0.111	0.525	0.135	0.435	0.028	0.200	0.284	0.045	0.149	0.415	0.036
π^3 -Long	958.7	0.106	0.151	0.534	0.113	0.515	0.022	0.232	0.352	0.036	0.166	0.467	0.029
DA3-Streaming	1356	0.114	0.125	0.642	0.094	0.567	0.018	0.136	0.414	0.031	0.118	0.541	0.025
SLAM-based													
MAS3R-SLAM	688.6	0.261	0.342	0.239	0.392	0.126	0.078	0.378	0.108	0.076	0.370	0.158	0.077
VGGT-SLAM	1257	0.121	0.111	0.525	0.141	0.383	0.034	0.232	0.179	0.059	0.161	0.362	0.047
Test-Time Training													
TTT3R	793.3	0.190	0.263	0.268	0.253	0.244	0.043	0.304	0.194	0.062	0.274	0.235	0.053
Scal3R	1266	0.159	0.252	0.571	0.186	0.495	0.022	0.302	0.279	0.035	0.247	0.448	0.028
LoGeR	1255	0.102	0.140	0.490	0.142	0.445	0.032	0.269	0.394	0.033	0.183	0.443	0.032
LoGeR*	1255	0.095	0.120	0.518	0.105	0.437	0.028	0.214	0.387	0.036	0.146	0.447	0.032

Table 16 | **Per-Dataset Results on DTU**. Performance across different input regimes: *Single Frame*, *Sparse*, *Medium*, *Dense*, and the *Average*. The best, second-best, and third-best results in each column are highlighted in **deep blue**, **medium blue**, and **light blue**, respectively. This dataset is not evaluated under the *Dense* regime, so the corresponding cells are marked as “-”. Within each sub-category, the **bold** value marks the in-group best. Note that DA-Next (Ours) is excluded from the per-column rankings.

Method	#Params (M)	Single Frame	Sparse		Medium				Dense				Average			
		AbsRel↓	AbsRel↓	AUC@30↑	AbsRel↓	AUC@30↑	ATE↓	F-Score↑	AbsRel↓	AUC@30↑	ATE↓	F-Score↑	AbsRel↓	AUC@30↑	ATE↓	F-Score↑
Optimization-based																
DUST3R	571.2	0.049	0.064	0.627	0.077	0.613	0.045	0.385	-	-	-	-	0.070	0.620	0.045	0.385
MAT3R	688.6	0.078	0.069	0.723	0.065	0.686	0.034	0.436	-	-	-	-	0.067	0.704	0.034	0.436
End-to-End Feed-Forward																
VGGT	1257	0.009	0.008	0.997	0.005	0.995	0.002	0.797	-	-	-	-	0.007	0.996	0.002	0.797
Fast3R	647.5	0.059	0.074	0.764	0.064	0.716	0.038	0.318	-	-	-	-	0.069	0.740	0.038	0.318
FastVGGT	1158	0.009	0.009	0.968	0.007	0.960	0.005	0.809	-	-	-	-	0.008	0.964	0.005	0.809
MUST3R	423.4	0.059	0.058	0.797	0.042	0.823	0.023	0.468	-	-	-	-	0.050	0.810	0.023	0.468
MapAnything	1228	0.090	0.084	0.624	0.083	0.621	0.044	0.290	-	-	-	-	0.084	0.622	0.044	0.290
OmniVGGT	1217	0.022	0.013	0.962	0.012	0.962	0.005	0.735	-	-	-	-	0.012	0.962	0.005	0.735
π^3	958.7	0.027	0.016	0.945	0.013	0.950	0.006	0.669	-	-	-	-	0.015	0.947	0.006	0.669
π^3 -X	1360	0.027	0.018	0.943	0.014	0.958	0.005	0.649	-	-	-	-	0.016	0.951	0.005	0.649
AMB3R	1563	0.012	0.009	0.994	0.007	0.990	0.003	0.581	-	-	-	-	0.008	0.992	0.003	0.581
DA3-Small	34.3	0.069	0.034	0.831	0.028	0.798	0.019	0.625	-	-	-	-	0.031	0.814	0.019	0.625
DA3-Base	135.4	0.055	0.021	0.898	0.017	0.898	0.010	0.689	-	-	-	-	0.019	0.898	0.010	0.689
DA3-Large	410.9	0.035	0.017	0.972	0.012	0.966	0.004	0.727	-	-	-	-	0.015	0.969	0.004	0.727
DA3-Giant	1356	0.033	0.014	0.992	0.011	0.987	0.002	0.747	-	-	-	-	0.013	0.990	0.002	0.747
DA3-Nested	1690	0.028	0.019	0.993	0.013	0.986	0.002	0.739	-	-	-	-	0.016	0.989	0.002	0.739
WorldMirror	1263	0.039	0.024	0.898	0.021	0.899	0.011	0.571	-	-	-	-	0.022	0.898	0.011	0.571
VGGT-Omega	1144	0.018	0.014	0.989	0.011	0.973	0.003	0.679	-	-	-	-	(0.012)	(0.981)	(0.003)	(0.679)
DA-Next (Ours)	1304	0.121	0.054	0.898	0.020	0.901	0.013	0.643	-	-	-	-	(0.065)	(0.900)	(0.011)	(0.643)
Online																
Spann3r ²²⁴	658.7	0.040	0.047	0.602	0.044	0.634	0.043	0.473	-	-	-	-	0.045	0.618	0.043	0.473
CUT3R	793.3	0.050	0.056	0.763	0.053	0.724	0.028	0.375	-	-	-	-	0.054	0.744	0.028	0.375
MonST3R	571.2	0.104	0.101	0.470	0.123	0.014	0.214	0.007	-	-	-	-	0.112	0.242	0.214	0.007
Point3R	828	0.038	0.061	0.596	0.063	0.499	0.048	0.239	-	-	-	-	0.062	0.547	0.048	0.239
Stream3R-S	1191	0.010	0.011	0.965	0.010	0.937	0.008	0.726	-	-	-	-	0.011	0.951	0.008	0.726
Stream3R-W	1191	0.010	0.011	0.965	0.011	0.896	0.013	0.720	-	-	-	-	0.011	0.931	0.013	0.720
StreamVGGT	1257	0.012	0.012	0.971	0.011	0.963	0.005	0.795	-	-	-	-	0.012	0.967	0.005	0.795
Page4D	1257	0.019	0.022	0.877	0.015	0.860	0.011	0.568	-	-	-	-	0.018	0.869	0.011	0.568
InfiniteVGGT	1257	0.011	0.012	0.972	0.011	0.962	0.006	0.804	-	-	-	-	0.012	0.967	0.006	0.804
Wint3R	749.5	0.033	0.028	0.791	0.026	0.785	0.020	0.610	-	-	-	-	0.027	0.788	0.020	0.610
LongStream-B	1191	0.037	0.038	0.851	0.062	0.715	0.031	0.247	-	-	-	-	0.050	0.783	0.031	0.247
LongStream-S	1191	0.037	0.038	0.851	0.032	0.707	0.030	0.267	-	-	-	-	0.035	0.779	0.030	0.267
LingbotMap*-W	1158	0.058	0.048	0.776	0.048	0.719	0.032	0.300	-	-	-	-	0.048	0.748	0.032	0.300
LingbotMap*-S	1158	0.058	0.048	0.776	0.048	0.719	0.032	0.300	-	-	-	-	0.048	0.748	0.032	0.300
Chunk-wise																
VGGT-Long	1257	0.009	0.008	0.997	0.005	0.995	0.002	0.797	-	-	-	-	0.007	0.996	0.002	0.797
π^3 -Long	958.7	0.027	0.016	0.945	0.013	0.950	0.006	0.669	-	-	-	-	0.015	0.947	0.006	0.669
DA3-Streaming	1356	0.033	0.014	0.993	0.011	0.987	0.002	0.746	-	-	-	-	0.013	0.990	0.002	0.746
SLAM-based																
MAT3R-SLAM	688.6	0.126	0.120	0.251	0.140	0.320	0.093	0.189	-	-	-	-	0.130	0.285	0.093	0.189
VGGT-SLAM	1257	0.009	0.008	0.997	0.005	0.995	0.002	0.797	-	-	-	-	0.007	0.996	0.002	0.797
Test-Time Training																
TTT3R	793.3	0.050	0.059	0.696	0.055	0.702	0.042	0.345	-	-	-	-	0.057	0.699	0.042	0.345
Scal3R	1266	0.010	0.008	0.991	0.007	0.981	0.002	0.773	-	-	-	-	0.008	0.986	0.002	0.773
LoGeR	1255	0.031	0.031	0.890	0.020	0.897	0.011	0.639	-	-	-	-	0.026	0.893	0.011	0.639
LoGeR*	1255	0.038	0.021	0.888	0.018	0.889	0.011	0.658	-	-	-	-	0.020	0.889	0.011	0.658

Table 17 | **Per-Dataset Results on ETH3D**. Performance across different input regimes: *Single Frame*, *Sparse*, *Medium*, *Dense*, and the *Average*. The best, second-best, and third-best results in each column are highlighted in **deep blue**, **medium blue**, and **light blue**, respectively. This dataset is not evaluated under the *Dense* regime, so the corresponding cells are marked as “-”. Within each sub-category, the **bold** value marks the in-group best. Note that DA-Next (Ours) is excluded from the per-column rankings.

Method	#Params (M)	Single Frame	Sparse		Medium			Dense			Average		
		AbsRel↓	AbsRel↓	AUC@30↑	AbsRel↓	AUC@30↑	ATE↓	AbsRel↓	AUC@30↑	ATE↓	AbsRel↓	AUC@30↑	ATE↓
Optimization-based													
DUS3R	571.2	0.046	0.099	0.482	0.084	0.528	1.297	-	-	-	0.092	0.505	1.297
MAS3R	688.6	0.051	0.086	0.690	0.057	0.793	0.597	-	-	-	0.071	0.742	0.597
End-to-End Feed-Forward													
VGGT	1257	0.033	0.050	0.686	0.039	0.715	0.460	-	-	-	0.044	0.701	0.460
Fast3R	647.5	0.083	0.163	0.267	0.208	0.285	2.747	-	-	-	0.186	0.276	2.747
FastVGGT	1158	0.034	0.055	0.568	0.053	0.601	0.791	-	-	-	0.054	0.584	0.791
MUS3R	423.4	0.037	0.071	0.587	0.056	0.762	0.554	-	-	-	0.063	0.675	0.554
MapAnything	1228	0.038	0.047	0.670	0.048	0.736	0.314	-	-	-	0.048	0.703	0.314
OmniVGGT	1217	0.026	0.042	0.556	0.039	0.638	0.952	-	-	-	0.040	0.597	0.952
π^3	958.7	0.027	0.034	0.706	0.030	0.784	0.199	-	-	-	0.032	0.745	0.199
π^3 -X	1360	0.028	0.032	0.692	0.030	0.779	0.207	-	-	-	0.031	0.735	0.207
AMB3R	1563	0.022	0.050	0.684	0.037	0.779	0.280	-	-	-	0.043	0.731	0.280
DA3-Small	34.3	0.063	0.108	0.484	0.102	0.511	1.120	-	-	-	0.105	0.498	1.120
DA3-Base	135.4	0.045	0.080	0.655	0.068	0.677	0.685	-	-	-	0.074	0.666	0.685
DA3-Large	410.9	0.042	0.056	0.689	0.041	0.795	0.552	-	-	-	0.049	0.742	0.552
DA3-Giant	1356	0.031	0.035	0.802	0.028	0.880	0.196	-	-	-	0.031	0.841	0.196
DA3-Nested	1690	0.041	0.027	0.805	0.025	0.878	0.192	-	-	-	0.026	0.842	0.192
WorldMirror	1263	0.031	0.040	0.709	0.039	0.785	1.411	-	-	-	0.040	0.747	1.411
VGGT-Omega	1144	0.019	0.023	0.863	0.021	0.899	0.126	-	-	-	(0.022)	(0.881)	(0.126)
DA-Next (Ours)	1304	0.030	0.037	0.765	0.025	0.845	0.222	-	-	-	(0.031)	(0.805)	(0.222)
Online													
Spann3r ²²⁴	658.7	0.156	0.256	0.256	0.264	0.256	2.833	-	-	-	0.260	0.256	2.833
CUT3R	793.3	0.040	0.100	0.428	0.104	0.449	1.354	-	-	-	0.102	0.439	1.354
MonST3R	571.2	0.051	0.131	0.207	0.196	0.078	2.126	-	-	-	0.163	0.142	2.126
Point3R	828	0.046	0.173	0.223	0.177	0.181	2.042	-	-	-	0.175	0.202	2.042
Stream3R-S	1191	0.023	0.043	0.455	0.064	0.518	1.241	-	-	-	0.053	0.486	1.241
Stream3R-W	1191	0.023	0.043	0.455	0.069	0.493	1.290	-	-	-	0.056	0.474	1.290
StreamVGGT	1257	0.031	0.092	0.473	0.138	0.443	1.126	-	-	-	0.115	0.458	1.126
Page4D	1257	0.031	0.046	0.527	0.050	0.565	0.696	-	-	-	0.048	0.546	0.696
InfiniteVGGT	1257	0.031	0.092	0.470	0.138	0.442	1.129	-	-	-	0.115	0.456	1.129
Wint3R	749.5	0.043	0.093	0.416	0.093	0.321	1.556	-	-	-	0.093	0.369	1.556
LongStream-B	1191	0.031	0.071	0.472	0.081	0.389	1.802	-	-	-	0.076	0.431	1.802
LongStream-S	1191	0.031	0.071	0.472	0.081	0.385	1.798	-	-	-	0.076	0.429	1.798
LingbotMap*-W	1158	0.038	0.052	0.711	0.054	0.673	1.293	-	-	-	0.053	0.692	1.293
LingbotMap*-S	1158	0.038	0.052	0.711	0.054	0.673	1.293	-	-	-	0.053	0.692	1.293
Chunk-wise													
VGGT-Long	1257	0.033	0.050	0.686	0.039	0.715	0.460	-	-	-	0.044	0.701	0.460
π^3 -Long	958.7	0.027	0.034	0.706	0.030	0.784	0.199	-	-	-	0.032	0.745	0.199
DA3-Streaming	1356	0.031	0.035	0.803	0.028	0.880	0.196	-	-	-	0.031	0.841	0.196
SLAM-based													
MAS3R-SLAM	688.6	0.104	0.165	0.145	0.165	0.098	2.659	-	-	-	0.165	0.121	2.659
VGGT-SLAM	1257	0.033	0.050	0.686	0.039	0.715	0.460	-	-	-	0.044	0.701	0.460
Test-Time Training													
TTT3R	793.3	0.040	0.114	0.450	0.100	0.395	2.009	-	-	-	0.107	0.422	2.009
Scal3R	1266	0.027	0.035	0.717	0.033	0.772	0.234	-	-	-	0.034	0.744	0.234
LoGeR	1255	0.032	0.035	0.717	0.026	0.793	0.217	-	-	-	0.030	0.755	0.217
LoGeR*	1255	0.030	0.031	0.730	0.025	0.828	0.176	-	-	-	0.028	0.779	0.176

Table 18 | **Per-Dataset Results on Hiroom**. Performance across different input regimes: *Single Frame*, *Sparse*, *Medium*, *Dense*, and the *Average*. The best, second-best, and third-best results in each column are highlighted in **deep blue**, **medium blue**, and **light blue**, respectively. This dataset is not evaluated under the *Dense* regime, so the corresponding cells are marked as “-”. Within each sub-category, the **bold** value marks the in-group best. Note that DA-Next (Ours) is excluded from the per-column rankings.

Method	#Params (M)	Single Frame	Sparse			Medium			Dense			Average				
		AbsRel↓	AbsRel↓	AUC@30↑	AbsRel↓	AUC@30↑	ATE↓	F-Score↑	AbsRel↓	AUC@30↑	ATE↓	F-Score↑	AbsRel↓	AUC@30↑	ATE↓	F-Score↑
Optimization-based																
DUST3R	571.2	0.024	0.028	0.786	0.031	0.853	0.079	0.289	-	-	-	-	0.030	0.820	0.079	0.289
MAT3R	688.6	0.056	0.075	0.879	0.051	0.904	0.054	0.306	-	-	-	-	0.063	0.891	0.054	0.306
End-to-End Feed-Forward																
VGGT	1257	0.024	0.020	0.792	0.017	0.848	0.091	0.558	-	-	-	-	0.018	0.820	0.091	0.558
Fast3R	647.5	0.038	0.079	0.646	0.050	0.729	0.222	0.256	-	-	-	-	0.065	0.688	0.222	0.256
FastVGGT	1158	0.024	0.024	0.621	0.024	0.752	0.224	0.345	-	-	-	-	0.024	0.687	0.224	0.345
MUST3R	423.4	0.033	0.021	0.933	0.020	0.942	0.037	0.651	-	-	-	-	0.021	0.938	0.037	0.651
MapAnything	1228	0.021	0.028	0.890	0.027	0.898	0.063	0.584	-	-	-	-	0.028	0.894	0.063	0.584
OmniVGGT	1217	0.023	0.025	0.811	0.021	0.778	0.137	0.387	-	-	-	-	0.023	0.795	0.137	0.387
π^3	958.7	0.020	0.022	0.932	0.013	0.948	0.033	0.679	-	-	-	-	0.017	0.940	0.033	0.679
π^3 -X	1360	0.021	0.018	0.919	0.013	0.955	0.028	0.651	-	-	-	-	0.015	0.937	0.028	0.651
AMB3R	1563	0.027	0.020	0.871	0.021	0.897	0.057	0.390	-	-	-	-	0.021	0.884	0.057	0.390
DA3-Small	34.3	0.039	0.042	0.650	0.044	0.801	0.103	0.363	-	-	-	-	0.043	0.725	0.103	0.363
DA3-Base	135.4	0.036	0.032	0.848	0.029	0.869	0.086	0.454	-	-	-	-	0.031	0.859	0.086	0.454
DA3-Large	410.9	0.020	0.017	0.947	0.014	0.972	0.027	0.629	-	-	-	-	0.016	0.959	0.027	0.629
DA3-Giant	1356	0.017	0.009	0.966	0.005	0.996	0.008	0.960	-	-	-	-	0.007	0.981	0.008	0.960
DA3-Nested	1690	0.020	0.010	0.971	0.006	0.994	0.009	0.947	-	-	-	-	0.008	0.983	0.009	0.947
WorldMirror	1263	0.026	0.030	0.912	0.025	0.923	0.047	0.474	-	-	-	-	0.027	0.918	0.047	0.474
VGGT-Omega	1144	0.008	0.015	0.985	0.009	0.980	0.017	0.868	-	-	-	-	(0.012)	(0.983)	(0.017)	(0.868)
DA-Next (Ours)	1304	0.018	0.010	0.982	0.007	0.990	0.011	0.948	-	-	-	-	(0.012)	(0.986)	(0.011)	(0.948)
Online																
Spann3r ²²⁴	658.7	0.041	0.079	0.594	0.071	0.659	0.328	0.214	-	-	-	-	0.075	0.627	0.328	0.214
CUT3R	793.3	0.035	0.082	0.531	0.076	0.634	0.359	0.143	-	-	-	-	0.079	0.583	0.359	0.143
MonST3R	571.2	0.033	0.094	0.327	0.070	0.167	0.702	0.050	-	-	-	-	0.082	0.247	0.702	0.050
Point3R	828	0.038	0.088	0.417	0.074	0.422	0.456	0.138	-	-	-	-	0.081	0.419	0.456	0.138
Stream3R-S	1191	0.025	0.030	0.781	0.030	0.777	0.158	0.269	-	-	-	-	0.030	0.779	0.158	0.269
Stream3R-W	1191	0.025	0.030	0.781	0.030	0.771	0.159	0.256	-	-	-	-	0.030	0.776	0.159	0.256
StreamVGGT	1257	0.024	0.076	0.736	0.057	0.688	0.274	0.079	-	-	-	-	0.066	0.712	0.274	0.079
Page4D	1257	0.028	0.029	0.736	0.025	0.858	0.076	0.314	-	-	-	-	0.027	0.797	0.076	0.314
InfiniteVGGT	1257	0.023	0.075	0.731	0.057	0.687	0.274	0.078	-	-	-	-	0.066	0.709	0.274	0.078
Wint3R	749.5	0.028	0.035	0.728	0.034	0.648	0.268	0.252	-	-	-	-	0.035	0.688	0.268	0.252
LongStream-B	1191	0.019	0.033	0.819	0.030	0.759	0.224	0.052	-	-	-	-	0.031	0.789	0.224	0.052
LongStream-S	1191	0.019	0.033	0.819	0.030	0.759	0.224	0.053	-	-	-	-	0.031	0.789	0.224	0.053
LingbotMap*-W	1158	0.027	0.034	0.870	0.036	0.769	0.127	0.278	-	-	-	-	0.035	0.820	0.127	0.278
LingbotMap*-S	1158	0.027	0.034	0.870	0.036	0.769	0.127	0.278	-	-	-	-	0.035	0.820	0.127	0.278
Chunk-wise																
VGGT-Long	1257	0.024	0.020	0.792	0.017	0.848	0.091	0.559	-	-	-	-	0.018	0.820	0.091	0.559
π^3 -Long	958.7	0.020	0.022	0.932	0.013	0.948	0.033	0.679	-	-	-	-	0.017	0.940	0.033	0.679
DA3-Streaming	1356	0.017	0.009	0.966	0.005	0.996	0.008	0.960	-	-	-	-	0.007	0.981	0.008	0.960
SLAM-based																
MAT3R-SLAM	688.6	0.159	0.202	0.194	0.171	0.238	0.845	0.021	-	-	-	-	0.187	0.216	0.845	0.021
VGGT-SLAM	1257	0.024	0.020	0.792	0.017	0.848	0.091	0.558	-	-	-	-	0.018	0.820	0.091	0.558
Test-Time Training																
TTT3R	793.3	0.035	0.086	0.486	0.080	0.608	0.380	0.136	-	-	-	-	0.083	0.547	0.380	0.136
Scal3R	1266	0.022	0.019	0.859	0.014	0.958	0.034	0.651	-	-	-	-	0.016	0.909	0.034	0.651
LoGeR	1255	0.025	0.018	0.836	0.017	0.915	0.046	0.342	-	-	-	-	0.017	0.875	0.046	0.342
LoGeR*	1255	0.023	0.020	0.856	0.019	0.908	0.049	0.402	-	-	-	-	0.019	0.882	0.049	0.402

Table 19 | **Per-Dataset Results on KITTI-Odometry**. Only metrics available for the *Dense* regime are reported. The best, second-best, and third-best results in each column are highlighted in **deep blue**, **medium blue**, and **light blue**, respectively. Out-of-memory (OOM) and Timeout (T.O) cells are shaded **light red**; methods without dense-regime results use “-”. Within each sub-category, the **bold** value marks the in-group best. Note that DA-Next (Ours) is excluded from the per-column rankings.

Method	#Params (M)	Camera		Trajectory	
		AUC@30↑	ATE↓	RPE _t ↓	RPE _r ↓
Optimization-based					
DUS _t 3R	571.2	OOM	OOM	OOM	OOM
MAS _t 3R	688.6	OOM	OOM	OOM	OOM
End-to-End Feed-Forward					
VGGT	1257	OOM	OOM	OOM	OOM
Fast3R	647.5	0.000	134.5	29.12	27.34
FastVGGT	1158	0.307	181.9	9.827	3.338
MUS _t 3R	423.4	T.O	T.O	T.O	T.O
MapAnything	1228	OOM	OOM	OOM	OOM
OmniVGGT	1217	OOM	OOM	OOM	OOM
π^3	958.7	0.412	153	10.07	1.369
π^3 -X	1360	OOM	OOM	OOM	OOM
AMB3R	1563	OOM	OOM	OOM	OOM
DA3-Small	34.3	0.089	220.3	29	17.12
DA3-Base	135.4	0.067	211.7	30.08	40.69
DA3-Large	410.9	OOM	OOM	OOM	OOM
DA3-Giant	1356	OOM	OOM	OOM	OOM
DA3-Nested	1690	OOM	OOM	OOM	OOM
WorldMirror	1263	OOM	OOM	OOM	OOM
VGGT-Omega	1144	-	-	-	-
DA-Next (Ours)	1304	OOM	OOM	OOM	OOM
Online					
Spann3r ²²⁴	658.7	0.036	214.9	23.33	18.99
CUT3R	793.3	0.065	206.6	2.763	1.830
MonST3R	571.2	OOM	OOM	OOM	OOM
Point3R	828	0.051	206.5	7.671	4.421
Stream3R-S	1191	OOM	OOM	OOM	OOM
Stream3R-W	1191	OOM	OOM	OOM	OOM
StreamVGGT	1257	0.168	206.2	14	4.174
Page4D	1257	OOM	OOM	OOM	OOM
InfiniteVGGT	1257	0.169	206.7	13.87	4.164
Wint3R	749.5	0.074	211.3	5.458	1.624
LongStream-B	1191	0.317	47.33	0.348	0.331
LongStream-S	1191	0.211	88.6	0.885	0.620
LingbotMap*-W	1158	0.615	41.16	0.368	0.286
LingbotMap*-S	1158	0.729	29.31	2.440	0.663
Chunk-wise					
VGGT-Long	1257	0.465	76.14	0.798	0.468
π^3 -Long	958.7	0.702	31.91	0.362	0.181
DA3-Streaming	1356	0.221	79.26	0.633	0.689
SLAM-based					
MAS _t 3R-SLAM	688.6	0.158	196.5	1.737	0.561
VGGT-SLAM	1257	0.436	80.06	0.607	0.226
Test-Time Training					
TTT3R	793.3	0.086	182.1	3.824	2.146
Scal3R	1266	0.655	18.17	0.457	0.649
LoGeR	1255	0.457	45.03	0.382	0.238
LoGeR*	1255	0.456	39.62	0.286	0.220

Table 20 | **Per-Dataset Results on Lingbot-Depth**. Only metrics available for the *Single Frame* regime are reported. The best, second-best, and third-best results in each column are highlighted in **deep blue**, **medium blue**, and **light blue**, respectively. Within each sub-category, the **bold** value marks the in-group best. Note that DA-Next (Ours) is excluded from the per-column rankings.

Method	#Params (M)	Depth					
		AbsRel↓	SqRel↓	RMSE↓	$\delta_{1.03}$ ↑	$\delta_{1.05}$ ↑	$\delta_{1.10}$ ↑
Optimization-based							
DUST3R	571.2	0.949	18.34	0.836	0.308	0.439	0.636
MAST3R	688.6	1.227	35.58	0.911	0.349	0.485	0.682
End-to-End Feed-Forward							
VGGT	1257	0.428	2.572	0.692	0.387	0.519	0.709
Fast3R	647.5	0.804	11.42	0.826	0.285	0.390	0.543
FastVGGT	1158	0.424	2.505	0.692	0.388	0.520	0.710
MUST3R	423.4	1.110	30.18	0.831	0.368	0.484	0.681
MapAnything	1228	1.326	42.33	0.784	0.423	0.571	0.749
OmniVGGT	1217	0.419	2.593	0.614	0.428	0.557	0.751
π^3	958.7	1.485	59.37	0.793	0.480	0.622	0.771
π^3 -X	1360	1.118	31.36	0.674	0.461	0.592	0.780
AMB3R	1563	1.453	54.6	0.762	0.439	0.572	0.750
DA3-Small	34.3	0.973	22.16	0.796	0.240	0.359	0.578
DA3-Base	135.4	0.875	18.38	0.661	0.338	0.480	0.694
DA3-Large	410.9	0.881	19.73	0.628	0.382	0.534	0.726
DA3-Giant	1356	1.034	26.41	0.693	0.440	0.586	0.744
DA3-Nested	1690	1.015	25.81	0.707	0.448	0.594	0.758
WorldMirror	1263	0.962	27.24	0.681	0.434	0.567	0.746
VGGT-Omega	1144	1.647	73.16	0.889	0.450	0.582	0.768
DA-Next (Ours)	1304	0.405	3.183	0.611	0.399	0.529	0.715
Online							
Spann3r ²²⁴	658.7	0.843	13.87	1.055	0.203	0.321	0.509
CUT3R	793.3	0.543	4.487	0.611	0.347	0.482	0.677
MonST3R	571.2	0.660	8.235	0.792	0.332	0.455	0.636
Point3R	828	0.988	23.95	0.766	0.300	0.422	0.632
Stream3R-S	1191	1.228	40.11	0.741	0.474	0.615	0.773
Stream3R-W	1191	1.228	40.11	0.741	0.474	0.615	0.773
StreamVGGT	1257	0.553	5.858	0.611	0.399	0.528	0.727
Page4D	1257	0.566	6.851	0.734	0.355	0.474	0.667
InfiniteVGGT	1257	0.547	5.667	0.610	0.399	0.528	0.727
Wint3R	749.5	1.869	90.54	1.231	0.385	0.502	0.682
LongStream-B	1191	1.572	60.93	0.831	0.372	0.510	0.722
LongStream-S	1191	1.572	60.93	0.831	0.372	0.510	0.722
LingbotMap ⁺ -W	1158	0.883	15.64	0.768	0.385	0.516	0.693
LingbotMap ⁺ -S	1158	0.883	15.64	0.768	0.385	0.516	0.693
Chunk-wise							
VGGT-Long	1257	0.428	2.572	0.692	0.387	0.519	0.709
π^3 -Long	958.7	1.485	59.37	0.793	0.480	0.622	0.771
DA3-Streaming	1356	1.034	26.41	0.693	0.440	0.586	0.744
SLAM-based							
MAST3R-SLAM	688.6	0.619	4.389	0.784	0.150	0.241	0.438
VGGT-SLAM	1257	0.428	2.572	0.692	0.387	0.519	0.709
Test-Time Training							
TTT3R	793.3	0.543	4.488	0.611	0.347	0.482	0.677
Scal3R	1266	0.546	5.438	0.682	0.424	0.555	0.733
LoGeR	1255	0.662	9.432	0.617	0.465	0.607	0.764
LoGeR*	1255	0.506	4.440	0.607	0.487	0.605	0.769

Table 21 | **Per-Dataset Results on NRGBD**. Performance across different input regimes: *Single Frame*, *Sparse*, *Medium*, *Dense*, and the *Average*. The best, second-best, and third-best results in each column are highlighted in **deep blue**, **medium blue**, and **light blue**, respectively. Out-of-memory (OOM) and Timeout (T.O) cells are shaded **light red**; *Average* values for those rows are wrapped in parentheses and excluded from per-column ranking. Within each sub-category, the **bold** value marks the in-group best. Note that DA-Next (Ours) is excluded from the per-column rankings.

Method	#Params (M)	Single Frame	Sparse		Medium				Dense				Average			
		AbsRel↓	AbsRel↓	AUC@30↑	AbsRel↓	AUC@30↑	ATE↓	F-Score↑	AbsRel↓	AUC@30↑	ATE↓	F-Score↑	AbsRel↓	AUC@30↑	ATE↓	F-Score↑
Optimization-based																
DUST3R	571.2	0.028	0.038	0.843	0.036	0.783	0.265	0.327	OOM	OOM	OOM	OOM	(0.037)	(0.813)	(0.265)	(0.327)
MASt3R	688.6	0.036	0.043	0.891	0.048	0.778	0.205	0.290	OOM	OOM	OOM	OOM	(0.046)	(0.834)	(0.205)	(0.290)
End-to-End Feed-Forward																
VGGT	1257	0.024	0.016	0.926	0.012	0.956	0.039	0.696	OOM	OOM	OOM	OOM	(0.014)	(0.941)	(0.039)	(0.696)
Fast3R	647.5	0.042	0.073	0.779	0.041	0.858	0.102	0.345	0.039	0.592	0.157	0.351	0.051	0.743	0.130	0.348
FastVGGT	1158	0.026	0.023	0.888	0.014	0.947	0.044	0.569	0.019	0.831	0.162	0.470	0.019	0.889	0.103	0.519
MUST3R	423.4	0.024	0.026	0.912	0.021	0.932	0.053	0.569	T.O	T.O	T.O	T.O	(0.024)	(0.922)	(0.053)	(0.569)
MapAnything	1228	0.026	0.035	0.872	0.031	0.886	0.093	0.437	OOM	OOM	OOM	OOM	(0.033)	(0.879)	(0.093)	(0.437)
OmniVGGT	1217	0.016	0.020	0.913	0.013	0.948	0.039	0.728	OOM	OOM	OOM	OOM	(0.016)	(0.931)	(0.039)	(0.728)
π^3	958.7	0.021	0.017	0.930	0.012	0.958	0.030	0.735	0.074	0.158	1.158	0.039	0.034	0.682	0.594	0.387
π^3 -X	1360	0.023	0.016	0.940	0.012	0.962	0.029	0.770	OOM	OOM	OOM	OOM	(0.014)	(0.951)	(0.029)	(0.770)
AMB3R	1563	0.022	0.024	0.933	0.015	0.953	0.038	0.688	OOM	OOM	OOM	OOM	(0.020)	(0.943)	(0.038)	(0.688)
DA3-Small	34.3	0.043	0.034	0.822	0.031	0.888	0.080	0.428	0.032	0.861	0.094	0.412	0.033	0.857	0.087	0.420
DA3-Base	135.4	0.031	0.024	0.891	0.020	0.937	0.048	0.561	0.019	0.929	0.055	0.467	0.021	0.919	0.051	0.514
DA3-Large	410.9	0.024	0.019	0.918	0.014	0.962	0.030	0.624	OOM	OOM	OOM	OOM	(0.017)	(0.940)	(0.030)	(0.624)
DA3-Giant	1356	0.026	0.009	0.944	0.009	0.971	0.025	0.811	OOM	OOM	OOM	OOM	(0.009)	(0.957)	(0.025)	(0.811)
DA3-Nested	1690	0.023	0.013	0.942	0.010	0.971	0.025	0.811	OOM	OOM	OOM	OOM	(0.011)	(0.957)	(0.025)	(0.811)
WorldMirror	1263	0.020	0.019	0.916	0.014	0.948	0.041	0.603	OOM	OOM	OOM	OOM	(0.017)	(0.932)	(0.041)	(0.603)
VGGT-Omega	1144	0.008	0.010	0.935	0.007	0.961	0.031	0.732	-	-	-	-	(0.008)	(0.948)	(0.031)	(0.732)
DA-Next (Ours)	1304	0.028	0.014	0.943	0.011	0.966	0.028	0.837	OOM	OOM	OOM	OOM	(0.018)	(0.955)	(0.028)	(0.837)
Online																
Spann3r ²²⁴	658.7	0.040	0.083	0.600	0.053	0.711	0.241	0.149	0.067	0.687	0.258	0.185	0.068	0.666	0.250	0.167
CUT3R	793.3	0.044	0.044	0.847	0.056	0.738	0.208	0.250	0.089	0.085	1.308	0.074	0.063	0.557	0.758	0.162
MonST3R	571.2	0.026	0.064	0.260	0.050	0.377	0.574	0.151	OOM	OOM	OOM	OOM	(0.057)	(0.318)	(0.574)	(0.151)
Point3R	828	0.024	0.055	0.582	0.048	0.724	0.191	0.238	0.061	0.618	0.430	0.149	0.054	0.641	0.311	0.193
Stream3R-S	1191	0.024	0.031	0.893	0.105	0.384	1.039	0.100	OOM	OOM	OOM	OOM	(0.068)	(0.639)	(1.039)	(0.100)
Stream3R-W	1191	0.024	0.031	0.895	0.251	0.354	1.170	0.088	OOM	OOM	OOM	OOM	(0.141)	(0.625)	(1.170)	(0.088)
StreamVGGT	1257	0.026	0.046	0.871	0.051	0.890	0.136	0.196	0.051	0.739	0.241	0.211	0.049	0.834	0.188	0.204
Page4D	1257	0.030	0.029	0.877	0.024	0.898	0.063	0.364	OOM	OOM	OOM	OOM	(0.026)	(0.887)	(0.063)	(0.364)
InfiniteVGGT	1257	0.026	0.046	0.871	0.051	0.889	0.138	0.194	0.051	0.740	0.239	0.211	0.049	0.833	0.189	0.202
Wint3R	749.5	0.023	0.032	0.779	0.027	0.796	0.254	0.472	0.083	0.264	0.750	0.091	0.047	0.613	0.502	0.281
LongStream-B	1191	0.025	0.031	0.876	0.082	0.656	0.376	0.060	0.091	0.277	0.692	0.053	0.068	0.603	0.534	0.057
LongStream-S	1191	0.025	0.031	0.876	0.058	0.392	0.685	0.060	0.090	0.169	0.849	0.050	0.060	0.479	0.767	0.055
LingbotMap*-W	1158	0.028	0.030	0.885	0.027	0.911	0.085	0.364	0.049	0.790	0.176	0.288	0.035	0.862	0.130	0.326
LingbotMap*-S	1158	0.028	0.030	0.885	0.022	0.929	0.055	0.524	0.021	0.934	0.055	0.494	0.024	0.916	0.055	0.509
Chunk-wise																
VGGT-Long	1257	0.024	0.016	0.926	0.013	0.955	0.038	0.658	0.024	0.851	0.174	0.481	0.018	0.911	0.106	0.570
π^3 -Long	958.7	0.021	0.017	0.930	0.027	0.952	0.032	0.568	0.143	0.850	0.147	0.160	0.062	0.911	0.090	0.364
DA3-Streaming	1356	0.026	0.009	0.944	0.009	0.967	0.027	0.790	0.023	0.871	0.170	0.551	0.014	0.927	0.098	0.671
SLAM-based																
MASt3R-SLAM	688.6	0.096	0.103	0.258	0.111	0.674	0.482	0.134	0.116	0.791	0.230	0.130	0.110	0.574	0.356	0.132
VGGT-SLAM	1257	0.024	0.016	0.926	0.015	0.941	0.047	0.647	0.027	0.837	0.163	0.410	0.019	0.901	0.105	0.528
Test-Time Training																
TTT3R	793.3	0.044	0.048	0.800	0.047	0.846	0.114	0.333	0.070	0.302	0.686	0.095	0.055	0.649	0.400	0.214
Scal3R	1266	0.024	0.016	0.928	0.017	0.798	0.037	0.709	0.172	0.622	0.174	0.472	0.112	0.783	0.105	0.590
LoGeR	1255	0.020	0.021	0.912	0.022	0.922	0.067	0.502	0.055	0.731	0.215	0.268	0.033	0.855	0.141	0.385
LoGeR*	1255	0.015	0.013	0.935	0.017	0.938	0.056	0.593	0.052	0.828	0.187	0.289	0.028	0.900	0.121	0.441

Table 22 | **Per-Dataset Results on OmniWorld**. Performance across different input regimes: *Single Frame*, *Sparse*, *Medium*, *Dense*, and the *Average*. The best, second-best, and third-best results in each column are highlighted in **deep blue**, **medium blue**, and **light blue**, respectively. Out-of-memory (OOM) and Timeout (T.O) cells are shaded **light red**; *Average* values for those rows are wrapped in parentheses and excluded from per-column ranking. Within each sub-category, the **bold** value marks the in-group best. Note that DA-Next (Ours) is excluded from the per-column rankings.

Method	#Params (M)	Single Frame	Sparse		Medium			Dense			Average		
		AbsRel↓	AbsRel↓	AUC@30↑	AbsRel↓	AUC@30↑	ATE↓	AbsRel↓	AUC@30↑	ATE↓	AbsRel↓	AUC@30↑	ATE↓
Optimization-based													
DUS3R	571.2	0.211	0.305	0.601	0.371	0.550	2.484	OOM	OOM	OOM	(0.338)	(0.575)	(2.484)
MAS3R	688.6	0.216	0.247	0.598	0.248	0.595	2.923	OOM	OOM	OOM	(0.247)	(0.596)	(2.923)
End-to-End Feed-Forward													
VGGT	1257	0.147	0.170	0.774	0.176	0.752	3.763	OOM	OOM	OOM	(0.173)	(0.763)	(3.763)
Fast3R	647.5	0.246	0.352	0.449	0.348	0.337	7.692	0.438	0.165	12.5	0.380	0.317	10.1
FastVGGT	1158	0.148	0.176	0.672	0.166	0.739	3.956	0.161	0.735	4.926	0.168	0.715	4.441
MUS3R	423.4	0.215	0.205	0.762	0.291	0.724	1.362	T.O	T.O	T.O	(0.248)	(0.743)	(1.362)
MapAnything	1228	0.144	0.122	0.824	0.125	0.802	2.256	OOM	OOM	OOM	(0.123)	(0.813)	(2.256)
OmniVGGT	1217	0.143	0.125	0.713	0.140	0.691	2.765	OOM	OOM	OOM	(0.132)	(0.702)	(2.765)
π^3	958.7	0.123	0.042	0.956	0.037	0.962	0.270	0.037	0.959	0.286	0.039	0.959	0.278
π^3 -X	1360	0.125	0.041	0.972	0.035	0.965	0.217	OOM	OOM	OOM	(0.038)	(0.969)	(0.217)
AMB3R	1563	0.147	0.124	0.876	0.124	0.880	0.837	OOM	OOM	OOM	(0.124)	(0.878)	(0.837)
DA3-Small	34.3	0.223	0.211	0.531	0.227	0.476	5.359	0.261	0.462	7.659	0.233	0.490	6.509
DA3-Base	135.4	0.195	0.155	0.613	0.170	0.640	4.013	0.183	0.583	4.623	0.169	0.612	4.318
DA3-Large	410.9	0.110	0.074	0.956	0.069	0.959	0.436	OOM	OOM	OOM	(0.071)	(0.958)	(0.436)
DA3-Giant	1356	0.114	0.050	0.978	0.046	0.982	0.235	OOM	OOM	OOM	(0.048)	(0.980)	(0.235)
DA3-Nested	1690	0.106	0.050	0.981	0.044	0.985	0.186	OOM	OOM	OOM	(0.047)	(0.983)	(0.186)
WorldMirror	1263	0.180	0.173	0.733	0.167	0.787	1.836	OOM	OOM	OOM	(0.170)	(0.760)	(1.836)
VGGT-Omega	1144	0.061	0.050	0.969	0.047	0.960	0.299	-	-	-	(0.048)	(0.965)	(0.299)
DA-Next (Ours)	1304	0.135	0.057	0.973	0.049	0.974	0.278	OOM	OOM	OOM	(0.080)	(0.973)	(0.278)
Online													
Spann3r ²²⁴	658.7	0.269	0.385	0.434	0.394	0.367	5.645	0.417	0.259	8.475	0.399	0.353	7.060
CUT3R	793.3	0.172	0.216	0.726	0.312	0.608	2.828	0.389	0.373	9.160	0.306	0.569	5.994
MonST3R	571.2	0.200	0.223	0.394	0.242	0.495	3.075	OOM	OOM	OOM	(0.233)	(0.445)	(3.075)
Point3R	828	0.200	0.246	0.260	0.262	0.261	7.981	0.339	0.092	9.878	0.282	0.205	8.929
Stream3R-S	1191	0.160	0.146	0.637	0.184	0.643	6.196	OOM	OOM	OOM	(0.165)	(0.640)	(6.196)
Stream3R-W	1191	0.160	0.152	0.592	0.215	0.450	11.25	OOM	OOM	OOM	(0.183)	(0.521)	(11.25)
StreamVGGT	1257	0.158	0.298	0.622	0.382	0.578	6.522	0.376	0.383	9.389	0.352	0.528	7.956
Page4D	1257	0.148	0.135	0.720	0.147	0.740	4.709	OOM	OOM	OOM	(0.141)	(0.730)	(4.709)
InfiniteVGGT	1257	0.160	0.299	0.623	0.381	0.586	6.464	0.379	0.387	9.373	0.353	0.532	7.919
Wint3R	749.5	0.137	0.066	0.747	0.072	0.685	1.833	0.144	0.394	6.080	0.094	0.609	3.956
LongStream-B	1191	0.153	0.185	0.420	0.247	0.780	1.356	0.224	0.650	2.156	0.219	0.617	1.756
LongStream-S	1191	0.153	0.165	0.417	0.199	0.617	2.763	0.232	0.502	2.440	0.199	0.512	2.602
LingbotMap*-W	1158	0.131	0.080	0.948	0.094	0.936	0.402	0.117	0.906	0.881	0.097	0.930	0.642
LingbotMap*-S	1158	0.131	0.080	0.948	0.090	0.923	0.357	0.095	0.918	0.588	0.088	0.930	0.473
Chunk-wise													
VGGT-Long	1257	0.147	0.170	0.774	0.170	0.814	2.701	0.349	0.613	5.409	0.230	0.734	4.055
π^3 -Long	958.7	0.123	0.042	0.956	0.082	0.957	0.288	0.337	0.909	0.739	0.154	0.940	0.513
DA3-Streaming	1356	0.114	0.050	0.978	0.046	0.981	0.243	0.051	0.956	0.289	0.049	0.972	0.266
SLAM-based													
MAS3R-SLAM	688.6	0.281	0.331	0.342	0.280	0.610	3.683	0.344	0.616	3.616	0.318	0.523	3.649
VGGT-SLAM	1257	0.147	0.170	0.774	0.186	0.765	4.607	0.371	0.433	6.222	0.243	0.657	5.415
Test-Time Training													
TTT3R	793.3	0.172	0.236	0.506	0.249	0.645	3.182	0.284	0.631	4.303	0.257	0.594	3.742
Scal3R	1266	0.142	0.116	0.848	0.137	0.830	0.812	0.405	0.682	1.359	0.219	0.787	1.085
LoGeR	1255	0.131	0.039	0.936	0.048	0.960	0.311	0.087	0.939	0.605	0.058	0.945	0.458
LoGeR*	1255	0.130	0.041	0.942	0.033	0.971	0.238	0.074	0.939	0.602	0.050	0.951	0.420

Table 23 | **Per-Dataset Results on RLbench**. Performance across different input regimes: *Single Frame*, *Sparse*, *Medium*, *Dense*, and the *Average*. The best, second-best, and third-best results in each column are highlighted in **deep blue**, **medium blue**, and **light blue**, respectively. Out-of-memory (OOM) and Timeout (T.O) cells are shaded **light red**; *Average* values for those rows are wrapped in parentheses and excluded from per-column ranking. Within each sub-category, the **bold** value marks the in-group best. Note that DA-Next (Ours) is excluded from the per-column rankings.

Method	#Params (M)	Single Frame	Sparse		Medium			Dense			Average		
		AbsRel↓	AbsRel↓	AUC@30↑	AbsRel↓	AUC@30↑	ATE↓	AbsRel↓	AUC@30↑	ATE↓	AbsRel↓	AUC@30↑	ATE↓
Optimization-based													
DUS3R	571.2	0.437	0.830	0.181	0.746	0.148	0.154	OOM	OOM	OOM	(0.788)	(0.165)	(0.154)
MAS3R	688.6	0.308	0.419	0.216	0.790	0.133	0.150	OOM	OOM	OOM	(0.605)	(0.174)	(0.150)
End-to-End Feed-Forward													
VGGT	1257	0.190	0.296	0.302	0.608	0.177	0.133	OOM	OOM	OOM	(0.452)	(0.239)	(0.133)
Fast3R	647.5	0.367	0.432	0.147	0.630	0.082	0.150	0.722	0.055	0.155	0.595	0.095	0.153
FastVGGT	1158	0.192	0.304	0.172	0.351	0.139	0.152	0.368	0.158	0.126	0.341	0.156	0.139
MUS3R	423.4	0.394	0.382	0.267	0.480	0.308	0.056	T.O	T.O	T.O	(0.431)	(0.287)	(0.056)
MapAnything	1228	0.281	0.328	0.284	0.443	0.176	0.101	OOM	OOM	OOM	(0.386)	(0.230)	(0.101)
OmniVGGT	1217	0.300	0.283	0.521	0.306	0.323	0.104	OOM	OOM	OOM	(0.295)	(0.422)	(0.104)
π^3	958.7	0.201	0.205	0.559	0.204	0.433	0.061	0.210	0.439	0.062	0.207	0.477	0.062
π^3 -X	1360	0.205	0.260	0.440	0.212	0.385	0.072	OOM	OOM	OOM	(0.236)	(0.413)	(0.072)
AMB3R	1563	0.204	0.229	0.525	0.256	0.389	0.086	OOM	OOM	OOM	(0.243)	(0.457)	(0.086)
DA3-Small	34.3	0.350	0.435	0.283	0.482	0.183	0.088	0.536	0.140	0.088	0.484	0.202	0.088
DA3-Base	135.4	0.410	0.406	0.285	0.400	0.217	0.077	0.438	0.157	0.078	0.415	0.220	0.078
DA3-Large	410.9	0.364	0.336	0.431	0.353	0.315	0.078	OOM	OOM	OOM	(0.344)	(0.373)	(0.078)
DA3-Giant	1356	0.355	0.270	0.565	0.250	0.471	0.058	OOM	OOM	OOM	(0.260)	(0.518)	(0.058)
DA3-Nested	1690	0.385	0.311	0.560	0.241	0.521	0.051	OOM	OOM	OOM	(0.276)	(0.541)	(0.051)
WorldMirror	1263	0.322	0.329	0.318	0.340	0.245	0.116	OOM	OOM	OOM	(0.335)	(0.282)	(0.116)
VGGT-Omega	1144	0.193	0.194	0.596	0.182	0.589	0.043	-	-	-	(0.188)	(0.592)	(0.043)
DA-Next (Ours)	1304	0.088	0.046	0.893	0.037	0.807	0.019	OOM	OOM	OOM	(0.057)	(0.850)	(0.019)
Online													
Spann3r ²²⁴	658.7	0.444	0.434	0.131	0.618	0.129	0.108	0.813	0.045	0.167	0.622	0.102	0.138
CUT3R	793.3	0.329	0.543	0.187	0.440	0.171	0.102	0.557	0.051	0.148	0.513	0.137	0.125
MonST3R	571.2	0.393	0.553	0.080	0.476	0.147	0.125	OOM	OOM	OOM	(0.515)	(0.113)	(0.125)
Point3R	828	0.348	0.503	0.164	0.678	0.044	0.183	0.795	0.036	0.181	0.659	0.081	0.182
Stream3R-S	1191	0.262	0.326	0.134	0.352	0.099	0.153	OOM	OOM	OOM	(0.339)	(0.116)	(0.153)
Stream3R-W	1191	0.262	0.326	0.134	0.484	0.064	0.198	OOM	OOM	OOM	(0.405)	(0.099)	(0.198)
StreamVGGT	1257	0.239	0.316	0.151	0.358	0.132	0.162	0.379	0.119	0.163	0.351	0.134	0.162
Page4D	1257	0.219	0.338	0.330	0.327	0.211	0.113	OOM	OOM	OOM	(0.333)	(0.271)	(0.113)
InfiniteVGGT	1257	0.239	0.315	0.155	0.358	0.132	0.162	0.378	0.118	0.163	0.350	0.135	0.162
Wint3R	749.5	0.364	0.383	0.201	0.398	0.142	0.107	0.584	0.076	0.154	0.455	0.140	0.131
LongStream-B	1191	0.385	0.332	0.121	0.438	0.097	0.112	0.668	0.080	0.102	0.479	0.099	0.107
LongStream-S	1191	0.385	0.331	0.121	0.363	0.081	0.110	0.750	0.063	0.113	0.482	0.088	0.112
LingbotMap*-W	1158	0.300	0.339	0.387	0.282	0.257	0.091	0.364	0.269	0.095	0.328	0.304	0.093
LingbotMap*-S	1158	0.300	0.339	0.387	0.282	0.257	0.091	0.324	0.183	0.114	0.315	0.276	0.103
Chunk-wise													
VGGT-Long	1257	0.190	0.296	0.302	0.609	0.178	0.136	0.599	0.177	0.113	0.501	0.219	0.124
π^3 -Long	958.7	0.201	0.205	0.559	0.206	0.433	0.061	0.350	0.375	0.069	0.254	0.456	0.065
DA3-Streaming	1356	0.355	0.270	0.566	0.256	0.472	0.062	0.549	0.311	0.102	0.359	0.450	0.082
SLAM-based													
MAS3R-SLAM	688.6	0.410	0.594	0.106	0.773	0.148	0.139	0.859	0.201	0.107	0.742	0.152	0.123
VGGT-SLAM	1257	0.190	0.296	0.302	0.432	0.182	0.135	0.350	0.120	0.108	0.359	0.201	0.121
Test-Time Training													
TTT3R	793.3	0.329	0.559	0.156	0.493	0.158	0.106	0.506	0.112	0.113	0.519	0.142	0.110
Scal3R	1266	0.238	0.233	0.524	0.282	0.347	0.089	0.386	0.248	0.073	0.300	0.373	0.081
LoGeR	1255	0.235	0.202	0.428	0.321	0.452	0.052	0.433	0.435	0.066	0.319	0.438	0.059
LoGeR*	1255	0.210	0.171	0.523	0.202	0.525	0.040	0.349	0.465	0.077	0.241	0.505	0.059

Table 24 | **Per-Dataset Results on Robolab**. Performance across different input regimes: *Single Frame*, *Sparse*, *Medium*, *Dense*, and the *Average*. The best, second-best, and third-best results in each column are highlighted in **deep blue**, **medium blue**, and **light blue**, respectively. Out-of-memory (OOM) and Timeout (T.O) cells are shaded **light red**; *Average* values for those rows are wrapped in parentheses and excluded from per-column ranking. Within each sub-category, the **bold** value marks the in-group best. Note that DA-Next (Ours) is excluded from the per-column rankings.

Method	#Params (M)	Single Frame	Sparse		Medium			Dense			Average		
		AbsRel↓	AbsRel↓	AUC@30↑	AbsRel↓	AUC@30↑	ATE↓	AbsRel↓	AUC@30↑	ATE↓	AbsRel↓	AUC@30↑	ATE↓
Optimization-based													
DUS3R	571.2	0.371	0.495	0.274	0.512	0.132	0.117	OOM	OOM	OOM	(0.504)	(0.203)	(0.117)
MAS3R	688.6	0.386	0.515	0.429	0.463	0.242	0.103	OOM	OOM	OOM	(0.489)	(0.336)	(0.103)
End-to-End Feed-Forward													
VGGT	1257	0.174	0.201	0.566	0.177	0.504	0.035	OOM	OOM	OOM	(0.189)	(0.535)	(0.035)
Fast3R	647.5	0.340	0.412	0.174	0.403	0.176	0.085	0.480	0.099	0.103	0.432	0.150	0.094
FastVGGT	1158	0.171	0.215	0.453	0.175	0.483	0.038	0.180	0.468	0.041	0.190	0.468	0.040
MUS3R	423.4	0.491	0.457	0.376	0.262	0.505	0.036	T.O	T.O	T.O	(0.359)	(0.440)	(0.036)
MapAnything	1228	0.194	0.381	0.221	0.321	0.179	0.069	OOM	OOM	OOM	(0.351)	(0.200)	(0.069)
OmniVGGT	1217	0.157	0.185	0.601	0.162	0.562	0.030	OOM	OOM	OOM	(0.173)	(0.582)	(0.030)
π^3	958.7	0.168	0.171	0.663	0.150	0.742	0.018	0.183	0.458	0.049	0.168	0.621	0.033
π^3 -X	1360	0.157	0.155	0.635	0.137	0.682	0.024	OOM	OOM	OOM	(0.146)	(0.658)	(0.024)
AMB3R	1563	0.213	0.239	0.639	0.188	0.582	0.032	OOM	OOM	OOM	(0.213)	(0.611)	(0.032)
DA3-Small	34.3	0.338	0.490	0.198	0.389	0.134	0.082	0.402	0.100	0.093	0.427	0.144	0.087
DA3-Base	135.4	0.278	0.326	0.352	0.273	0.225	0.067	0.276	0.177	0.073	0.292	0.251	0.070
DA3-Large	410.9	0.243	0.237	0.447	0.184	0.469	0.036	OOM	OOM	OOM	(0.210)	(0.458)	(0.036)
DA3-Giant	1356	0.132	0.174	0.719	0.170	0.671	0.027	OOM	OOM	OOM	(0.172)	(0.695)	(0.027)
DA3-Nested	1690	0.148	0.194	0.716	0.137	0.721	0.018	OOM	OOM	OOM	(0.166)	(0.718)	(0.018)
WorldMirror	1263	0.271	0.311	0.409	0.275	0.405	0.050	OOM	OOM	OOM	(0.293)	(0.407)	(0.050)
VGGT-Omega	1144	0.207	0.147	0.742	0.149	0.811	0.012	-	-	-	(0.148)	(0.777)	(0.012)
DA-Next (Ours)	1304	0.025	0.030	0.802	0.018	0.916	0.006	OOM	OOM	OOM	(0.024)	(0.859)	(0.006)
Online													
Spann3r ²²⁴	658.7	0.380	0.485	0.041	0.399	0.154	0.079	0.434	0.076	0.108	0.439	0.090	0.094
CUT3R	793.3	0.274	0.451	0.287	0.404	0.122	0.090	0.449	0.029	0.123	0.434	0.146	0.107
MonST3R	571.2	0.381	0.501	0.152	0.416	0.124	0.114	OOM	OOM	OOM	(0.458)	(0.138)	(0.114)
Point3R	828	0.424	0.469	0.139	0.416	0.100	0.114	0.434	0.053	0.129	0.440	0.097	0.121
Stream3R-S	1191	0.196	0.270	0.424	0.244	0.260	0.092	OOM	OOM	OOM	(0.257)	(0.342)	(0.092)
Stream3R-W	1191	0.196	0.271	0.421	0.348	0.117	0.137	OOM	OOM	OOM	(0.310)	(0.269)	(0.137)
StreamVGGT	1257	0.170	0.266	0.392	0.240	0.335	0.060	0.254	0.175	0.092	0.253	0.301	0.076
Page4D	1257	0.189	0.259	0.494	0.222	0.389	0.051	OOM	OOM	OOM	(0.241)	(0.441)	(0.051)
InfiniteVGGT	1257	0.169	0.265	0.390	0.239	0.339	0.060	0.252	0.175	0.090	0.252	0.301	0.075
Wint3R	749.5	0.319	0.333	0.292	0.268	0.169	0.077	0.364	0.020	0.119	0.322	0.161	0.098
LongStream-B	1191	0.216	0.270	0.412	0.360	0.165	0.087	0.358	0.062	0.100	0.329	0.213	0.093
LongStream-S	1191	0.216	0.270	0.411	0.326	0.129	0.095	0.358	0.038	0.103	0.318	0.193	0.099
LingbotMap*-W	1158	0.202	0.327	0.394	0.201	0.360	0.044	0.323	0.200	0.077	0.284	0.318	0.060
LingbotMap*-S	1158	0.202	0.327	0.394	0.208	0.412	0.043	0.230	0.359	0.047	0.255	0.388	0.045
Chunk-wise													
VGGT-Long	1257	0.174	0.201	0.566	0.192	0.506	0.049	0.345	0.278	0.083	0.246	0.450	0.066
π^3 -Long	958.7	0.168	0.171	0.663	0.185	0.639	0.042	0.301	0.378	0.075	0.219	0.560	0.058
DA3-Streaming	1356	0.132	0.174	0.720	0.183	0.578	0.037	0.223	0.325	0.074	0.193	0.541	0.056
SLAM-based													
MAS3R-SLAM	688.6	0.473	0.547	0.118	0.471	0.147	0.110	0.459	0.181	0.094	0.492	0.149	0.102
VGGT-SLAM	1257	0.174	0.201	0.566	0.209	0.436	0.062	0.320	0.239	0.081	0.244	0.414	0.072
Test-Time Training													
TTT3R	793.3	0.274	0.464	0.278	0.367	0.212	0.082	0.412	0.075	0.109	0.415	0.189	0.096
Scal3R	1266	0.189	0.216	0.711	0.308	0.413	0.052	0.329	0.188	0.079	0.284	0.437	0.066
LoGeR	1255	0.190	0.220	0.586	0.301	0.448	0.066	0.452	0.223	0.100	0.324	0.419	0.083
LoGeR*	1255	0.142	0.130	0.617	0.206	0.490	0.057	0.325	0.240	0.096	0.220	0.449	0.077

Table 25 | **Per-Dataset Results on RoboTwin**. Performance across different input regimes: *Single Frame*, *Sparse*, *Medium*, *Dense*, and the *Average*. The best, second-best, and third-best results in each column are highlighted in **deep blue**, **medium blue**, and **light blue**, respectively. Out-of-memory (OOM) and Timeout (T.O) cells are shaded **light red**; *Average* values for those rows are wrapped in parentheses and excluded from per-column ranking. Within each sub-category, the **bold** value marks the in-group best. Note that DA-Next (Ours) is excluded from the per-column rankings.

Method	#Params (M)	Single Frame	Sparse		Medium			Dense			Average		
		AbsRel↓	AbsRel↓	AUC@30↑	AbsRel↓	AUC@30↑	ATE↓	AbsRel↓	AUC@30↑	ATE↓	AbsRel↓	AUC@30↑	ATE↓
Optimization-based													
DUS3R	571.2	0.342	0.728	0.061	0.928	0.067	0.120	OOM	OOM	OOM	(0.828)	(0.064)	(0.120)
MAS3R	688.6	0.388	0.756	0.190	0.695	0.132	0.107	OOM	OOM	OOM	(0.725)	(0.161)	(0.107)
End-to-End Feed-Forward													
VGGT	1257	0.218	0.369	0.253	0.323	0.105	0.093	OOM	OOM	OOM	(0.346)	(0.179)	(0.093)
Fast3R	647.5	0.351	0.698	0.079	0.580	0.030	0.109	0.624	0.045	0.110	0.634	0.051	0.110
FastVGGT	1158	0.218	0.416	0.185	0.317	0.100	0.085	0.300	0.088	0.090	0.345	0.124	0.088
MUS3R	423.4	0.366	0.507	0.126	0.473	0.137	0.093	T.O	T.O	T.O	(0.490)	(0.131)	(0.093)
MapAnything	1228	0.232	0.415	0.142	0.410	0.124	0.096	OOM	OOM	OOM	(0.412)	(0.133)	(0.096)
OmniVGGT	1217	0.212	0.333	0.090	0.495	0.070	0.106	OOM	OOM	OOM	(0.414)	(0.080)	(0.106)
π^3	958.7	0.181	0.309	0.482	0.317	0.250	0.064	0.313	0.263	0.066	0.313	0.332	0.065
π^3 -X	1360	0.170	0.271	0.345	0.310	0.090	0.084	OOM	OOM	OOM	(0.291)	(0.217)	(0.084)
AMB3R	1563	0.184	0.252	0.454	0.273	0.223	0.068	OOM	OOM	OOM	(0.263)	(0.339)	(0.068)
DA3-Small	34.3	0.310	0.575	0.060	0.485	0.106	0.087	0.494	0.108	0.091	0.518	0.091	0.089
DA3-Base	135.4	0.285	0.565	0.095	0.476	0.133	0.084	0.484	0.144	0.091	0.509	0.124	0.088
DA3-Large	410.9	0.255	0.426	0.285	0.348	0.210	0.070	OOM	OOM	OOM	(0.387)	(0.248)	(0.070)
DA3-Giant	1356	0.287	0.320	0.441	0.315	0.253	0.071	OOM	OOM	OOM	(0.318)	(0.347)	(0.071)
DA3-Nested	1690	0.259	0.317	0.385	0.280	0.263	0.069	OOM	OOM	OOM	(0.298)	(0.324)	(0.069)
WorldMirror	1263	0.205	0.363	0.179	0.344	0.121	0.095	OOM	OOM	OOM	(0.353)	(0.150)	(0.095)
VGGT-Omega	1144	0.182	0.217	0.529	0.189	0.372	0.058	-	-	-	(0.203)	(0.450)	(0.058)
DA-Next (Ours)	1304	0.072	0.068	0.765	0.045	0.541	0.036	OOM	OOM	OOM	(0.062)	(0.653)	(0.036)
Online													
Spann3r ²²⁴	658.7	0.307	0.612	0.085	0.421	0.067	0.099	0.460	0.072	0.103	0.498	0.075	0.101
CUT3R	793.3	0.320	0.617	0.043	0.501	0.064	0.101	0.539	0.032	0.104	0.552	0.046	0.102
MonST3R	571.2	0.361	0.627	0.027	0.427	0.061	0.127	OOM	OOM	OOM	(0.527)	(0.044)	(0.127)
Point3R	828	0.295	0.583	0.017	0.591	0.045	0.109	0.613	0.053	0.114	0.596	0.038	0.112
Stream3R-S	1191	0.216	0.354	0.289	0.449	0.106	0.091	OOM	OOM	OOM	(0.401)	(0.198)	(0.091)
Stream3R-W	1191	0.216	0.354	0.289	0.484	0.079	0.138	OOM	OOM	OOM	(0.419)	(0.184)	(0.138)
StreamVGGT	1257	0.203	0.372	0.155	0.391	0.128	0.085	0.369	0.116	0.081	0.377	0.133	0.083
Page4D	1257	0.224	0.326	0.122	0.347	0.082	0.092	OOM	OOM	OOM	(0.337)	(0.102)	(0.092)
InfiniteVGGT	1257	0.203	0.369	0.152	0.392	0.131	0.085	0.369	0.121	0.080	0.377	0.135	0.082
Wint3R	749.5	0.245	0.569	0.106	0.438	0.111	0.085	0.517	0.078	0.095	0.508	0.099	0.090
LongStream-B	1191	0.243	0.462	0.199	0.512	0.098	0.098	0.444	0.070	0.092	0.473	0.122	0.095
LongStream-S	1191	0.243	0.462	0.199	0.420	0.085	0.097	0.448	0.106	0.083	0.443	0.130	0.090
LingbotMap*-W	1158	0.303	0.509	0.262	0.336	0.201	0.082	0.354	0.191	0.088	0.400	0.218	0.085
LingbotMap*-S	1158	0.303	0.509	0.262	0.361	0.202	0.081	0.429	0.199	0.084	0.433	0.221	0.082
Chunk-wise													
VGGT-Long	1257	0.218	0.369	0.253	0.334	0.088	0.093	0.415	0.100	0.096	0.373	0.147	0.095
π^3 -Long	958.7	0.181	0.309	0.482	0.309	0.238	0.068	0.439	0.243	0.076	0.353	0.321	0.072
DA3-Streaming	1356	0.287	0.320	0.442	0.310	0.257	0.074	0.461	0.189	0.098	0.364	0.296	0.086
SLAM-based													
MAS3R-SLAM	688.6	0.504	0.937	0.109	0.806	0.094	0.100	0.854	0.151	0.101	0.866	0.118	0.101
VGGT-SLAM	1257	0.218	0.369	0.253	0.423	0.110	0.085	0.426	0.110	0.099	0.406	0.158	0.092
Test-Time Training													
TTT3R	793.3	0.320	0.606	0.051	0.480	0.070	0.103	0.502	0.062	0.097	0.529	0.061	0.100
Scal3R	1266	0.193	0.350	0.280	0.309	0.147	0.083	0.391	0.132	0.085	0.350	0.186	0.084
LoGeR	1255	0.223	0.350	0.195	0.354	0.160	0.070	0.466	0.181	0.083	0.390	0.178	0.076
LoGeR*	1255	0.191	0.259	0.233	0.271	0.173	0.070	0.430	0.203	0.077	0.320	0.203	0.074

Table 26 | **Per-Dataset Results on Xperience**. Performance across different input regimes: *Single Frame*, *Sparse*, *Medium*, *Dense*, and the *Average*. The best, second-best, and third-best results in each column are highlighted in **deep blue**, **medium blue**, and **light blue**, respectively. Out-of-memory (OOM) and Timeout (T.O) cells are shaded **light red**; *Average* values for those rows are wrapped in parentheses and excluded from per-column ranking. Within each sub-category, the **bold** value marks the in-group best. Note that DA-Next (Ours) is excluded from the per-column rankings.

Method	#Params (M)	Single Frame	Sparse		Medium			Dense			Average		
		AbsRel↓	AbsRel↓	AUC@30↑	AbsRel↓	AUC@30↑	ATE↓	AbsRel↓	AUC@30↑	ATE↓	AbsRel↓	AUC@30↑	ATE↓
Optimization-based													
DUS3R	571.2	0.054	0.092	0.471	0.240	0.079	4.312	OOM	OOM	OOM	(0.166)	(0.275)	(4.312)
MAS3R	688.6	0.087	0.068	0.694	0.261	0.202	4.373	OOM	OOM	OOM	(0.164)	(0.448)	(4.373)
End-to-End Feed-Forward													
VGGT	1257	0.126	0.051	0.070	0.078	0.047	7.239	OOM	OOM	OOM	(0.065)	(0.059)	(7.239)
Fast3R	647.5	0.085	0.359	0.005	0.468	0.001	7.571	-	-	-	0.413	0.003	7.571
FastVGGT	1158	0.128	0.048	0.073	0.076	0.036	7.024	0.113	0.062	7.943	0.079	0.057	7.483
MUS3R	423.4	0.058	0.059	0.496	0.111	0.282	5.645	T.O	T.O	T.O	(0.085)	(0.389)	(5.645)
MapAnything	1228	0.062	0.040	0.617	0.098	0.138	5.422	OOM	OOM	OOM	(0.069)	(0.377)	(5.422)
OmniVGGT	1217	0.056	0.033	0.042	0.072	0.042	6.971	OOM	OOM	OOM	(0.052)	(0.042)	(6.971)
π^3	958.7	0.133	0.031	0.127	0.050	0.130	7.219	0.265	0.009	7.460	0.115	0.089	7.340
π^3 -X	1360	0.089	0.029	0.421	0.046	0.022	6.461	OOM	OOM	OOM	(0.038)	(0.221)	(6.461)
AMB3R	1563	0.104	0.041	0.022	0.069	0.045	7.102	OOM	OOM	OOM	(0.055)	(0.034)	(7.102)
DA3-Small	34.3	0.112	0.061	0.011	0.094	0.025	6.493	0.104	0.041	6.741	0.086	0.026	6.617
DA3-Base	135.4	0.103	0.053	0.071	0.078	0.053	5.507	0.088	0.081	5.624	0.073	0.068	5.565
DA3-Large	410.9	0.099	0.064	0.103	0.073	0.116	5.989	OOM	OOM	OOM	(0.068)	(0.109)	(5.989)
DA3-Giant	1356	0.162	0.049	0.291	0.057	0.193	4.895	OOM	OOM	OOM	(0.053)	(0.242)	(4.895)
DA3-Nested	1690	0.180	0.044	0.201	0.051	0.185	6.236	OOM	OOM	OOM	(0.047)	(0.193)	(6.236)
WorldMirror	1263	0.076	0.048	0.197	0.091	0.040	7.172	OOM	OOM	OOM	(0.069)	(0.118)	(7.172)
VGGT-Omega	1144	0.070	0.038	0.528	0.069	0.275	5.317	-	-	-	(0.054)	(0.401)	(5.317)
DA-Next (Ours)	1304	0.064	0.037	0.703	0.046	0.385	4.508	OOM	OOM	OOM	(0.041)	(0.544)	(4.508)
Online													
Spann3r ²²⁴	658.7	0.156	0.292	0.066	0.221	0.012	5.472	0.171	0.216	4.852	0.228	0.098	5.162
CUT3R	793.3	0.148	0.074	0.124	0.114	0.027	4.663	0.316	0.029	7.244	0.168	0.060	5.954
MonST3R	571.2	0.191	0.116	0.021	0.283	0.007	5.104	OOM	OOM	OOM	(0.200)	(0.014)	(5.104)
Point3R	828	0.114	0.074	0.031	0.156	0.017	6.804	0.234	0.029	7.762	0.154	0.025	7.283
Stream3R-S	1191	0.083	0.055	0.046	0.419	0.005	7.469	OOM	OOM	OOM	(0.237)	(0.025)	(7.469)
Stream3R-W	1191	0.083	0.056	0.047	0.407	0.006	7.484	OOM	OOM	OOM	(0.231)	(0.027)	(7.484)
StreamVGGT	1257	0.108	0.131	0.054	0.159	0.033	7.306	0.185	0.053	8.103	0.158	0.047	7.705
Page4D	1257	0.134	0.049	0.075	0.073	0.032	7.165	OOM	OOM	OOM	(0.061)	(0.054)	(7.165)
InfiniteVGGT	1257	0.109	0.131	0.051	0.159	0.033	7.317	0.185	0.054	8.087	0.159	0.046	7.702
Wint3R	749.5	0.053	0.054	0.039	0.074	0.065	6.512	0.290	0.059	7.698	0.139	0.054	7.105
LongStream-B	1191	0.142	0.079	0.029	0.118	0.004	6.245	0.259	0.027	2.884	0.152	0.020	4.565
LongStream-S	1191	0.142	0.075	0.028	0.137	0.004	6.278	0.223	0.020	6.397	0.145	0.017	6.337
LingbotMap*-W	1158	0.060	0.050	0.197	0.086	0.299	2.164	0.157	0.193	1.458	0.098	0.230	1.811
LingbotMap*-S	1158	0.060	0.050	0.197	0.097	0.270	2.445	0.100	0.451	3.616	0.082	0.306	3.031
Chunk-wise													
VGGT-Long	1257	0.126	0.051	0.070	0.244	0.067	7.389	1.390	0.075	5.495	0.562	0.071	6.442
π^3 -Long	958.7	0.133	0.031	0.127	0.091	0.134	6.415	0.465	0.809	0.215	0.196	0.357	3.315
DA3-Streaming	1356	0.162	0.049	0.285	0.175	0.173	5.291	0.474	0.319	2.817	0.233	0.259	4.054
SLAM-based													
MAS3R-SLAM	688.6	0.206	0.144	0.000	0.201	0.001	6.986	0.279	0.423	4.841	0.208	0.141	5.913
VGGT-SLAM	1257	0.126	0.051	0.070	0.302	0.044	7.735	0.973	0.051	5.342	0.442	0.055	6.538
Test-Time Training													
TTT3R	793.3	0.148	0.064	0.107	0.102	0.061	7.159	0.143	0.119	5.582	0.103	0.096	6.371
Scal3R	1266	0.256	0.045	0.056	0.192	0.010	7.411	0.462	0.195	3.739	0.233	0.087	5.575
LoGeR	1255	0.122	0.040	0.036	0.076	0.043	4.821	0.158	0.400	1.088	0.092	0.160	2.954
LoGeR*	1255	0.113	0.034	0.071	0.066	0.093	7.053	0.090	0.583	0.608	0.064	0.249	3.830

Table 27 | **Per-Dataset Results on Scannet++**. Performance across different input regimes: *Single Frame*, *Sparse*, *Medium*, *Dense*, and *Average*. The best, second-best, and third-best results in each column are highlighted in **deep blue**, **medium blue**, and **light blue**, respectively. Out-of-memory (OOM) and Timeout (T.O) cells are shaded **light red**; *Average* values for those rows are wrapped in parentheses and excluded from per-column ranking. Within each sub-category, the **bold** value marks the in-group best. Note that DA-Next (Ours) is excluded from the per-column rankings.

Method	#Params (M)	Single Frame	Sparse		Medium			Dense				Average				
		AbsRel↓	AbsRel↓	AUC@30↑	AbsRel↓	AUC@30↑	ATE↓	F-Score↑	AbsRel↓	AUC@30↑	ATE↓	F-Score↑	AbsRel↓	AUC@30↑	ATE↓	F-Score↑
Optimization-based																
DUST3R	571.2	0.038	0.064	0.762	0.057	0.713	0.392	0.374	OOM	OOM	OOM	OOM	(0.060)	(0.738)	(0.392)	(0.374)
MASt3R	688.6	0.061	0.069	0.858	0.073	0.757	0.184	0.431	OOM	OOM	OOM	OOM	(0.071)	(0.807)	(0.184)	(0.431)
End-to-End Feed-Forward																
VGGT	1257	0.038	0.049	0.901	0.043	0.942	0.067	0.657	OOM	OOM	OOM	OOM	(0.046)	(0.921)	(0.067)	(0.657)
Fast3R	647.5	0.046	0.102	0.567	0.095	0.619	0.555	0.325	0.112	0.599	0.639	0.308	0.103	0.595	0.597	0.316
FastVGGT	1158	0.038	0.052	0.838	0.043	0.922	0.079	0.524	0.040	0.915	0.104	0.536	0.045	0.892	0.092	0.530
MUST3R	423.4	0.039	0.044	0.881	0.042	0.921	0.077	0.506	T.O	T.O	T.O	T.O	(0.043)	(0.901)	(0.077)	(0.506)
MapAnything	1228	0.041	0.039	0.854	0.039	0.897	0.100	0.498	OOM	OOM	OOM	OOM	(0.039)	(0.875)	(0.100)	(0.498)
OmniVGGT	1217	0.047	0.033	0.728	0.039	0.875	0.162	0.526	OOM	OOM	OOM	OOM	(0.036)	(0.801)	(0.162)	(0.526)
π^3	958.7	0.035	0.031	0.901	0.031	0.952	0.044	0.709	0.030	0.953	0.058	0.723	0.031	0.935	0.051	0.716
π^3 -X	1360	0.036	0.031	0.903	0.031	0.951	0.039	0.728	OOM	OOM	OOM	OOM	(0.031)	(0.927)	(0.039)	(0.728)
AMB3R	1563	0.035	0.036	0.871	0.035	0.929	0.084	0.557	OOM	OOM	OOM	OOM	(0.036)	(0.900)	(0.084)	(0.557)
DA3-Small	34.3	0.073	0.075	0.677	0.071	0.614	0.616	0.262	0.073	0.533	0.787	0.216	0.073	0.608	0.701	0.239
DA3-Base	135.4	0.058	0.056	0.795	0.048	0.799	0.215	0.388	0.048	0.759	0.288	0.346	0.050	0.785	0.251	0.367
DA3-Large	410.9	0.036	0.039	0.899	0.035	0.941	0.062	0.609	OOM	OOM	OOM	OOM	(0.037)	(0.920)	(0.062)	(0.609)
DA3-Giant	1356	0.035	0.032	0.959	0.031	0.983	0.020	0.761	OOM	OOM	OOM	OOM	(0.031)	(0.971)	(0.020)	(0.761)
DA3-Nested	1690	0.035	0.031	0.958	0.031	0.983	0.020	0.758	OOM	OOM	OOM	OOM	(0.031)	(0.970)	(0.020)	(0.758)
WorldMirror	1263	0.037	0.037	0.889	0.033	0.932	0.070	0.686	OOM	OOM	OOM	OOM	(0.035)	(0.911)	(0.070)	(0.686)
VGGT-Omega	1144	0.035	0.042	0.946	0.041	0.969	0.036	0.709	-	-	-	-	(0.042)	(0.958)	(0.036)	(0.709)
DA-Next (Ours)	1304	0.039	0.029	0.949	0.026	0.976	0.025	0.805	OOM	OOM	OOM	OOM	(0.032)	(0.962)	(0.025)	(0.805)
Online																
Spann3r ²²⁴	658.7	0.072	0.175	0.337	0.123	0.431	0.731	0.161	0.130	0.361	0.925	0.154	0.143	0.376	0.828	0.158
CUT3R	793.3	0.042	0.069	0.717	0.070	0.673	0.506	0.264	0.083	0.275	1.132	0.169	0.074	0.555	0.819	0.217
MonST3R	571.2	0.049	0.110	0.232	0.157	0.022	1.189	0.084	OOM	OOM	OOM	OOM	(0.133)	(0.127)	(1.189)	(0.084)
Point3R	828	0.040	0.061	0.445	0.062	0.459	0.528	0.189	0.067	0.412	0.597	0.159	0.063	0.438	0.562	0.174
Stream3R-S	1191	0.032	0.045	0.836	0.226	0.514	1.088	0.291	OOM	OOM	OOM	OOM	(0.136)	(0.675)	(1.088)	(0.291)
Stream3R-W	1191	0.032	0.046	0.828	0.217	0.437	1.299	0.236	OOM	OOM	OOM	OOM	(0.131)	(0.633)	(1.299)	(0.236)
StreamVGGT	1257	0.038	0.077	0.837	0.088	0.740	0.500	0.302	0.087	0.670	0.622	0.263	0.084	0.749	0.561	0.283
Page4D	1257	0.044	0.054	0.812	0.050	0.867	0.130	0.385	OOM	OOM	OOM	OOM	(0.052)	(0.840)	(0.130)	(0.385)
InfiniteVGGT	1257	0.035	0.078	0.811	0.087	0.759	0.477	0.313	0.085	0.676	0.602	0.267	0.083	0.749	0.540	0.290
Wint3R	749.5	0.049	0.057	0.565	0.058	0.442	0.920	0.213	0.067	0.344	0.982	0.169	0.061	0.450	0.951	0.191
LongStream-B	1191	0.047	0.062	0.574	0.110	0.309	1.044	0.123	0.125	0.280	1.018	0.119	0.099	0.388	1.031	0.121
LongStream-S	1191	0.047	0.062	0.574	0.089	0.158	1.313	0.104	0.118	0.055	1.351	0.133	0.090	0.262	1.332	0.119
LingbotMap*-W	1158	0.042	0.042	0.906	0.046	0.869	0.165	0.494	0.044	0.875	0.124	0.481	0.044	0.884	0.145	0.488
LingbotMap*-S	1158	0.042	0.042	0.906	0.040	0.900	0.082	0.556	0.038	0.912	0.088	0.565	0.040	0.906	0.085	0.561
Chunk-wise																
VGGT-Long	1257	0.038	0.049	0.901	0.046	0.911	0.126	0.597	0.045	0.893	0.111	0.543	0.047	0.902	0.119	0.570
π^3 -Long	958.7	0.035	0.031	0.901	0.043	0.946	0.050	0.643	0.102	0.929	0.085	0.342	0.059	0.925	0.067	0.493
DA3-Streaming	1356	0.035	0.032	0.958	0.032	0.956	0.084	0.707	0.054	0.817	0.381	0.606	0.039	0.910	0.233	0.656
SLAM-based																
MASt3R-SLAM	688.6	0.165	0.205	0.096	0.199	0.093	1.638	0.043	0.188	0.164	1.500	0.074	0.197	0.118	1.569	0.059
VGGT-SLAM	1257	0.038	0.049	0.901	0.048	0.884	0.134	0.538	0.053	0.759	0.275	0.437	0.050	0.848	0.204	0.487
Test-Time Training																
TTT3R	793.3	0.042	0.071	0.634	0.067	0.637	0.662	0.261	0.071	0.679	0.484	0.244	0.069	0.650	0.573	0.253
Scal3R	1266	0.065	0.043	0.891	0.097	0.843	0.056	0.707	0.144	0.728	0.092	0.651	0.095	0.821	0.074	0.679
LoGeR	1255	0.038	0.033	0.908	0.040	0.908	0.077	0.574	0.058	0.826	0.182	0.447	0.043	0.881	0.129	0.510
LoGeR*	1255	0.035	0.030	0.900	0.034	0.923	0.073	0.632	0.040	0.865	0.143	0.548	0.035	0.896	0.108	0.590

Table 28 | **Per-Dataset Results on Tanks and Temples**. Performance across different input regimes: *Single Frame*, *Sparse*, *Medium*, *Dense*, and the *Average*. The best, second-best, and third-best results in each column are highlighted in **deep blue**, **medium blue**, and **light blue**, respectively. Out-of-memory (OOM) and Timeout (T.O) cells are shaded **light red**; *Average* values for those rows are wrapped in parentheses and excluded from per-column ranking. Within each sub-category, the **bold** value marks the in-group best. Note that DA-Next (Ours) is excluded from the per-column rankings.

Method	#Params (M)	Single Frame	Sparse		Medium			Dense			Average		
		AbsRel↓	AbsRel↓	AUC@30↑	AbsRel↓	AUC@30↑	ATE↓	AbsRel↓	AUC@30↑	ATE↓	AbsRel↓	AUC@30↑	ATE↓
Optimization-based													
DUS3R	571.2	0.045	0.097	0.368	0.132	0.333	11.93	OOM	OOM	OOM	(0.114)	(0.351)	(11.93)
MAS3R	688.6	0.043	0.074	0.548	0.113	0.578	7.868	OOM	OOM	OOM	(0.094)	(0.563)	(7.868)
End-to-End Feed-Forward													
VGGT	1257	0.022	0.039	0.712	0.038	0.780	4.238	OOM	OOM	OOM	(0.038)	(0.746)	(4.238)
Fast3R	647.5	0.045	0.182	0.303	0.181	0.342	11.37	0.172	0.354	14.09	0.178	0.333	12.73
FastVGGT	1158	0.022	0.043	0.507	0.039	0.748	4.854	0.027	0.832	3.614	0.036	0.695	4.234
MUS3R	423.4	0.054	0.070	0.670	0.064	0.729	5.223	T.O	T.O	T.O	(0.067)	(0.699)	(5.223)
MapAnything	1228	0.027	0.054	0.604	0.045	0.696	4.929	OOM	OOM	OOM	(0.050)	(0.650)	(4.929)
OmniVGGT	1217	0.023	0.052	0.419	0.051	0.498	11.06	OOM	OOM	OOM	(0.051)	(0.458)	(11.06)
π^3	958.7	0.026	0.053	0.626	0.043	0.732	4.345	0.030	0.813	7.929	0.042	0.724	6.137
π^3 -X	1360	0.023	0.048	0.479	0.038	0.730	3.709	OOM	OOM	OOM	(0.043)	(0.605)	(3.709)
AMB3R	1563	0.021	0.040	0.561	0.039	0.779	7.555	OOM	OOM	OOM	(0.039)	(0.670)	(7.555)
DA3-Small	34.3	0.093	0.075	0.373	0.069	0.457	9.981	0.072	0.499	10.56	0.072	0.443	10.27
DA3-Base	135.4	0.066	0.073	0.385	0.060	0.613	8.527	0.060	0.624	11.09	0.064	0.541	9.807
DA3-Large	410.9	0.034	0.076	0.468	0.063	0.713	6.316	OOM	OOM	OOM	(0.069)	(0.590)	(6.316)
DA3-Giant	1356	0.023	0.041	0.624	0.034	0.751	6.912	OOM	OOM	OOM	(0.037)	(0.687)	(6.912)
DA3-Nested	1690	0.022	0.043	0.625	0.042	0.688	7.066	OOM	OOM	OOM	(0.043)	(0.657)	(7.066)
WorldMirror	1263	0.031	0.061	0.389	0.055	0.682	7.159	OOM	OOM	OOM	(0.058)	(0.535)	(7.159)
VGGT-Omega	1144	0.028	0.041	0.593	0.037	0.629	10.21	-	-	-	(0.039)	(0.611)	(10.21)
DA-Next (Ours)	1304	0.030	0.040	0.444	0.035	0.813	7.456	OOM	OOM	OOM	(0.035)	(0.628)	(7.456)
Online													
Spann3r ²²⁴	658.7	0.142	0.677	0.260	0.517	0.316	11.5	0.410	0.261	13.84	0.535	0.279	12.67
CUT3R	793.3	0.040	0.105	0.335	0.150	0.535	9.351	0.153	0.385	10.4	0.136	0.418	9.877
MonST3R	571.2	0.058	0.108	0.088	0.179	0.029	10.42	OOM	OOM	OOM	(0.143)	(0.059)	(10.42)
Point3R	828	0.038	0.284	0.244	0.218	0.226	13.01	0.593	0.229	14	0.365	0.233	13.51
Stream3R-S	1191	0.022	0.050	0.366	0.081	0.488	10.99	OOM	OOM	OOM	(0.065)	(0.427)	(10.99)
Stream3R-W	1191	0.022	0.065	0.373	0.090	0.411	13.03	OOM	OOM	OOM	(0.078)	(0.392)	(13.03)
StreamVGGT	1257	0.023	0.100	0.378	0.085	0.510	11.51	0.085	0.590	8.610	0.090	0.493	10.06
Page4D	1257	0.029	0.036	0.695	0.038	0.730	4.257	OOM	OOM	OOM	(0.037)	(0.712)	(4.257)
InfiniteVGGT	1257	0.026	0.099	0.412	0.087	0.507	11.88	0.089	0.615	9.897	0.092	0.511	10.89
Wint3R	749.5	0.037	0.094	0.344	0.104	0.448	10.57	0.092	0.361	14.37	0.097	0.384	12.47
LongStream-B	1191	0.034	0.097	0.374	0.171	0.327	11.43	0.191	0.284	12.92	0.153	0.329	12.18
LongStream-S	1191	0.034	0.068	0.368	0.141	0.320	11.48	0.166	0.108	12	0.125	0.265	11.74
LingbotMap*-W	1158	0.031	0.060	0.532	0.058	0.647	7.800	0.060	0.636	7.732	0.059	0.605	7.766
LingbotMap*-S	1158	0.031	0.060	0.532	0.057	0.667	7.531	0.054	0.740	7.282	0.057	0.646	7.406
Chunk-wise													
VGGT-Long	1257	0.022	0.039	0.712	0.038	0.779	4.242	0.044	0.586	6.455	0.040	0.692	5.349
π^3 -Long	958.7	0.026	0.053	0.626	0.047	0.732	4.331	0.134	0.698	6.858	0.078	0.685	5.594
DA3-Streaming	1356	0.023	0.041	0.624	0.034	0.750	6.913	2.078	0.537	9.225	0.718	0.637	8.069
SLAM-based													
MAS3R-SLAM	688.6	0.074	0.173	0.052	0.178	0.049	12.21	0.196	0.172	15.25	0.182	0.091	13.73
VGGT-SLAM	1257	0.022	0.039	0.712	0.051	0.698	4.195	0.139	0.491	8.844	0.076	0.633	6.520
Test-Time Training													
TTT3R	793.3	0.040	0.109	0.373	0.119	0.413	11.95	0.180	0.567	11.93	0.136	0.451	11.94
Scal3R	1266	0.027	0.041	0.531	0.056	0.629	4.730	0.234	0.504	6.711	0.110	0.555	5.720
LoGeR	1255	0.031	0.044	0.413	0.066	0.650	8.799	0.135	0.478	10.81	0.082	0.513	9.803
LoGeR*	1255	0.034	0.053	0.482	0.061	0.671	8.614	0.087	0.536	9.533	0.067	0.563	9.073

Table 29 | **Per-Dataset Results on TUM.** Performance across different input regimes: *Single Frame*, *Sparse*, *Medium*, *Dense*, and the *Average*. The best, second-best, and third-best results in each column are highlighted in **deep blue**, **medium blue**, and **light blue**, respectively. Out-of-memory (OOM) and Timeout (T.O) cells are shaded **light red**; *Average* values for those rows are wrapped in parentheses and excluded from per-column ranking. Within each sub-category, the **bold** value marks the in-group best. Note that DA-Next (Ours) is excluded from the per-column rankings.

Method	#Params (M)	Single Frame	Sparse		Medium			Dense			Average		
		AbsRel↓	AbsRel↓	AUC@30↑	AbsRel↓	AUC@30↑	ATE↓	AbsRel↓	AUC@30↑	ATE↓	AbsRel↓	AUC@30↑	ATE↓
Optimization-based													
DUS3R	571.2	0.235	0.123	0.418	0.237	0.251	0.208	OOM	OOM	OOM	(0.180)	(0.335)	(0.208)
MAS3R	688.6	0.223	0.125	0.472	0.201	0.376	0.168	OOM	OOM	OOM	(0.163)	(0.424)	(0.168)
End-to-End Feed-Forward													
VGGT	1257	0.120	0.070	0.728	0.075	0.836	0.017	OOM	OOM	OOM	(0.072)	(0.782)	(0.017)
Fast3R	647.5	0.350	0.258	0.323	0.237	0.507	0.176	0.258	0.097	0.127	0.251	0.309	0.152
FastVGGT	1158	0.119	0.075	0.703	0.074	0.812	0.023	0.070	0.821	0.022	0.073	0.778	0.022
MUS3R	423.4	0.237	0.124	0.627	0.194	0.714	0.032	T.O	T.O	T.O	(0.159)	(0.670)	(0.032)
MapAnything	1228	0.175	0.089	0.542	0.092	0.656	0.062	OOM	OOM	OOM	(0.090)	(0.599)	(0.062)
OmniVGGT	1217	0.140	0.063	0.727	0.072	0.786	0.057	OOM	OOM	OOM	(0.068)	(0.756)	(0.057)
π^3	958.7	0.089	0.046	0.700	0.045	0.806	0.023	0.057	0.161	0.454	0.049	0.556	0.238
π^3 -X	1360	0.084	0.046	0.730	0.045	0.833	0.018	OOM	OOM	OOM	(0.046)	(0.781)	(0.018)
AMB3R	1563	0.087	0.056	0.690	0.065	0.734	0.033	OOM	OOM	OOM	(0.061)	(0.712)	(0.033)
DA3-Small	34.3	0.180	0.134	0.546	0.116	0.632	0.092	0.105	0.616	0.151	0.118	0.598	0.121
DA3-Base	135.4	0.181	0.112	0.561	0.109	0.703	0.075	0.094	0.697	0.106	0.105	0.654	0.091
DA3-Large	410.9	0.160	0.089	0.643	0.081	0.811	0.038	OOM	OOM	OOM	(0.085)	(0.727)	(0.038)
DA3-Giant	1356	0.189	0.088	0.747	0.079	0.865	0.014	OOM	OOM	OOM	(0.084)	(0.806)	(0.014)
DA3-Nested	1690	0.180	0.088	0.769	0.080	0.854	0.015	OOM	OOM	OOM	(0.084)	(0.812)	(0.015)
WorldMirror	1263	0.121	0.082	0.694	0.090	0.795	0.023	OOM	OOM	OOM	(0.086)	(0.744)	(0.023)
VGGT-Omega	1144	0.066	0.042	0.821	0.040	0.899	0.013	-	-	-	(0.041)	(0.860)	(0.013)
DA-Next (Ours)	1304	0.151	0.057	0.697	0.048	0.813	0.016	OOM	OOM	OOM	(0.085)	(0.755)	(0.016)
Online													
Spann3r ²²⁴	658.7	0.195	0.220	0.239	0.133	0.391	0.241	0.130	0.250	0.432	0.161	0.293	0.336
CUT3R	793.3	0.154	0.102	0.634	0.088	0.551	0.088	0.105	0.115	0.478	0.099	0.433	0.283
MonST3R	571.2	0.237	0.127	0.342	0.235	0.141	0.303	OOM	OOM	OOM	(0.181)	(0.241)	(0.303)
Point3R	828	0.153	0.134	0.410	0.110	0.421	0.145	0.114	0.218	0.292	0.119	0.350	0.218
Stream3R-S	1191	0.106	0.069	0.591	0.262	0.208	0.519	OOM	OOM	OOM	(0.166)	(0.400)	(0.519)
Stream3R-W	1191	0.106	0.069	0.591	0.221	0.221	0.553	OOM	OOM	OOM	(0.145)	(0.406)	(0.553)
StreamVGGT	1257	0.106	0.087	0.621	0.094	0.699	0.052	0.108	0.553	0.115	0.097	0.624	0.084
Page4D	1257	0.098	0.053	0.634	0.045	0.726	0.033	OOM	OOM	OOM	(0.049)	(0.680)	(0.033)
InfiniteVGGT	1257	0.106	0.087	0.601	0.093	0.701	0.052	0.108	0.554	0.117	0.096	0.619	0.084
Wint3R	749.5	0.147	0.102	0.588	0.108	0.489	0.165	0.126	0.163	0.301	0.112	0.413	0.233
LongStream-B	1191	0.108	0.064	0.573	0.145	0.576	0.104	0.183	0.188	0.262	0.131	0.446	0.183
LongStream-S	1191	0.108	0.064	0.573	0.108	0.448	0.179	0.181	0.146	0.271	0.118	0.389	0.225
LingbotMap*-W	1158	0.167	0.066	0.655	0.116	0.671	0.048	0.207	0.378	0.265	0.130	0.568	0.157
LingbotMap*-S	1158	0.167	0.066	0.655	0.104	0.677	0.048	0.095	0.658	0.051	0.088	0.663	0.049
Chunk-wise													
VGGT-Long	1257	0.120	0.070	0.728	0.080	0.757	0.036	0.227	0.266	0.311	0.126	0.584	0.174
π^3 -Long	958.7	0.089	0.046	0.700	0.057	0.784	0.025	0.172	0.441	0.146	0.091	0.642	0.086
DA3-Streaming	1356	0.189	0.088	0.747	0.081	0.822	0.019	0.107	0.429	0.144	0.092	0.666	0.081
SLAM-based													
MAS3R-SLAM	688.6	0.230	0.232	0.129	0.337	0.306	0.361	0.323	0.426	0.125	0.297	0.287	0.243
VGGT-SLAM	1257	0.120	0.070	0.728	0.085	0.653	0.056	0.303	0.196	0.352	0.152	0.526	0.204
Test-Time Training													
TTT3R	793.3	0.154	0.097	0.613	0.084	0.651	0.058	0.090	0.257	0.325	0.090	0.507	0.192
Scal3R	1266	0.186	0.070	0.668	0.126	0.680	0.054	0.217	0.197	0.260	0.138	0.515	0.157
LoGeR	1255	0.085	0.045	0.746	0.068	0.690	0.064	0.103	0.411	0.142	0.072	0.616	0.103
LoGeR*	1255	0.079	0.045	0.717	0.053	0.761	0.035	0.074	0.657	0.061	0.057	0.712	0.048

Table 30 | **Per-Dataset Results on Vkiti**. Performance across different input regimes: *Single Frame*, *Sparse*, *Medium*, *Dense*, and the *Average*. The best, second-best, and third-best results in each column are highlighted in **deep blue**, **medium blue**, and **light blue**, respectively. Out-of-memory (OOM) and Timeout (T.O) cells are shaded **light red**; *Average* values for those rows are wrapped in parentheses and excluded from per-column ranking. Within each sub-category, the **bold** value marks the in-group best. Note that DA-Next (Ours) is excluded from the per-column rankings.

Method	#Params (M)	Single Frame			Sparse			Medium			Dense			Average		
		AbsRel↓	AbsRel↓	AUC@30↑	AbsRel↓	AUC@30↑	ATE↓	AbsRel↓	AUC@30↑	ATE↓	AbsRel↓	AUC@30↑	ATE↓	AbsRel↓	AUC@30↑	ATE↓
Optimization-based																
DUS3R	571.2	0.215	0.286	0.668	0.326	0.702	16.67	OOM	OOM	OOM	(0.306)	(0.685)	(16.67)			
MASt3R	688.6	0.114	0.210	0.386	0.504	0.677	21.24	OOM	OOM	OOM	(0.357)	(0.532)	(21.24)			
End-to-End Feed-Forward																
VGGT	1257	0.037	0.055	0.922	0.046	0.921	5.778	OOM	OOM	OOM	(0.051)	(0.922)	(5.778)			
Fast3R	647.5	0.228	0.424	0.115	0.303	0.135	72.45	0.324	0.146	75.05	0.350	0.132	73.75			
FastVGGT	1158	0.038	0.062	0.918	0.048	0.918	4.304	0.047	0.784	6.673	0.052	0.873	5.488			
MUS3R	423.4	0.117	0.108	0.634	0.094	0.583	47.54	T.O	T.O	T.O	(0.101)	(0.608)	(47.54)			
MapAnything	1228	0.120	0.113	0.690	0.106	0.681	28.69	OOM	OOM	OOM	(0.109)	(0.685)	(28.69)			
OmniVGGT	1217	0.045	0.058	0.816	0.070	0.795	12.71	OOM	OOM	OOM	(0.064)	(0.806)	(12.71)			
π^3	958.7	0.112	0.082	0.843	0.076	0.898	5.051	0.074	0.804	5.849	0.077	0.848	5.450			
π^3 -X	1360	0.062	0.064	0.882	0.056	0.903	1.783	OOM	OOM	OOM	(0.060)	(0.892)	(1.783)			
AMB3R	1563	0.045	0.061	0.950	0.050	0.921	4.534	OOM	OOM	OOM	(0.056)	(0.936)	(4.534)			
DA3-Small	34.3	0.119	0.122	0.448	0.120	0.458	55.2	0.123	0.397	59.85	0.122	0.434	57.52			
DA3-Base	135.4	0.142	0.105	0.550	0.105	0.485	45.83	0.103	0.440	56.79	0.104	0.492	51.31			
DA3-Large	410.9	0.085	0.079	0.655	0.075	0.649	44.85	OOM	OOM	OOM	(0.077)	(0.652)	(44.85)			
DA3-Giant	1356	0.072	0.064	0.787	0.061	0.749	20.83	OOM	OOM	OOM	(0.063)	(0.768)	(20.83)			
DA3-Nested	1690	0.071	0.072	0.767	0.072	0.655	37.2	OOM	OOM	OOM	(0.072)	(0.711)	(37.2)			
WorldMirror	1263	0.081	0.104	0.734	0.099	0.773	13.65	OOM	OOM	OOM	(0.101)	(0.754)	(13.65)			
VGGT-Omega	1144	0.110	0.100	0.793	0.094	0.787	4.123	-	-	-	(0.097)	(0.790)	(4.123)			
DA-Next (Ours)	1304	0.083	0.073	0.742	0.073	0.691	26.178	OOM	OOM	OOM	(0.077)	(0.717)	(26.178)			
Online																
Spann3r ²²⁴	658.7	0.327	0.453	0.366	0.443	0.346	38.77	0.497	0.278	33.67	0.464	0.330	36.22			
CUT3R	793.3	0.070	0.075	0.650	0.069	0.588	41.24	0.063	0.349	58.95	0.069	0.529	50.1			
MonST3R	571.2	0.254	0.216	0.485	0.391	0.478	17.98	OOM	OOM	OOM	(0.304)	(0.482)	(17.98)			
Point3R	828	0.064	0.073	0.348	0.067	0.244	70.09	0.062	0.249	60.33	0.067	0.280	65.21			
Stream3R-S	1191	0.053	0.092	0.708	0.128	0.584	51.36	OOM	OOM	OOM	(0.110)	(0.646)	(51.36)			
Stream3R-W	1191	0.053	0.126	0.666	0.133	0.479	63.01	OOM	OOM	OOM	(0.130)	(0.572)	(63.01)			
StreamVGGT	1257	0.054	0.322	0.808	0.280	0.602	58.14	0.227	0.417	65.29	0.276	0.609	61.71			
Page4D	1257	0.043	0.061	0.823	0.053	0.837	7.484	OOM	OOM	OOM	(0.057)	(0.830)	(7.484)			
InfiniteVGGT	1257	0.054	0.322	0.809	0.281	0.588	59.06	0.223	0.415	65.02	0.275	0.604	62.04			
Wint3R	749.5	0.126	0.142	0.688	0.110	0.505	48.24	0.146	0.317	74.98	0.133	0.503	61.61			
LongStream-B	1191	0.055	0.073	0.822	0.069	0.875	2.261	0.069	0.585	2.175	0.070	0.760	2.218			
LongStream-S	1191	0.055	0.073	0.787	0.074	0.805	3.625	0.072	0.557	2.488	0.073	0.716	3.057			
LingbotMap*-W	1158	0.075	0.079	0.884	0.060	0.927	1.310	0.063	0.815	1.637	0.067	0.875	1.473			
LingbotMap*-S	1158	0.075	0.079	0.884	0.059	0.923	1.464	0.055	0.827	1.396	0.064	0.878	1.430			
Chunk-wise																
VGGT-Long	1257	0.037	0.055	0.922	0.041	0.959	0.719	0.044	0.853	1.324	0.047	0.911	1.021			
π^3 -Long	958.7	0.112	0.082	0.843	0.095	0.930	2.012	0.159	0.722	6.218	0.112	0.831	4.115			
DA3-Streaming	1356	0.072	0.064	0.787	0.116	0.897	5.066	0.052	0.779	1.386	0.077	0.821	3.226			
SLAM-based																
MASt3R-SLAM	688.6	0.253	0.459	0.165	0.492	0.152	77.07	0.566	0.139	68.34	0.506	0.152	72.71			
VGGT-SLAM	1257	0.037	0.055	0.922	0.054	0.956	2.172	0.045	0.847	1.076	0.051	0.909	1.624			
Test-Time Training																
TTT3R	793.3	0.070	0.073	0.541	0.069	0.655	32.52	0.064	0.405	33	0.068	0.534	32.76			
Scal3R	1266	0.036	0.048	0.928	0.087	0.905	0.437	0.089	0.804	0.650	0.075	0.879	0.543			
LoGeR	1255	0.054	0.065	0.751	0.061	0.819	3.494	0.058	0.707	2.756	0.061	0.759	3.125			
LoGeR*	1255	0.054	0.068	0.715	0.056	0.846	2.877	0.052	0.771	2.949	0.059	0.778	2.913			

Table 31 | **Per-Dataset Results on Waymo**. Performance across different input regimes: *Single Frame*, *Sparse*, *Medium*, *Dense*, and the *Average*. The best, second-best, and third-best results in each column are highlighted in **deep blue**, **medium blue**, and **light blue**, respectively. Out-of-memory (OOM) and Timeout (T.O) cells are shaded **light red**; *Average* values for those rows are wrapped in parentheses and excluded from per-column ranking. Within each sub-category, the **bold** value marks the in-group best. Note that DA-Next (Ours) is excluded from the per-column rankings.

Method	#Params (M)	Single Frame	Sparse		Medium			Dense			Average		
		AbsRel↓	AbsRel↓	AUC@30↑	AbsRel↓	AUC@30↑	ATE↓	AbsRel↓	AUC@30↑	ATE↓	AbsRel↓	AUC@30↑	ATE↓
Optimization-based													
DUS3R	571.2	0.125	0.270	0.725	0.256	0.601	5.117	OOM	OOM	OOM	(0.263)	(0.663)	(5.117)
MAS3R	688.6	0.119	0.224	0.751	0.334	0.682	8.506	OOM	OOM	OOM	(0.279)	(0.716)	(8.506)
End-to-End Feed-Forward													
VGGT	1257	0.053	0.048	0.975	0.035	0.958	0.683	OOM	OOM	OOM	(0.042)	(0.966)	(0.683)
Fast3R	647.5	0.159	0.226	0.508	0.285	0.230	43.43	0.274	0.248	47.63	0.262	0.329	45.53
FastVGGT	1158	0.053	0.049	0.962	0.037	0.946	0.944	0.036	0.946	0.776	0.041	0.951	0.860
MUS3R	423.4	0.125	0.128	0.792	0.147	0.648	14.2	T.O	T.O	T.O	(0.138)	(0.720)	(14.2)
MapAnything	1228	0.110	0.293	0.905	0.137	0.863	3.648	OOM	OOM	OOM	(0.215)	(0.884)	(3.648)
OmniVGGT	1217	0.055	0.054	0.951	0.044	0.923	5.228	OOM	OOM	OOM	(0.049)	(0.937)	(5.228)
π^3	958.7	0.101	0.086	0.887	0.069	0.883	1.200	0.068	0.866	1.207	0.074	0.879	1.203
π^3 -X	1360	0.060	0.058	0.972	0.044	0.968	0.601	OOM	OOM	OOM	(0.051)	(0.970)	(0.601)
AMB3R	1563	0.054	0.047	0.975	0.037	0.956	0.666	OOM	OOM	OOM	(0.042)	(0.965)	(0.666)
DA3-Small	34.3	0.144	0.179	0.671	0.145	0.537	30.89	0.141	0.532	30.19	0.155	0.580	30.54
DA3-Base	135.4	0.112	0.147	0.754	0.114	0.580	23.83	0.112	0.543	22.18	0.124	0.626	23.01
DA3-Large	410.9	0.115	0.164	0.862	0.117	0.851	9.856	OOM	OOM	OOM	(0.140)	(0.856)	(9.856)
DA3-Giant	1356	0.083	0.078	0.985	0.067	0.986	0.303	OOM	OOM	OOM	(0.072)	(0.985)	(0.303)
DA3-Nested	1690	0.099	0.125	0.905	0.094	0.903	2.907	OOM	OOM	OOM	(0.110)	(0.904)	(2.907)
WorldMirror	1263	0.068	0.104	0.902	0.075	0.875	4.761	OOM	OOM	OOM	(0.090)	(0.888)	(4.761)
VGGT-Omega	1144	0.088	0.088	0.972	0.073	0.949	0.975	-	-	-	(0.081)	(0.960)	(0.975)
DA-Next (Ours)	1304	0.064	0.059	0.943	0.052	0.960	0.884	OOM	OOM	OOM	(0.058)	(0.952)	(0.884)
Online													
Spann3r ²²⁴	658.7	0.178	0.335	0.526	0.288	0.431	29.38	0.294	0.360	29.13	0.306	0.439	29.25
CUT3R	793.3	0.057	0.072	0.865	0.062	0.709	6.451	0.061	0.573	10.89	0.065	0.716	8.670
MonST3R	571.2	0.092	0.232	0.730	0.296	0.726	9.918	OOM	OOM	OOM	(0.264)	(0.728)	(9.918)
Point3R	828	0.062	0.074	0.577	0.062	0.331	43.64	0.062	0.282	44.75	0.066	0.396	44.19
Stream3R-S	1191	0.059	0.069	0.879	0.240	0.573	42.25	OOM	OOM	OOM	(0.155)	(0.726)	(42.25)
Stream3R-W	1191	0.059	0.071	0.850	0.205	0.514	47.43	OOM	OOM	OOM	(0.138)	(0.682)	(47.43)
StreamVGGT	1257	0.050	0.205	0.856	0.297	0.674	28.85	0.308	0.600	29.34	0.270	0.710	29.09
Page4D	1257	0.050	0.048	0.954	0.041	0.947	0.696	OOM	OOM	OOM	(0.045)	(0.950)	(0.696)
InfiniteVGGT	1257	0.050	0.204	0.856	0.293	0.676	28.54	0.305	0.603	29.63	0.268	0.712	29.09
Wint3R	749.5	0.130	0.124	0.765	0.125	0.597	21.38	0.131	0.458	25.96	0.127	0.607	23.67
LongStream-B	1191	0.057	0.065	0.895	0.057	0.906	0.786	0.058	0.840	0.896	0.060	0.880	0.841
LongStream-S	1191	0.057	0.064	0.839	0.056	0.855	2.367	0.053	0.806	1.323	0.058	0.833	1.845
LingbotMap*-W	1158	0.073	0.086	0.950	0.060	0.967	0.509	0.063	0.954	0.644	0.069	0.957	0.576
LingbotMap*-S	1158	0.073	0.086	0.950	0.060	0.965	0.645	0.058	0.945	0.659	0.068	0.954	0.652
Chunk-wise													
VGGT-Long	1257	0.053	0.048	0.975	0.047	0.930	0.889	0.059	0.878	1.408	0.051	0.927	1.148
π^3 -Long	958.7	0.101	0.086	0.887	0.117	0.865	1.642	0.111	0.812	2.409	0.105	0.855	2.026
DA3-Streaming	1356	0.083	0.078	0.985	0.065	0.981	0.286	0.062	0.967	0.233	0.068	0.977	0.260
SLAM-based													
MAS3R-SLAM	688.6	0.216	0.494	0.478	0.477	0.392	32.29	0.468	0.422	23.64	0.480	0.430	27.96
VGGT-SLAM	1257	0.053	0.048	0.975	0.061	0.841	1.431	0.095	0.797	2.519	0.068	0.871	1.975
Test-Time Training													
TTT3R	793.3	0.057	0.072	0.815	0.061	0.847	3.565	0.061	0.813	4.001	0.065	0.825	3.783
Scal3R	1266	0.059	0.049	0.968	0.180	0.870	0.673	0.088	0.856	1.382	0.106	0.898	1.027
LoGeR	1255	0.058	0.057	0.944	0.051	0.966	0.681	0.043	0.953	0.428	0.050	0.954	0.555
LoGeR*	1255	0.054	0.053	0.949	0.039	0.976	0.391	0.037	0.965	0.275	0.043	0.963	0.333

Table 32 | **Metric-Depth Comparison on SpatialBench.** We compare the native metric-depth predictions (no median/scale alignment) of all 6 methods on SpatialBench that emit metric-scale depth, across the *Single Frame*, *Sparse*, and *Medium* settings, together with the *Average* across all three settings. The best, second-best, and third-best results in each column are highlighted in **deep blue**, **medium blue**, and **light blue**, respectively.

Method	#Params (M)	Single Frame				Sparse				Medium				Average			
		AbsRel↓	SqRel↓	RMSE↓	$\delta_{1.25}$ ↑	AbsRel↓	SqRel↓	RMSE↓	$\delta_{1.25}$ ↑	AbsRel↓	SqRel↓	RMSE↓	$\delta_{1.25}$ ↑	AbsRel↓	SqRel↓	RMSE↓	$\delta_{1.25}$ ↑
DA3-Nested	1689.85	1.599	16.57	1.477	0.507	0.870	5.295	1.569	0.617	1.188	19.64	2.000	0.552	1.219	13.83	1.682	0.559
MapAnything	1228.49	2.476	31.96	2.440	0.365	2.368	23.54	2.592	0.437	3.103	27.87	2.374	0.407	2.649	27.79	2.469	0.403
AMB3R	1563.12	2.235	48.59	1.473	0.388	1.133	4.934	1.360	0.519	1.407	3.990	1.242	0.521	1.592	19.17	1.358	0.476
π^3 -X	1360.03	3.187	13.87	1.842	0.400	1.771	9.361	1.779	0.461	1.957	6.269	1.705	0.449	2.305	9.832	1.775	0.436
DANext	1303.76	1.484	3.369	3.595	0.070	0.713	3.280	4.235	0.117	0.713	3.350	4.261	0.116	0.970	3.333	4.030	0.101
MAS3R-SLAM	688.64	2.672	5.479	2.962	0.231	1.570	4.043	3.468	0.191	2.264	4.992	3.555	0.209	2.169	4.838	3.329	0.210

G. Limitations

We report the limitations of SpatialBench in this section.

Evaluation Cost. Evaluating 41 models across 100+ scenes per model under the dense regime is time-consuming. This can be mitigated by distributing evaluation across multiple GPUs in parallel.

Memory Constraints. All evaluations are conducted on H200 GPUs with 141 GB VRAM. We have not tested models under larger memory configurations such as B100 or B200, and performance or behavior may differ on such hardware.

Hyperparameter Selection. We acknowledge that some evaluated methods may require task- or scene-specific hyperparameter tuning to achieve optimal performance. However, such tuning falls outside the scope of this benchmark. We follow the recommended configurations provided in each method’s official codebase to ensure a fair and consistent comparison across all methods.

Expanding Method Coverage. As of the submission deadline, a number of newly released models continue to be open-sourced. Therefore, we cannot guarantee complete coverage of all existing methods. We commit to continuously integrating and evaluating new methods as they become available.